

**STRUCTURAL, BIOCHEMICAL, AND CELL BIOLOGICAL
CHARACTERIZATION OF RAB7 MUTANTS THAT CAUSE PERIPHERAL
NEUROPATHY**

Brett A. McCray

A Dissertation

In

Neuroscience

Presented to the Faculties of the University of Pennsylvania

In Partial Fulfillment to the Requirements for the Degree of Doctor of Philosophy

2010

J. Paul Taylor, M.D., Ph.D.
Dissertation Supervisor

Rita Balice-Gordon, Ph.D.
Graduate Group Chairperson

Dissertation Committee
Steven Scherer, M.D., Ph.D.
Erika Holzbaur, Ph.D.
Virginia M.-Y. Lee, Ph.D.
Randall Pittman, Ph.D.

**STRUCTURAL, BIOCHEMICAL, AND CELL BIOLOGICAL
CHARACTERIZATION OF RAB7 MUTANTS THAT CAUSE PERIPHERAL
NEUROPATHY**

Copyright

2010

Brett A. McCray

ABSTRACT

STRUCTURAL, BIOCHEMICAL, AND CELL BIOLOGICAL CHARACTERIZATION OF RAB7 MUTANTS THAT CAUSE PERIPHERAL NEUROPATHY

Brett A. McCray

Supervisor: J. Paul Taylor

Coordinated trafficking of intracellular vesicles is of critical importance for the maintenance of cellular health and homeostasis. Members of the Rab GTPase family serve as master regulators of vesicular trafficking, maturation, and fusion by reversibly associating with distinct target membranes and recruiting specific effector proteins. Rabs act as molecular switches by cycling between an active, GTP-bound form and an inactive, GDP-bound form. The activity cycle is coupled to GTP hydrolysis and is tightly controlled by regulatory proteins such as guanine nucleotide exchange factors and GTPase activating proteins. Rab7 specifically regulates the trafficking and maturation of vesicle populations that are involved in protein degradation including late endosomes, lysosomes, and autophagic vacuoles. Missense mutations of Rab7 cause a dominantly-inherited axonal degeneration known as Charcot-Marie-Tooth type 2B (CMT2B) through an unknown mechanism. Patients with CMT2B present with length-dependent degeneration of peripheral sensory and motor neurons that leads to weakness and profound sensory loss. To gain insight into the pathogenesis of CMT2B, we undertook

extensive characterization of two disease-causing Rab7 mutants, L129F and V162M. We present the 2.8 Å crystal structure of GTP-bound L129F mutant Rab7 which reveals normal conformations of the effector binding regions and catalytic site, but an alteration to the nucleotide binding pocket that is predicted to alter GTP binding. We further demonstrate that disease-associated mutations in Rab7 do not lead to an intrinsic GTPase defect as previously suggested, but permit unregulated nucleotide exchange leading to both excessive activation and hydrolysis-independent inactivation. Using an unbiased proteomics approach, we characterize effector interactions in wild-type and mutant Rab7 and identify several novel Rab7 interactors. Consistent with augmented activity, mutant Rab7 shows significantly enhanced interaction with a subset of effector proteins. In addition, dynamic imaging demonstrates that mutant Rab7 is abnormally retained on target membranes. However, we show that increased activation of mutant Rab7 is counterbalanced by unregulated, GTP-hydrolysis-independent membrane cycling. Thus, we demonstrate that disease mutations uncouple Rab7 from the spatial and temporal control normally imposed by regulatory proteins and cause disease by misregulation of native Rab7 activity. Future experiments will address the impact of Rab7 misregulation on neuronal trafficking and trophic signaling.

TABLE OF CONTENTS

Cover Page	i
Title Page	ii
Abstract	iii
Table of Contents	v
List of Tables	viii
List of Illustrations	ix
Chapter 1: Introduction	
Intracellular vesicular dynamics	2
Microtubules and vesicular trafficking	2
Specification of organelle identity	4
The endo-lysosomal pathway	6
The autophagy-lysosomal pathway	8
Rab GTPases	9
The Rab GTPase activity cycle	12
Rab7 and vesicular trafficking	17
Signaling endosomes and axonal transport	23
Retrograde axonal trafficking and disease	26
Charcot-Marie-Tooth disease	28
Charcot-Marie-Tooth disease type 2B	32
Chapter 2: Disease mutations in Rab7 result in unregulated nucleotide exchange and inappropriate activation	
Abstract	38

Introduction	39
Materials and Methods	43
Results	55
Tables	73
Supplementary Data	75
Discussion	83
Chapter 3: Conclusions and Future Directions	
CMT2B disease mutations and misregulation of the Rab7 activity cycle	91
Rab7 disease mutations and trafficking of signaling endosomes	93
Characterization of Rab7-effector interactions in neurons	98
Functional characterization of the Rab7-VapB interaction	100
Concluding remarks	104
Appendix 1: The role of autophagy in age-related neurodegeneration	
Abstract	111
Living may be hazardous to your health	112
Induction and maturation of autophagosomes	116
Regulation of autophagy	117
Multiple roles for autophagy: matters of life and death	118
Decline of autophagy with aging	120
Accumulation of autophagic vacuoles in patients and models of neurodegeneration	122
Autophagy is neuroprotective	124

Can autophagy be co-opted for therapeutic benefit?	127
Unanswered questions and future directions	128
Appendix 2: HDAC6 regulates the steady-state levels and turnover of polyglutamine-expanded androgen receptor	
Abstract	132
Introduction	134
Materials and Methods	136
Results and Discussion	139
References	143

LIST OF TABLES

Chapter 3: Disease mutations in Rab7 result in unregulated nucleotide exchange and inappropriate activation

Table 2.1. Data collection and refinement statistics	73
Table 2.2. Proteomics summary and statistics	74

LIST OF ILLUSTRATIONS

Chapter 1: Introduction

Fig. 1.1. Intersection of the endocytic and autophagic pathways	7
Fig. 1.2. Structure of the Rab GTPase Rab7	10
Fig. 1.3. The Rab GTPase activity cycle	13
Fig. 1.4. Localization of Rab7 disease mutations	34

Chapter 3: Disease mutations in Rab7 result in unregulated nucleotide exchange and inappropriate activation

Fig. 2.1. Structural insights into the disease-causing Rab7 L129F mutant	56
Fig. 2.2. Rab7 disease-causing mutants have decreased GTPase activity and increased guanine nucleotide dissociation	59
Fig. 2.3. Rab7 disease mutants lead to GEF-independent nucleotide exchange	61
Fig. 2.4. Rab7 disease mutants lead to an increase in the GTP-bound, active fraction	63
Fig. 2.5. Rab7 disease mutants demonstrate quantitative changes in effector interactions	65
Fig. 2.6. Rab7 disease mutants have grossly normal subcellular localization but decreased membrane cycling	67
Fig. 2.7. Rab7 disease mutants have decreased membrane cycling	69
Fig. 2.8. Rab7 disease mutants lead to GTPase-independent membrane cycling	71
Fig. 2.9. Model of how Rab7 disease mutants cause misregulation of the activation cycle	85
Fig. S2.1. Stereo views of wild-type and L129F Rab7	75

Fig. S2.2. L129F Rab7 omit map	76
Fig. S3.3. Stereo views of the wild-type and L129F Rab7 GTP binding pocket	77
Fig. S2.4. Analysis of Rab7 interacting proteins	78
Fig. S2.5. Verification of interaction with protein identified by LC-MS/MS	79
Fig. S2.6. Examples of vesicular phenotypes in cells expressing GFP-Rab7 constructs	80
Fig. S2.7. Rab7 mutants associate with autophagosomes and do not alter autophagic flux	81
Chapter 3: Conclusions and Future Directions	
Fig. 3.1. Rab7 disease mutants disrupt axonal trafficking	94
Fig. 3.2. Model of disruption of TrkA signaling in Rab7 disease mutants	96
Fig. 3.3. Rab7 disease mutants cause accumulation of enlarged acidic vesicles in sympathetic neurons	98
Fig. 3.4. Rab7 specifically interacts with VapB	103
Fig. 3.5. The vesicular transport pathway is a hotspot for genetic neurologic diseases	105
Appendix 1: The role of autophagy in age-related neurodegeneration	
Fig. A1.1. Intracellular protein degradation pathways	114
Fig. A1.2. The process of macroautophagy	115
Fig. A1.3. Ubiquitin-like conjugation systems in autophagosome formation	117
Fig. A1.4. Accumulation of autophagic structures in Alzheimer's disease brain	123
Appendix 2: HDAC6 regulates the steady-state levels and turnover of polyglutamine-expanded androgen receptor	

Fig. A2.1. HDAC6 rescues degeneration in SBMA flies	139
Fig. A2.2. HDAC6 accelerates the turnover of polyglutamine-expanded AR	141

Chapter 1: Introduction

This chapter was written by Brett McCray.

Intracellular vesicular dynamics

Maintenance of cellular homeostasis requires regulation of the biogenesis and trafficking of diverse membranous subcellular organelles and vesicles. Membranous compartments such as the endoplasmic reticulum (ER), the Golgi apparatus, endosomes, lysosomes, and autophagic vacuoles are in constant flux and undergo considerable interconversion and crosstalk. The trafficking and regulation of membranous organelles within the cell is vital for coordinating the flow of plasma membrane proteins, nutrient and cholesterol uptake and homeostasis, regulation of secretion, immune function, anabolism and catabolism, and energetic homeostasis. Vesicular compartments are able to undergo directed trafficking, generally using the microtubule network and microtubule-specific motor complexes. In addition, vesicles undergo both homotypic and heterotypic fusion events. As the coordination of vesicular trafficking is of critical importance, cells have evolved multiple protein networks and complex, multifactorial regulatory mechanisms to regulate and carry out this vital task. In particular, members of the Rab family of small GTPases exert tremendous control over multiple aspects of vesicular identity and transport dynamics. The function and regulation of Rabs, and Rab7 specifically, will be the focus of this introduction.

Microtubules and vesicular trafficking

For directed movement throughout the cytoplasm, vesicles often travel along cytoskeletal tracks using various motor complexes. Actin, intermediate filaments, and microtubules constitute the major components of the cellular cytoskeleton, with microtubules being the most common cytoskeletal track used for regulated vesicular transport. Microtubules are

cylindrical structures. The end that elongates more rapidly is designated the plus end, while the other end, which associates with the microtubule organizing center (MTOC) and colocalizes with the centrosome, is designated the minus end.

Microtubules are required for transport of various organelles and protein cargoes.

Anterograde movement (towards the plus end) is mediated by the kinesin superfamily, whereas retrograde movement (towards the minus end) is primarily accomplished by dynein motor complexes (Caviston and Holzbaur, 2006). Although Rab GTPases regulate both anterograde and retrograde transport processes, this dissertation will focus on Rab7-mediated retrograde microtubule transport. The retrograde transport machinery includes two multiprotein subcomplexes: the cytoplasmic dynein motor complex and its adaptor, the dynactin complex. The cytoplasmic dynein complex couples the hydrolysis of ATP to minus end-directed movement and is composed of two dynein heavy chains, two intermediate chains, four light intermediate chains, and several light chains (Kamal and Goldstein, 2002; Schroer, 2004). Cytoplasmic dynein not only plays a role in vesicular trafficking, but is also involved in many biological processes including mRNA localization, assembly of the mitotic spindle, and the transport of organelles and neurofilaments. Dynactin is a multiprotein complex that binds to cytoplasmic dynein to increase its processivity and mediate motor cargo binding (Schroer, 2004). Dynactin is composed of p150^{glued}, which forms a projection arm that interacts with microtubules, Arp1, Arp11, p62, and various other components that interact with motor cargoes, and p50/dynamitin, which connects these two functional units (Schroer, 2004). The p150^{glued} subunit links dynactin to cytoplasmic dynein by binding the intermediate chain subunit of

dynein (Waterman-Storer et al., 1995). In vesicular transport, dynactin functions as an adaptor by binding both to proteins in the vesicular membrane and the cytoplasmic dynein motor.

Specification of organelle identity

While at any given time specific vesicular compartments can be distinguished within the cell, it is currently unclear whether there is a predominance of stable vesicular compartments with carrier vesicles transporting among them (stable compartment model), or whether membranous vesicles are in a constant state of flux and maturation, interconverting among various vesicle identities (maturation model). Evidence suggests that aspects of both of these models are valid. Indeed, dynamic imaging has demonstrated that certain vesicle subtypes can mature and convert into other populations, consistent with the maturation model (Rink et al., 2005; Zoncu et al., 2009). However, ample evidence also exists to demonstrate budding of vesicles from relatively stable compartments before trafficking and fusion to another compartment (Gu and Gruenberg, 1999). In addition, content mixing experiments have demonstrated that endocytic vesicles can undergo transient or protracted fusion with other vesicles, and luminal contents can be shared by these brief contacts (Bright et al., 2005). Thus, in some cases, vesicles go through a stepwise maturation process, and in other cases transport and fusion events cause a change in vesicle identity.

Organelle identity is largely determined by the content of phospholipids and proteins that reside within the limiting membrane. In particular, the presence of small GTPases and the

membrane composition of specific phosphoinositides are critical in regulating vesicle dynamics and in defining organelle identity. The coordination of vesicular trafficking and fusion and fission events is largely regulated by members of the Rab and Arf families of small GTPases which bind to the cytosolic face of specific membranous populations and recruit various effector proteins. The function and regulation of Rab GTPases will be discussed in detail in subsequent sections. Like Rabs, phosphoinositides reside within the limiting membranes of vesicles where they have diverse functions in the regulation of compartmental identity and recruitment of specific proteins (Di Paolo and De Camilli, 2006). Phosphorylation and dephosphorylation of hydroxyl groups at the 3, 4, or 5 position of the inositol ring generates distinct species that are recognized by protein motifs and localize specifically to certain vesicular populations. The head group of phosphoinositides binds to cytosolic proteins or the cytosolic face of membrane proteins; thus they can recruit proteins to specific membranes or organize resident membrane-bound proteins. For example, early endosomes predominantly contain phosphatidylinositol 3-phosphate (PI(3)P), which is produced by the class III phosphoinositide 3-kinase (PI3K) Vps34 and is selectively bound by the FYVE and PX domains present in early-endosomal proteins. In contrast, late endosomes predominantly contain PI(3,5)P, which is largely generated from PI(3)P by Fab1p/PIKfyve kinase (Di Paolo and De Camilli, 2006). Phosphoinositide-protein interactions are generally of low affinity, but stable recruitment of proteins to specific membranes can be achieved through cooperativity of phosphoinositide binding and additional binding events with other proteins or lipids. In this way, phosphoinositide binding provides a mechanism of coincidence detection wherein proteins are recruited to specific membranes by the

cooperative action of multiple signals. Phosphoinositides and Rabs together coordinate vesicular trafficking and engage in reciprocal regulation of each other. Phosphoinositides can assist in the recruitment of Rabs to membranes and in the localization of Rab regulatory proteins, and proteins recruited by Rabs can lead to interconversion of phosphoinositides. Such dual regulation places Rab-phosphoinositide dynamics at the center of the specification of organelle identity and vesicular transport.

The endo-lysosomal pathway

The endosomal pathway consists of vesicles that are derived by various mechanisms of endocytosis, a process which involves invagination and subsequent fission of regions of the plasma membrane. Endosomes arise from diverse entry points such as clathrin- or caveolin-mediated endocytosis, macropinocytosis, and phagocytosis (Conner and Schmid, 2003). Endosomes then undergo a maturation and trafficking process with multiple potential outcomes (Fig. 1.1). Endosomes can undergo homotypic fusion and assimilation into the tubular endosome network, or they can be directed to a recycling endosome compartment for return to the plasma membrane. Portions of the tubular endosomal network can also bud and undergo maturation to late endosomes, which directs them to a lysosomal fate. The maturation of late endosomes involves acidification by delivery of vacuolar proton pump ATPases and fusion with other late endosomes. In some cases, early and late endosomes form multivesicular bodies (MVBs) which contain vesicles within the limiting membrane of the endosome whose contents are topologically equivalent to the cytosol. The formation of MVBs involves the stepwise recruitment of Hrs and three ESCRT (endosomal sorting complex required for transport) complexes

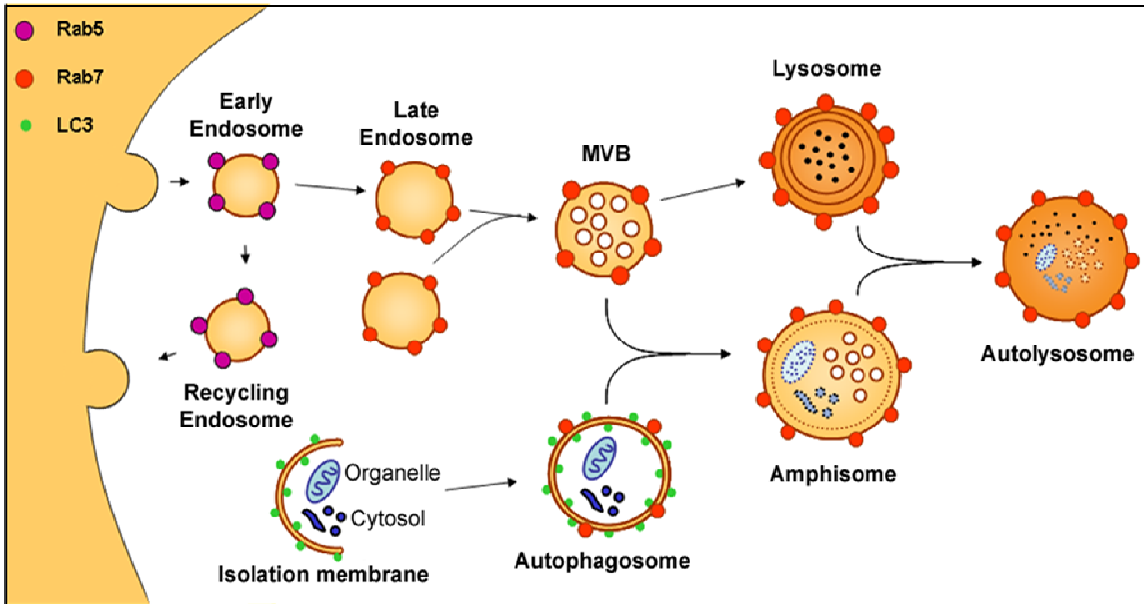


Figure 1.1. Intersection of the endocytic and autophagic pathways. Rab5 regulates endocytosis and early endosome maturation, whereas Rab7 regulates late endosome, lysosome, and autophagosome dynamics. Early endosomes can be recycled to the cell surface or mature into late endosomes, which can then form MVBs. The endocytic and autophagic pathways culminate in fusion with lysosomes where vesicle contents are degraded.

which regulate the invagination and budding of the internalized vesicles (Raiborg et al., 2003). Following maturation, late endosomes and MVBs are targeted to or mature into lysosomes, highly acidic vesicles that degrade their luminal contents. Lysosomes are generated by the delivery of hydrolases to late endosomes by the mannose-6 phosphate receptor (MPR), and their acidic pH (~4.6-5.0) is maintained by vacuolar proton pump ATPases (Luzio et al., 2007). Lysosomes also fuse with vesicles in the autophagic pathway, a pathway which involves the sequestration of portions of cytosol into a double-membrane structure. Thus, the lysosome marks a point of intersection for the endocytic and autophagic pathways and serves as the final common degradative compartment for both pathways.

The autophagy-lysosomal pathway

The autophagy-lysosomal pathway is a relatively non-selective, bulk degradation process wherein long-lived proteins and organelles are delivered for lysosomal degradation through multiple pathways. In contrast, short-lived and misfolded proteins are degraded by the other major degradative pathway, the ubiquitin proteasome system (UPS) (Ciechanover et al., 1984). In the autophagy-lysosomal system, extracellular material can reach the lysosome through the endocytic pathway as described above, or through a process termed macroautophagy (hereafter referred to as autophagy). In this latter process, cytosolic materials are engulfed in crescent-shaped double-membrane structures that close to form autophagosomes which eventually fuse with lysosomes (Cuervo, 2004). The activation of autophagosome membrane formation occurs through a ubiquitin-like conjugation system involving various autophagy proteins (Ohsumi, 2001). One of the terminal steps in this pathway is the proteolytic cleavage of microtubule-associated protein light chain 3-I (LC3-I or atg8) to generate LC3-II which associates with autophagosome membranes. Autophagosomes can be monitored by the localization and amount of LC3-II present in a cell. In mammals, newly formed autophagosomes undergo a stepwise maturation process involving fusion with late endosomes and multivesicular bodies to form a structure termed an amphisome (Berg et al., 1998). Autolysosomes are formed when amphisomes ultimately fuse with lysosomes to deliver their contents for degradation by lysosomal hydrolases. Finally, the breakdown products from the autolysosome are translocated back across the lysosomal membrane for reuse in metabolic processes. Similar to most intracellular vesicles, autophagic vacuole

maturation seems to depend on the function of Rab GTPases (Gutierrez et al., 2004; Jager et al., 2004).

Rab GTPases

The Ras superfamily of small GTPases includes Ras, Rho, Ran, Arf, and Rab GTPases, which regulate diverse processes in intracellular transport, signaling, and cytoskeletal dynamics (Wennerberg et al., 2005). Members of the Rab (for Ras in brain) family of small GTPases are master regulators of vesicular trafficking, maturation, and fusion. Rab GTPases function as molecular switches by cycling between active, GTP-bound states where they are reversibly associated with specific vesicular membranes and inactive, GDP-bound states in which they are predominantly cytosolic and dissociated from their target membranes.

Nucleotide binding and specificity are determined by the five highly conserved G-loops, or G-boxes, of Rabs and related GTPases (Fig. 1.2). The first G-loop, which consists of the sequence GxxxxGK(S/T) and is often referred to as the phosphate loop or P-loop, makes polar contacts with the α - and β -phosphate groups of the nucleotide. GTP binding requires coordination of Mg^{++} , which makes bonding contacts with the γ -phosphate group of GTP and a conserved threonine residue (G2) of Rab GTPases. G3 consists of the sequence DxxGQ which lies near the γ -phosphate group of GTP and provides a catalytic glutamine residue that facilitates GTP hydrolysis. Specificity for binding guanine nucleotides is largely conferred by the conserved G4 loop sequence NKxD, with the residues of this motif forming polar contacts with the guanine ring of the nucleotide. The

final G5 loop contains the consensus sequence SAK/L/T with the final residue directly participating in binding to the guanine ring (Paduch et al., 2001).

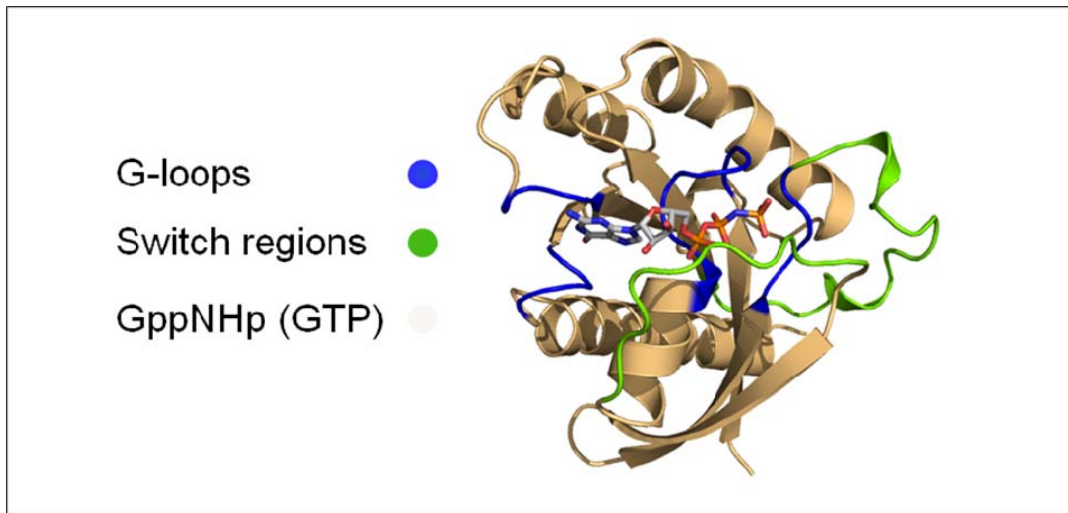


Figure 1.2. Structure of the Rab GTPase Rab7. Rab GTPases contain five G-loops which participate in nucleotide binding. The two switch regions of Rabs change conformation depending on the identity of the bound nucleotide. In the GTP-bound state (shown above), the switch regions are capable of binding to specific effector proteins.

Following membrane association and GTP binding, Rab GTPases recruit effector proteins that exert specific biological activities. In this way, Rab GTPases serve as adaptors to bring effector complexes to specific membrane compartments. Rab effector proteins mediate diverse cellular functions through the recruitment of proteins involved in vesicular trafficking, vesicle tethering and docking, homo- and heterotypic membrane fusion, and even the function of other Rab GTPases. Two “switch” regions of Rabs, designated switch I and II, are the only portions of Rabs that undergo conformational changes depending on the identity of the bound guanine nucleotide. Most Rab effector proteins specifically recognize the GTP-bound conformation of the switch regions and are therefore recruited only to activated Rabs. The effector-Rab GTPase binding interface

usually occurs between coiled-coil domains of the effector and the switch I or II region of the Rab. In most cases, effector binding serves to maintain the bound Rab in its active, GTP-bound state (Jordens et al., 2001), while some effectors seem to facilitate inactivation of their cognate Rabs. Although the tertiary structure of switch regions of Rabs are strikingly similar, effector proteins demonstrate remarkable specificity and minimal overlap in their binding to various Rabs. In fact, single amino acid changes to critical residues within the effector binding switch regions can dramatically alter affinity for effectors (Eathiraj et al., 2005).

The most well-established function of Rab GTPases is the facilitation of vesicle fusion. The process of vesicle fusion can be subdivided into multiple steps: priming, tethering, docking, and fusion. In the priming step, soluble *N*-ethylmaleimide sensitive factor (NSF) attachment protein receptor (SNARE) proteins are activated in a process that requires ATP hydrolysis and NSF. Vesicle tethering is required for fusion and involves the formation of contacts between vesicle membranes mediated by sets of SNARE proteins that interact in *trans* via parallel helical bundles (Sudhof and Rothman, 2009). Docking defines a series of complex interactions that occur after tethering and prior to vesicle fusion. The mechanical force required for vesicle fusion can be entirely provided by trans-SNARE interactions *in vitro* (Weber et al., 1998), although multiple regulatory proteins such as Rabs likely control this process *in vivo*. Rab GTPases, including Rab7, generally facilitate vesicle fusion by recruiting protein complexes that are directly involved in steps of vesicle tethering, docking, and the final fusion event.

The Rab GTPase activity cycle

For each of the more than 60 human Rabs, multiple regulatory proteins have evolved to modulate Rab membrane targeting and activity (Fig. 1.3). Membrane association of Rabs is mediated by a geranyl-geranyl group, also referred to as a prenyl group, which is added post-translationally to successive cysteine residues present at the extreme C-terminus.

The addition of this lipid is coordinated by the activity of Rab geranyl-geranyl transferase (Rab GGT) and Rab escort protein-1 (REP-1). The C-terminal “hypervariable” region of Rabs is the least conserved region across members of the Rab family. This disordered region provides flexibility for the insertion of the geranyl-geranyl membrane anchor.

Inactive Rabs are largely sequestered in the cytosol by Rab GDP-dissociation inhibitor (GDI) which recognizes GDP-bound Rabs and binds their C-terminal prenyl group (Sasaki et al., 1990; Rak et al., 2003). In humans, two forms of Rab GDI exist with GDI1 being highly expressed in the central nervous system (CNS) and GDI2 being expressed ubiquitously. GDI proteins do not discriminate among different Rab proteins but function as general regulators of extraction and sequestration for all Rab GTPases. Aside from protecting the hydrophobic C-terminal lipids of Rabs, GDI also inhibits the dissociation of GDP from Rabs by inducing a conformational change that sterically blocks the opening to the nucleotide binding pocket (Rak et al., 2004). GDI is also important for delivery of inactive, GDP-bound Rabs to the appropriate membrane compartment (Ullrich et al., 1993; Soldati et al., 1994).

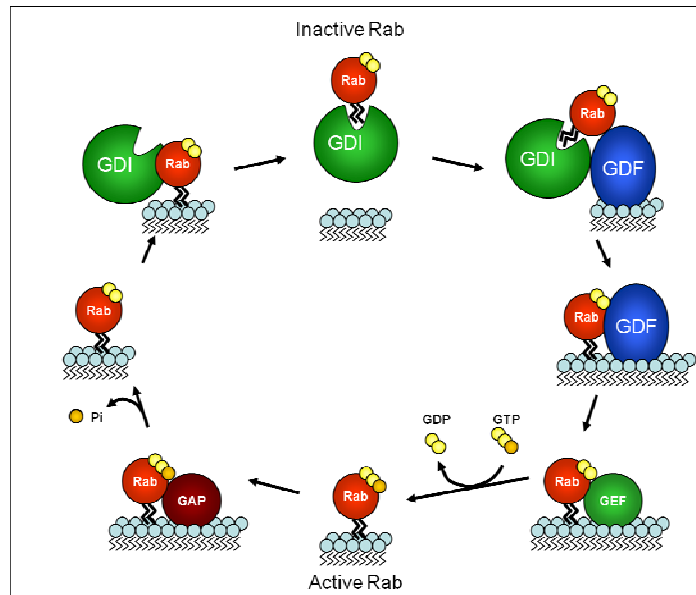


Figure 1.3. The Rab GTPase activity cycle. Inactive Rabs are sequestered in the cytosol by GDI. GDF facilitates extraction from GDI and membrane insertion. Membrane-bound Rabs are then activated by GEF proteins which catalyze GDP release and subsequent GTP binding. Hydrolysis of GTP is facilitated by GAP proteins and leads to Rab inactivation and membrane extraction by GDI.

Activation of Rabs requires extraction from Rab GDI and insertion into membranes.

Targeting of Rabs to the proper vesicular compartment is multifactorial and complex.

The hypervariable C-terminal regions of Rabs may provide some specificity to Rab targeting, as substitution of hypervariable regions on different Rabs can partially redirect Rabs to the vesicle corresponding to the donor C-terminal protein (Chavrier et al., 1991).

However, more extensive analysis of hybrid proteins suggests that the hypervariable domain is insufficient for membrane targeting and that additional determinants seem to work combinatorially (Ali et al., 2004). Extraction from GDI is often facilitated by GDI displacement factors (GDFs) which reside on vesicular membranes and catalyze the release of Rabs from GDI (Dirac-Svejstrup et al., 1997). Additional specificity for membrane targeting is likely mediated by the local concentration of regulatory proteins

such as GDF and guanine nucleotide exchange factors (GEFs) within specific target membranes.

Once Rab GTPases are inserted into the membrane in their GDP-bound, inactive form, their activation requires the exchange of GTP for GDP. Spontaneous GDP dissociation rates for Rabs are typically very low making GDP dissociation the rate-limiting step in Rab activation. To facilitate GTP exchange, GEFs bind the GDP-bound conformation of Rabs and lead to structural alterations to the nucleotide binding pocket that facilitate GDP release (Itzen et al., 2006; Delprato and Lambright, 2007; Dong et al., 2007; Sato et al., 2007; Cai et al., 2008). Evidence suggests that multiple individual GEFs can regulate the same Rab protein, perhaps imparting activation on a subset of vesicular populations or for specific cellular functions. For example, Rabex-5, ALS2 (Alsin), and RIN family members all exhibit GEF activity towards Rab5, and specificity of action of each GEF is further regulated by distinct protein complexes (Esters et al., 2001; Tall et al., 2001; Kajiho et al., 2003; Otomo et al., 2003). In general, structures determined from Rab proteins co-crystallized with GEF proteins demonstrate reorganization of switch I away from the bound nucleotide, thus opening the nucleotide binding pocket and specifically disrupting an edge-to-face aromatic interaction between the guanine ring and a conserved aromatic residue in switch I (Delprato and Lambright, 2007; Dong et al., 2007; Sato et al., 2007; Cai et al., 2008). In the case of the Rab GTPase Sec4p, which plays a role in exocytosis, the structural details of GEF-catalyzed GDP release have been described in detail. The GEF Sec2p adopts a coiled coil structure and binds the switch I and switch II regions of Sec4p. These contacts induce dramatic reorganization of switch I and

specifically two residues of switch I, F45 and P47, which make contacts with the guanine base and ribose, respectively (Dong et al., 2007; Sato et al., 2007). The Sec2p-induced structural rearrangements essentially open the nucleotide binding pocket and decrease affinity for GDP. After GDP release, the P-loop shifts to reside within the region normally occupied by the nucleotide, thus blocking GDP rebinding (Dong et al., 2007). Similar rearrangements to switch I and the P-loop are observed in the complex of Rab21 and the GEF Rabex-5 and in the complex of Ypt1 and the GEF TRAPP (Delprato and Lambright, 2007; Cai et al., 2008), and these mechanisms for GDP release are quite similar to those described for Rho family GTPases (Worthylake et al., 2000). Presently, there is no structural information regarding the mechanism by which GTP binding is facilitated following GDP release. Since intracellular concentrations of GTP are generally 10-fold higher than GDP (500 μ M vs. 50 μ M), a preference for GTP binding following GDP release may be favored simply based on increased relative abundance of GTP *in vivo* (Traut, 1994).

Termination of Rab function is mediated through hydrolysis of the γ -phosphate of GTP to yield GDP, which allows extraction of GDP-bound Rabs by GDI (Ullrich et al., 1993). Intrinsic GTP hydrolysis rates of Rabs are characteristically low, and efficient hydrolysis generally requires the activity of a GTPase activating protein (GAP). GAPs accelerate the hydrolysis reaction by catalyzing the nucleophilic attack of a water molecule on the γ -phosphate of GTP. Like other effector proteins, GAPs specifically recognize the GTP-bound conformation of Rabs. GAP proteins typically display strong preference for specific Rabs, although promiscuity has been observed in cell-free conditions (Pan et al.,

2006). While some GAPs have been paired with specific Rab GTPases (Haas et al., 2005), the identities of many Rab-specific GAPs are unknown. In addition, it seems that each Rab may bind to a host of different GAPs that might each contribute to the inactivation of a subset of functions in specific compartments (Zhang et al., 2005; Seaman et al., 2009). Known GAPs for mammalian Rabs belong to multiple families, and the process of defining specific GAP-Rab pairs is only just beginning. Most known Rab GAPs belong to the Tre-2/Bub2/Cdc16 (TBC) domain containing family of proteins (Lanzetti et al., 2000; Pei et al., 2002), although non-TBC GAPs have been described (Fukui et al., 1997; Xiao et al., 1997). Although the glutamine residue of the DxxGQ (Q67 in Rab7) is generally considered to be catalytic in GTP hydrolysis, recent evidence suggests that this might not be the case in Rab GTPases that bind TBC family members. Instead, the conserved glutamine residue contributes to stabilization of the Rab-GAP interface, and the GAP provides arginine and glutamine fingers that catalyze GTP hydrolysis (Pan et al., 2006). While this mechanism has been verified in Ypt7, the yeast homolog of Rab7, it is currently unclear whether hydrolysis in mammalian forms of Rab7 also occurs in this fashion.

Notably, most Rab GTPases have intrinsically low rates of GDP dissociation and GTP hydrolysis. Because of these properties, both the spontaneous rates of activation and inactivation of Rab GTPases are usually quite slow and allow the Rab activity cycle to be under positive and negative modulatory influences of GEF and GAP proteins. As such, recruitment to target membranes and subsequent activation and inactivation are tightly regulated processes that occur under the control of multiple accessory proteins such as

GDI, GDFs, GEFs, and GAPs. The necessity of such tight regulation is underscored by the demonstration that mutations to activity cycle regulatory proteins (e.g. GDI, REP-1, GEFs) have been found to cause multiple human diseases (D'Adamo et al., 1998; Hadano et al., 2001; Yang et al., 2001).

Rab7 and vesicular trafficking

Rab7 is a ubiquitously expressed protein that plays a vital role in the regulation of the trafficking, maturation, and fusion of endocytic and autophagic vesicles. Rab7 localizes primarily to acidic, pre-degradative, and degradative organelles such as late endosomes, lysosomes, MVBs, phagosomes, autophagosomes, and autophagolysosomes (Feng et al., 1995; Vitelli et al., 1997; Bucci et al., 2000; Harrison et al., 2003). Rab7 specifically controls the transit of early endosomes into the late-endosomal/lysosomal system and subsequent degradation of cargoes associated with target vesicles. As such, Rab7 activity regulates the lysosome-mediated degradation of endocytic cargoes such as activated EGF receptors, internalized cholesterol, and neurotrophic factor receptors such as TrkA (Bucci et al., 2000; Saxena et al., 2005; Ceresa and Bahr, 2006). In general, loss of Rab7 activity leads to a failure in the maintenance of the juxtannuclear lysosomal compartment and dispersal of Rab7-related organelles (Feng et al., 1995; Bucci et al., 2000). Decreased Rab7 activity also slows the degradation of internalized cargoes such as cholesterol and EGF receptors (Bucci et al., 2000). Conversely, augmented Rab7 activity through overexpression of a constitutively active, GTPase deficient mutant (Q67L) leads to more rapid turnover of endocytosed molecules and enhanced juxtannuclear clustering of late endosomes and lysosomes (Bucci et al., 2000; Cantalupo et al., 2001).

In addition to its role in regulation of the endo-lysosomal system, Rab7 also regulates the autophagic pathway. The fusion of autophagic vacuoles with lysosomes requires Rab7 (Gutierrez et al., 2004; Jager et al., 2004; Kimura et al., 2007), although it is unclear whether autophagic vacuole trafficking likewise depends on Rab7 function. Rab7 is not required for MVB formation, but is necessary for their proper maturation, fusion with lysosomes, and subsequent lysosomal degradation (Vanlandingham and Ceresa, 2009). Thus, Rab7 is critical in the trafficking and terminal maturation of vesicles in the late-endosomal, lysosomal, and autophagic pathways.

Similar to other Rabs, Rab7 functions by recruiting specific effector proteins to membranes when it is in the active, GTP-bound state. Known Rab7 effectors include Rab interacting lysosomal protein (RILP), Oxysterol-binding protein-related protein 1L (ORP1L), the homotypic vacuole fusion and vacuole protein sorting (HOPS) complex, Rabring7, the proteasomal subunit XAPC7, and components of the retromer complex (Seals et al., 2000; Cantalupo et al., 2001; Mizuno et al., 2003; Dong et al., 2004; Johansson et al., 2005; Rojas et al., 2008). These effectors have diverse roles in the regulation of Rab7-dependent processes such as recruitment of motor proteins and vesicle fusion machinery.

RILP and ORP1L cooperate to regulate the maturation and retrograde microtubule transport of late endosomes and lysosomes (Cantalupo et al., 2001; Jordens et al., 2001; Johansson et al., 2005; Johansson et al., 2007). The coiled-coil region of RILP forms a

homodimer that can interact with two separate Rab7-GTP molecules (Wu et al., 2005). RILP then recruits cytoplasmic dynein by direct interaction with the extreme C-terminus of the p150^{glued} subunit of dynactin, thereby acting as a linker between dynein motors and Rab7-positive late endosomes and lysosomes (Johansson et al., 2007). Overexpression of a dynactin-binding-deficient RILP causes peripheral redistribution of lysosomes from their usual perinuclear location (Bucci et al., 2000; Jordens et al., 2001). Conversely, overexpression of wild type RILP leads to clustering of lysosomes to a single juxtannuclear region (Cantalupo et al., 2001; Jordens et al., 2001). In addition to RILP, ORP1L is required for efficient retrograde trafficking of Rab7-positive vesicles. RILP and ORP1L bind noncompetitively to Rab7, and ORP1L facilitates the transfer of the RILP-dynein motor complex to the membrane-bound adaptor β III spectrin, thereby ensuring stable docking of the dynein motor complex and efficient retrograde transport (Johansson et al., 2007).

The HOPS complex is another well-characterized Rab7 effector that mediates the biological activity of Rab7. The molecular details of HOPS assembly and function have been largely elucidated in yeast using the Rab7 homolog Ypt7 and by examining the formation and function of the vacuole, the yeast equivalent of the lysosome. The HOPS complex includes the class C vacuolar protein sorting (Vps) proteins Vps11, 16, 18, 33, 39, and 41, which are conserved from yeast to humans (Raymond et al., 1992; Seals et al., 2000). Loss of function of any of these proteins leads to disruption of vacuole formation and improper secretion of the normally vacuole-targeted protease carboxypeptidase Y (Raymond et al., 1992). The interaction of the HOPS complex with

Ypt7 is complex and illustrates the elegant coordination of Rab GTPase activation and effector recruitment. Through different subunits, HOPS can bind both the GDP-bound and GTP-bound forms of Ypt7 (Eitzen et al., 2000; Wurmser et al., 2000; Brett et al., 2008). The Vps39 subunit of the HOPS complex binds GDP-bound Ypt7 and acts as a GEF to facilitate GDP release and subsequent GTP binding to Ypt7 (Wurmser et al., 2000). Interestingly, the early endosomal Rab GTPase Rab5 also binds the HOPS subunit Vps11, which may localize the HOPS complex to early endosomes and facilitate the interaction of Ypt7 and Vps39 (Rink et al., 2005). In this way, Rab5 might coordinate the recruitment of Rab7 to vesicles and the subsequent transition from early endosomes to late endosomes. Once activated by Vps39 GEF activity, Ypt7 can interact with HOPS and facilitate more stable recruitment of HOPS to target membranes. Thus, through different protein subunits, HOPS both participates in the activation of Ypt7 on target membranes and is then itself recruited by active, GTP-bound Ypt7, creating a feed forward loop that serves to concentrate Ypt7 and HOPS together onto specific membrane domains. The activity of membrane-associated HOPS is further regulated by post-translational modifications such as the phosphorylation state of various HOPS subunits. In particular, the vacuolar kinase Yck3p phosphorylates the HOPS subunit Vps41 and negatively regulates HOPS membrane binding (Brett et al., 2008; Cabrera et al., 2009). However, the phosphorylation and inactivation of Vps41 is inhibited by active Ypt7 (Brett et al., 2008). Thus, Ypt7 plays a dual role in HOPS membrane recruitment through direct binding and through opposing the phosphorylation-dependent inactivation of HOPS. Once recruited to membranes, Ypt7 and HOPS coordinate the recruitment of multiple vacuolar SNAREs that facilitate vesicle fusion by tethering donor and acceptor

vesicles together in close proximity (Stroupe et al., 2006). While many of the details of Ypt7 and HOPS functions in vesicle fusion have been elucidated in yeast, it remains to be seen whether the functions and regulatory mechanisms of Rab7 and HOPS are conserved in higher organisms.

The mammalian retromer complex is a recently discovered Rab7 effector complex whose function requires Rab7 activity (Rojas et al., 2008; Seaman et al., 2009). The retromer is a multiprotein complex that functions to retrieve transmembrane proteins, such as the MPR, from late endosomes and deliver them to the trans-Golgi network (Seaman et al., 1998). Retromer is composed of two subcomplexes: a dimer of sorting nexins, and a heterotrimer consisting of Vps26, Vps29, and Vps35. Active, GTP-bound Rab7 binds directly to Vps35 and thereby recruits the retromer complex to late endosome compartments (Rojas et al., 2008). Impairment of Rab7 activity leads to dissociation of retromer from late-endosomal membranes, disruption of late endosome-Golgi trafficking, and inappropriate secretion of lysosomal hydrolases (Rojas et al., 2008; Seaman et al., 2009). Thus, Rab7 seems to play a critical role in retromer membrane recruitment and in the sorting of lysosomal enzymes.

Another Rab7-specific effector is the E3 ubiquitin ligase Rabring7, which regulates transit of EGFR through the late-endosomal/lysosomal pathway (Mizuno et al., 2003). As receptor internalization and the formation of MVBs depend on monoubiquitination, Rabring7 might serve to facilitate these processes through catalysis of ubiquitin conjugation. However, additional work is needed to determine the function of Rab7-

Rab7 interactions.

In addition to the identified effector proteins for active Rab7, some of the proteins that regulate the activity cycle of Rab7 have been identified and characterized. Prenylated Rab acceptor1 (PRA1), the human homolog of Ypt-interacting protein-3 (Yip3) in yeast, is likely to be the GDF that mediates the extraction of Rab7 from GDI (Sivars et al., 2003). PRA1 contains multiple transmembrane domains and is localized to late endosomes and the Golgi network (Sivars et al., 2003). In yeast, Vps39 clearly has GEF activity toward Ypt7, the yeast Rab7 homolog (Wurmser et al., 2000). However, evidence of conserved function in mammals is lacking. Knockdown of Vam6, the mammalian homolog of Vps39, was shown to inhibit the maturation of early endosomes into late endosomes (Rink et al., 2005), but another study failed to find a functional or physical interaction between Rab7 and Vam6 (Caplan et al., 2001). To date, no other putative GEF for Rab7 has been identified, and no evidence of Vam6 GEF activity towards Rab7 has been documented in mammalian systems. However, Vam6 does appear to play a role in late endosome and lysosome fusion, as overexpression leads to prominent vesicular clustering (Caplan et al., 2001). Clearly, further characterization is needed to elucidate the role Vam6 in Rab7-dependent pathways.

In yeast, Ypt7 GTPase activity is stimulated roughly 40-fold by the GAP Gyp7 (Vollmer et al., 1999). Two TBC domain family members have been proposed as putative GAPs for mammalian Rab7 (Zhang et al., 2005; Seaman et al., 2009). TBC1D15, a putative mammalian homolog of Gyp7, shows a partial vesicular localization and has Rab7 GAP

activity *in vitro* (Zhang et al., 2005). However, a functional role in the regulation of Rab7-dependent processes for TBC1D15 has not been shown. TBC1D5 seems to be specifically recruited by the retromer complex and regulates Rab7 activity chiefly in the endosome-to-Golgi sorting pathway (Seaman et al., 2009). A broader role for TBC1D5 in Rab7 biology has not been demonstrated. Further study to define GEF and GAP proteins for Rab7 will likely provide useful tools for further characterization of the diverse functions of Rab7.

Signaling endosomes and axonal transport

In addition to a general role in vesicle trafficking and fusion, Rab7 has been implicated in the regulation of long-range vesicular trafficking in neurons (Deinhardt et al., 2006). In particular, Rab7 may regulate the transport and signaling of neurotrophic factor receptors within axons. Neurotrophins are signaling molecules that are secreted from neuronal target tissues and bind with high affinity to specific receptor tyrosine kinases (Trks). Mammalian neurotrophin receptors include nerve growth factor (NGF), brain-derived neurotrophic factor (BDNF), and neurotrophins 3 and 4/5 (NT3, NT4/5). Receptors for these factors include TrkA, which predominantly binds NGF, TrkB, which binds BDNF and NT4/5, and TrkC, which binds NT3 (Huang and Reichardt, 2001). TrkA is specifically expressed in sensory and sympathetic neurons, making NGF-TrkA signaling critical for the development and survival of these neuron subtypes. Once bound to their receptors, neurotrophins induce dimerization, endocytosis, and autophosphorylation of their cognate receptors (Zweifel et al., 2005). The activated, phosphorylated receptors then initiate pro-survival signaling cascades in the PI3K-Akt and Mitogen-activated

protein kinase-extracellular signal-related kinase (MAPK-ERK) pathways (Zweifel et al., 2005). However, in many neurons, especially peripheral neurons, there is considerable distance between the distal axonal process and the cell body where survival signals must be transmitted. In cell culture paradigms, the requirement for retrograde trafficking of neurotrophin-receptor complexes has been elegantly documented using culture conditions in which the cell body of sympathetic neurons is isolated from the distal processes (Campenot, 1977). In these cultures, NGF applied exclusively to the distal process can provide trophic support and promote survival, but survival requires dynein-mediated axonal trafficking along microtubules (Heerssen et al., 2004). Transmission of target-derived trophic support in these cases requires that the receptor-ligand complex be transported from the axon terminal to the cell body, as simple diffusion of the signal is insufficient. In addition, the complex must be transported intact, and its kinase activity must be maintained in order to promote survival (Ye et al., 2003). The process of transporting activated receptors is accomplished primarily by the “signaling endosome,” a specialized endocytic vesicle that harbors ligand-bound receptors within its membrane. Signaling endosome formation requires endocytosis of ligand-bound receptors at the plasma membrane and subsequent sorting of the receptors into carrier vesicles (Ye et al., 2003). Once endocytosed to form signaling endosomes, the activated neurotrophin receptor is accessible to the cytosol and acts to phosphorylate downstream signaling proteins that generate survival signals (Zweifel et al., 2005). However, for trophic support to reach the nucleus and influence the transcription of pro-survival genes, the signaling endosome must be retrogradely transported over great distances using the microtubule network.

While the details of signaling endosome biology have been the focus of much research over recent decades, the exact nature and properties of the signaling endosome are still under intense debate. Isolated NGF-TrkA complexes have been found to reside in vesicles positive for both early endosomal antigen 1 (EEA1) and Rab5 suggesting that at least some signaling endosomes have properties of early endosomes (Delcroix et al., 2003). Furthermore, experiments in cultured rat pheochromocytoma (PC12) cells, which depend on NGF-TrkA signaling for survival, have demonstrated that NGF, TrkA, and Rab5 colocalize to the same axonal vesicles (Cui et al., 2007). However, experiments using primary mouse motor and sensory neurons suggest that Rab5-positive vesicles only undergo short-range movements and that Rab5 may be responsible for early steps in signaling endosome biogenesis and not long-range trafficking. In these experiments, Rab7 seems to be the primary protein localized to vesicles undergoing long-range axonal trafficking (Deinhardt et al., 2006). Further supporting a role for Rab7, a dominant-negative form of Rab7 inhibits trafficking of signaling endosomes (Deinhardt et al., 2006). In addition to a potential role in axonal trafficking, Rab7 is also likely to play a role in the degradation of neurotrophic factor receptors. Indeed, disruption of Rab7 activity sensitizes PC12 cells to low-dose NGF by delaying degradation of activated TrkA receptors (Saxena et al., 2005). Despite these conflicting reports of the role of Rab5 and Rab7, it seems likely that both play some role in signaling endosome biogenesis and transport. Additional debate concerns whether signaling endosomes display features of MVBs. Electron microscopy demonstrates that immunolabeled NGF partially colocalizes to MVBs within sympathetic neurons (Sandow et al., 2000), although a subsequent study

reported that quantum dot-labeled NGF resides in vesicles without intraluminal vesicles (Cui et al., 2007). If neurotrophin-receptor complexes are found in internal vesicles of MVBs, an important outstanding question would be how the activated receptors could initiate downstream signaling events from within the lumen of MVBs.

While the body of data available at this point does not provide definite characterization of the signaling endosome, it is clear that there is heterogeneity among vesicles that contain activated neurotrophin factor receptors (Cui et al., 2007). Such heterogeneity would account for the discrepancies in data across different systems and experimental paradigms. Even in the absence of a clear consensus on the nature of the signaling endosome, data suggest that signaling endosomes variably display features of early and late endosomes en route to the cell body where they are eventually targeted for degradation in lysosomes (Claude et al., 1982). It will be important for future work to dissect how differences in signaling endosome properties affect their trafficking and signaling and how these differences relate to the recruitment and activity of Rab GTPases.

Retrograde axonal trafficking and disease

Several lines of evidence have highlighted retrograde microtubule transport machinery as critical for maintaining neuronal homeostasis and survival. In mice, two mutant strains that display progressive degenerative motor symptoms (*Legs at odd angles (Loa)* and *Cramping 1 (Cra1)*) were found to have point mutations in dynein heavy chain (Hafezparast et al., 2003). While these mutants were originally reported to display

selective loss of lower motor neurons, further pathological examination demonstrated specific loss of proprioceptive sensory neurons and relative sparing of motor neurons (Ilieva et al., 2008; Dupuis et al., 2009). A third mouse strain with a mutation in dynein (*Sprawling (Swl)*) also displays a sensory neuropathy due to loss of proprioceptive neurons within the dorsal root ganglion and subsequent muscle spindle loss (Chen et al., 2007). Together, the characterization of these mutants suggests that dynein mutations lead to selective degeneration of sensory neurons and that motor symptoms are a result of muscle spindle deficiency, not motor neuron loss. However, there is evidence to suggest that motor neurons are also sensitive to defects in retrograde trafficking: targeted disruption of microtubule transport specifically within motor neurons causes neuron loss and a late-onset neurodegenerative phenotype (LaMonte et al., 2002). Furthermore, the most compelling evidence for the involvement of dynein in motor neuron survival comes from the identification of a mutation in the p150^{glued} subunit of dynactin (G59S) that leads to a human lower motor neuron degenerative disease (distal spinobulbar muscular atrophy) (Puls et al., 2003). Mice expressing the G59S mutant display age-related degeneration of motor neurons, altered morphology of lysosomes, abnormal accumulations of vesicles within axons and terminals, and dynactin-positive inclusions (Chevalier-Larsen et al., 2008; Laird et al., 2008). However, the G59S mutant protein shows only minimal defects in microtubule transport in cell culture (Levy et al., 2006), and no observable transport defect *in vivo* (Chevalier-Larsen et al., 2008). Thus, further elucidation of the functional consequences of the G59S mutation for vesicular trafficking will be required to understand the pathogenesis of this disease.

While it is clear from human and mouse genetic studies that disruption of dynein function can lead to degeneration of sensory or motor neurons, the mechanisms underlying such degeneration remain unclear. The involvement of dynein motors in multiple cellular processes raises numerous possibilities including disrupted ER-Golgi transport, mislocalization of mRNA, and impairment of the trafficking and function of protein degradation machinery. However, a prevailing hypothesis is that dysfunction of cytoplasmic dynein may compromise the efficient retrograde transport of signaling endosomes and attenuate trophic support in the soma. This hypothesis holds particular appeal given that mutations affecting transport often lead to a pattern of disease that is restricted to neurons with the longest axonal processes which are presumably more sensitive to subtle trafficking defects. As axonal transport of signaling endosomes proceeds at $\sim 1-3 \mu\text{m/s}$, transport between the distal process and the soma in the longest axons of the human body would be expected to take $\sim 4-10$ days (Ure and Campenot, 1997; Cui et al., 2007). Thus, it is not surprising that such long neurons display a unique sensitivity to disruption of axonal transport pathways that could influence signaling endosome trafficking. Potentially related to this idea is the discovery that mutations in the axonal trafficking protein Rab7 cause a form of Charcot-Marie-Tooth (CMT) disease characterized by length-dependent axonal degeneration in motor and sensory neurons (Verhoeven et al., 2003). Although it has not been formally tested, it is tempting to speculate that the pathogenesis of this form of CMT may be related to defects in the axonal trafficking of Rab7-related organelles such as signaling endosomes.

Charcot-Marie-Tooth disease

Charcot-Marie-Tooth disease, alternatively known as hereditary sensory and motor neuropathy (HSMN), is a broad clinical entity composed of a heterogeneous group of inherited forms of peripheral neuropathy (Barisic et al., 2008). CMT represents the most common form of hereditary peripheral neuropathy with a prevalence of approximately 1 in 2500 (Zuchner and Vance, 2006). CMT diseases are generally autosomal dominant genetic diseases with complete penetrance. Patients with CMT present with length-dependent sensory, motor, or autonomic dysfunction either alone or in combination (Barisic et al., 2008). Life expectancy is not affected, although patients can develop significant difficulty with ambulation. No effective treatments exist to alter the course of the disease, making treatment primarily supportive (Young and Suter, 2001). There are numerous subtypes of CMT that are recognized, and the associated clinical picture for each subtype is highly variable. To date, over 30 causative genes have been identified in various forms of CMT, and the list continues to grow rapidly. Depending on the form of CMT, patients can experience a range of symptoms including muscle wasting, weakness, sensory loss, paresthesias, decreased deep tendon reflexes, and deformities (Kuhlenbaumer et al., 2002). Symptoms occur in a symmetric distribution with the most distally innervated regions of the feet affected first. The time course and pattern of symptoms is highly correlated with axonal length; the longest axons in the body are affected first and involvement then spreads to shorter axons over time. Thus, disease progresses from distal to proximal regions of the lower limbs with the hands variably becoming affected later in the course of the disease. Differential loss of antagonistic muscles of the feet often leads to foot deformities such as pes cavus and hammer toes (Barisic et al., 2008). In some cases, severe sensory loss can lead to ulcero-mutilating

complications. Wasting of the muscles of the lower limbs is also prominent in many cases and can result in so called “stork leg” deformity from atrophy of peroneal muscles.

Two major subtypes of CMT, designated CMT1 and CMT2, are recognized and distinguished by the primary pathology underlying symptoms. CMT1, which makes up a majority of cases of CMT, is characterized by prominent demyelination and is most commonly caused by mutations in myelin-specific proteins expressed in Schwann cells (Suter and Scherer, 2003). Electrophysiological examination demonstrates decreased nerve conduction velocities reflecting the loss of myelin in affected neurons. Repeated demyelination and remyelination events lead to characteristic onion bulb formation seen in pathological sections of affected nerves (Suter and Scherer, 2003). In some cases, this process leads to prominent enlargement of axonal processes that can be palpated on physical exam. Mutations in the gene coding for peripheral myelin protein 22 (*PMP22*) cause CMT1A, which accounts for the majority of cases of CMT1 (~60-90%) and roughly half of all cases of CMT (Valentijn et al., 1992a; Valentijn et al., 1992b). Other causative proteins in CMT1 include myelin protein zero (MPZ) (Hayasaka et al., 1993) which is the most abundant protein in peripheral myelin, small integral membrane protein of lysosome-late endosome (SIMPLE) (Street et al., 2003), the gap junction protein connexin 32 (GJB1) (Bergoffen et al., 1993), the myelin gene transcription factor early growth response element 2 (EGR2) (Warner et al., 1998), and neurofilament light chain (NEFL) (Jordanova et al., 2003).

In CMT2, the primary pathological feature is axonal degeneration with relative sparing of myelin sheaths. As a result, nerve conduction velocities are generally normal or only slightly reduced whereas compound action potential amplitudes are more markedly reduced. While genetic mutations that cause CMT2 affect a variety of cellular processes, defects in mitochondrial physiology, chaperone activity, and axonal transport pathways are most commonly implicated (Zuchner and Vance, 2006). Mutations in mitofusin 2 (MFN2), a GTPase involved in mitochondrial fusion, cause CMT2A and account for roughly 20% of all cases of CMT2 (Zuchner et al., 2004; Zuchner and Vance, 2006). Other causative proteins in forms of CMT2 include the small heat shock proteins HSP22 (Tang et al., 2005) and HSP27 (Evgrafov et al., 2004), NEFL (Mersiyanova et al., 2000), and the small GTPase Rab7 (Verhoeven et al., 2003). A form of dominant intermediate CMT, so-called for its features of both axonal degeneration and demyelination, is caused by mutations in the gene encoding dynamin 2, a GTPase which regulates membrane fission events (Zuchner et al., 2005).

CMT is notable for marked phenotypic and genetic heterogeneity; different mutations in the same gene can lead to markedly different clinical phenotypes. For example, genetic studies have demonstrated that different mutations in the same gene can sometimes cause either CMT1 or CMT2. This phenomenon is demonstrated by NEFL, where different mutations cause either the demyelinating disease CMT1F or the axonal disease CMT2E (Mersiyanova et al., 2000; Jordanova et al., 2003). Similarly, more than 100 mutation in MPZ have been identified, and depending on the specific mutation, patients can present with demyelination (CMT1B) (Hayasaka et al., 1993) or axonal degeneration (CMT2I

(Marrosu et al., 1998) or CMT2J (De Jonghe et al., 1999)). As an extreme example of phenotypic heterogeneity, the same recessive mutation in the gene for ganglioside-induced differentiation-associated protein-1 (GDAP1) leads to clinically distinct neuropathies in different families (Nelis et al., 2002). Although in some cases inconsistency in classification due to mixed features of axonal degeneration and demyelination might contribute to the apparent genetic heterogeneity, it is quite clear that there can be very poor genotype-phenotype correlation in CMT.

Charcot-Marie-Tooth disease type 2B

Charcot-Marie-Tooth disease type 2B (CMT2B) is a rare form of axonal degeneration accounting for less than 1% of all cases of CMT. Inheritance of CMT2B is autosomal dominant with complete penetrance (Kwon et al., 1995). The clinical picture is notable for the occurrence of profound loss of distal pain sensation leading to recurrent ulcers, deformities, and frequent need for amputation of the lower limbs (Kwon et al., 1995; Auer-Grumbach et al., 2000b; Auer-Grumbach et al., 2000a). As such, CMT2B is alternatively classified as ulcero-mutilating neuropathy. Degeneration of motor neurons and prominent muscle weakness and atrophy are also associated with CMT2B (Auer-Grumbach et al., 2000b). Muscles of the hands are much less affected than the distal muscles of the legs. Affected individuals usually develop symptoms in their second or third decade, although careful questioning can reveal onset of symptoms in childhood (Auer-Grumbach et al., 2000b; Auer-Grumbach et al., 2000a). Patients most commonly initially present with painless infections of the feet that are associated with enlarged inguinal lymph nodes and fevers, and many patients experience recurrent infections of

the feet that can be complicated by osteomyelitis and osteolysis (Auer-Grumbach et al., 2000a). Sensory loss includes small and large fiber modalities. However, the extent of sensory loss across modalities varies in different pedigrees, with some families experiencing equal sensory loss across all modalities and others experiencing preservation of proprioception (Auer-Grumbach et al., 2000b; Auer-Grumbach et al., 2000a). Patellar tendon reflexes are variable within pedigrees and range from brisk to diminished, but patients never display a positive Babinski sign (Auer-Grumbach et al., 2000b; Auer-Grumbach et al., 2000a). In some cases, patients complain of excessive sweating on the distal limbs, but no other autonomic symptoms have been described (Auer-Grumbach et al., 2000b; Auer-Grumbach et al., 2000a). In electrophysiological studies, CMT2B patients show evidence of a primarily axonal degeneration with normal or only slightly reduced motor neuron conduction velocities, markedly reduced compound motor action potential amplitudes, absent or severely reduced action potentials amplitudes in sensory neurons, and electromyogram evidence of denervation in distal muscles (Kwon et al., 1995). Nerve biopsy studies demonstrate signs of axonal degeneration and regeneration and involvement of all fiber types (Auer-Grumbach et al., 2000b). In late stages of the disease, evidence of demyelination and remyelination have been noted (Auer-Grumbach et al., 2000b).

To date, four missense mutations in the *RAB7* gene have been associated with CMT2B (Verhoeven et al., 2003; Houlden et al., 2004; Meggouh et al., 2006). A leucine to phenylalanine (L129F) and a valine to methionine substitution (V162M) have been found in multiple families with CMT2B (Verhoeven et al., 2003) whereas only single patients

with K157N (Meggouh et al., 2006) and N161T (Houlden et al., 2004) mutations have been described. All of the residues mutated in CMT2B are perfectly conserved from humans to worms, although the L129 residue demonstrates homology but not identity in yeast and *Arabidopsis*. CMT2B mutations cluster near the conserved G4 and G5 loops that participate in nucleotide binding (Fig. 1.4). The L129 residue immediately follows the NKxD G4 loop, and the K157 residue is part of the conserved SAK/L/T G5 motif. Residues N161 and V162 are positioned at the transition between the $\alpha 4$ helix and the G5 loop.

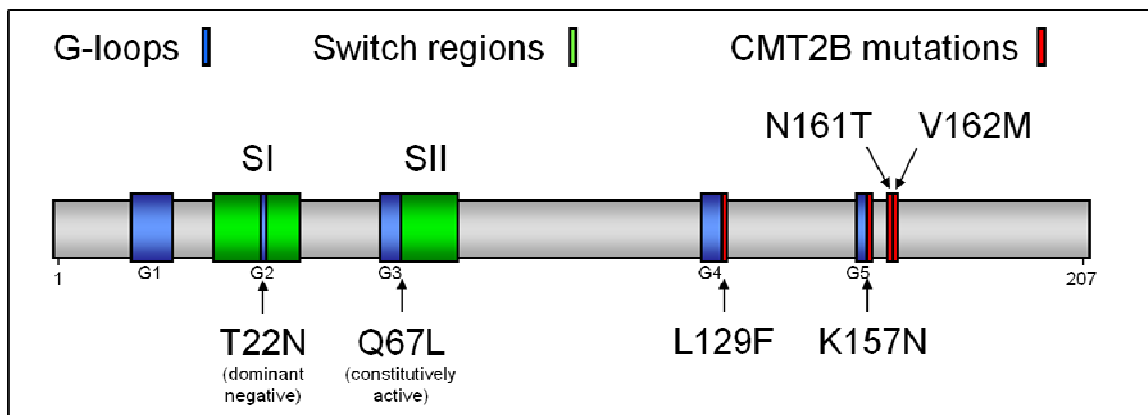


Figure 1.4. Localization of Rab7 disease mutations. CMT2B disease-causing mutations in Rab7 cluster near the highly conserved G4 and G5 loops which directly participate in guanine nucleotide binding. The mutations are localized at a distance from the switch regions and the conserved T22 and Q67 residues which are involved in Mg^{++} binding and GTP hydrolysis, respectively.

At present it is unknown how mutations in Rab7 lead to axonal degeneration. There are currently no animal models of CMT2B, and pathological information regarding this disease is minimal. As Rab7 is a ubiquitously expressed protein that plays a general role in late-endosomal/lysosomal trafficking, one would expect Rab7 to be an essential protein for a variety of cellular processes. Indeed, overexpression of a constitutively

active Rab7 mutant (Q67L) leads to developmental defects in *Drosophila* (Entchev et al., 2000; Wilkin et al., 2008). Given that Rab7 mutations cause a tissue-specific neuronal disease, the effect of these mutations on Rab7 function is likely to be subtle. Given the localization of mutations near G-loops, it is likely that some aspects of the nucleotide cycle are affected. A prior study suggested that disease mutations impair Rab7 GTPase activity and might lead to constitutive activation (Spinosa et al., 2008), but this result was enigmatic considering that none of the four known disease-causing mutations are located near the catalytic site of Rab7.

In the present work, we undertook extensive characterization of Rab7 disease-causing proteins in order to elucidate the specific defects associated with CMT2B mutations. First, we present the high resolution crystal structure of the L129F Rab7 mutant which reveals changes to the nucleotide binding pocket that likely influence nucleotide binding. We follow up our structural studies through biochemical characterization of nucleotide dissociation rates and GTP hydrolysis in wild-type and disease mutant Rab7. We further demonstrate mutation-dependent misregulation of nucleotide exchange leading to excessive activation and shifts in effector binding. We use dynamic live-cell imaging to examine the activity cycle in Rab7 disease mutants and to demonstrate subtle changes in membrane association. Together, our analysis reveals mutation-dependent structural changes that correlate with biochemical and cellular abnormalities resulting in misregulation of the Rab7 activity cycle in disease mutants. We conclude that such misregulation forms the pathological basis of CMT2B and speculate on how such misregulation could lead to axonal trafficking defects and the specific pattern of axonal

degeneration seen in CMT2B. Finally, we present follow-up of proteomic analysis of Rab7 interactors that suggests that the vesicle-associated protein VapB is a novel Rab7 effector. Also included in this dissertation is a review of the role of autophagy in neurodegeneration and specific contributions to a previous publication regarding HDAC6 and autophagy-mediated degradation of misfolded disease proteins.

Chapter 2: Disease mutations in Rab7 result in unregulated nucleotide exchange and inappropriate activation

All work presented in this chapter, except for structural analysis of Rab7 L129F, was performed by Brett McCray. Preparation of Rab7 L129F protein and crystallization of Rab7 L129F was performed by Brett McCray with help from Emmanuel Skordalakes (Wistar Institute). X-ray diffraction data sets were collected at the Brookhaven National Laboratory National Synchrotron Light Source. Structural determination and refinement were performed by Emmanuel Skordalakes. The chapter was written by Brett McCray and J. Paul Taylor with contributions from Emmanuel Skordalakes and is currently in press in *Human Molecular Genetics* (McCray et al., 2009).

Abstract

Rab GTPases are molecular switches that orchestrate vesicular trafficking, maturation, and fusion by cycling between an active, GTP-bound form and an inactive, GDP-bound form. The activity cycle is coupled to GTP hydrolysis and is tightly controlled by regulatory proteins. Missense mutations of the GTPase Rab7 cause a dominantly inherited axonal degeneration known as Charcot-Marie-Tooth type 2B through an unknown mechanism. We present the 2.8 Å crystal structure of GTP-bound L129F mutant Rab7 which reveals normal conformations of the effector binding regions and catalytic site, but an alteration to the nucleotide binding pocket that is predicted to alter GTP binding. Through extensive biochemical analysis, we demonstrate that disease-associated mutations in Rab7 do not lead to an intrinsic GTPase defect, but permit unregulated nucleotide exchange leading to both excessive activation and hydrolysis-independent inactivation. Consistent with augmented activity, mutant Rab7 shows significantly enhanced interaction with a subset of effector proteins. In addition, dynamic imaging demonstrates that mutant Rab7 is abnormally retained on target membranes. However, we show that increased activation of mutant Rab7 is counterbalanced by unregulated, GTP hydrolysis-independent membrane cycling. Notably, disease mutations are able to rescue the membrane cycling of a GTPase deficient mutant. Thus, we demonstrate that disease mutations uncouple Rab7 from the spatial and temporal control normally imposed by regulatory proteins and cause disease not by a gain of novel toxic function, but by misregulation of native Rab7 activity.

Introduction

Members of the Rab family of small GTPases such as Rab7 are master regulators of vesicular trafficking, maturation, and fusion. Rab GTPases function as molecular switches by cycling between active, GTP-bound states in which they are reversibly associated with specific vesicular membranes and inactive, GDP-bound states in which they are predominantly cytosolic and dissociated from their target membranes. Following GTP binding, Rabs recruit specific effector proteins that are involved in vesicular transport and hetero- and homotypic fusion events. For each of the more than 60 human Rabs, multiple regulatory proteins have evolved to modulate Rab membrane targeting and activity. Inactive Rabs are largely sequestered in the cytosol by Rab GDP-dissociation inhibitor (GDI) which recognizes GDP-bound Rabs and binds their C-terminal geranyl geranyl group (Sasaki et al., 1990; Rak et al., 2003). Activation of Rabs requires extraction from Rab GDI, insertion into membranes, and GTP exchange. To facilitate GTP exchange, guanine nucleotide exchange factors (GEFs) bind the GDP-bound conformation of Rabs and lead to structural alterations that facilitate GDP release and allow subsequent GTP binding (Sato et al., 2007). Two “switch” regions of Rabs undergo conformational changes depending on the identity of the bound guanine nucleotide. Rab effector proteins specifically recognize the GTP-bound conformation of the switch regions and are therefore recruited only to activated Rabs. Termination of Rab function is mediated through hydrolysis of the γ -phosphate of GTP to yield GDP. GTPase activating proteins (GAPs) accelerate the hydrolysis reaction by catalyzing the nucleophilic attack of a water molecule on the γ -phosphate of GTP. Following

hydrolysis, GDP-bound Rabs are recognized and extracted from the membrane by GDI (Ullrich et al., 1993). Thus, GEF and GAP proteins along with GDI play a critical role in the regulation of the Rab activity cycle.

Rab7 is a ubiquitously expressed protein that plays a vital role in the regulation of the trafficking, maturation, and fusion of endocytic and autophagic vesicles. Rab7 localizes primarily to acidic, pre-degradative, and degradative organelles such as late endosomes, lysosomes, multivesicular bodies, phagosomes, autophagosomes, and autophagolysosomes (Feng et al., 1995; Vitelli et al., 1997; Bucci et al., 2000; Harrison et al., 2003). Rab7 specifically controls the transition of early endosomes into the late-endosomal/lysosomal system and subsequent degradation of cargoes associated with target vesicles. As such, Rab7 activity regulates the lysosome-mediated degradation of endocytic cargoes such as activated EGF receptors, internalized cholesterol, and neurotrophic factor receptors such as TrkA (Bucci et al., 2000; Saxena et al., 2005; Ceresa and Bahr, 2006). In addition, fusion of autophagic vacuoles with lysosomes requires Rab7 activity (Gutierrez et al., 2004; Jager et al., 2004). Rab7 has also been implicated in the regulation of long-range axonal trafficking (Deinhardt et al., 2006). Although there is no consensus as to the exact role of Rab7 in axonal transport, evidence suggests that Rab5 and Rab7 together regulate the retrograde trafficking of signaling endosomes that supply trophic support to neurons in the peripheral nervous system (Zweifel et al., 2005).

Charcot-Marie-Tooth disease comprises a heterogeneous group of inherited peripheral neuropathies (Barisic et al., 2008). Patients with CMT present with length-dependent sensory, motor, or autonomic dysfunction either alone or in combination. Two major subtypes of CMT are recognized and distinguished by the primary pathology. CMT type 1 is characterized by prominent demyelination and decreased nerve conduction velocities and is most commonly caused by mutations in myelin-specific proteins. In contrast, the primary pathological feature in CMT type 2 is axonal degeneration. While genetic mutations that cause CMT type 2 affect a variety of cellular processes, defects in mitochondrial physiology, chaperone activity, and axonal transport pathways are most commonly implicated (Zuchner and Vance, 2006). To date, four missense mutations in Rab7 have been associated with Charcot-Marie-Tooth disease type 2B (OMIM 600882) (Verhoeven et al., 2003; Houlden et al., 2004; Meggouh et al., 2006). This subtype of CMT is distinguished by profound loss of pain sensation leading to recurrent ulcers, deformities, and frequent need for amputation of the lower limbs (Auer-Grumbach et al., 2000b). As such, CMT2B is alternatively classified as ulcero-mutilating neuropathy. Degeneration of motor neurons and subsequent muscle weakness are also associated with CMT2B (Auer-Grumbach et al., 2000b).

At present it is unknown how mutations in Rab7 lead to axonal degeneration. A prior study suggested that disease mutations reduce nucleotide affinity, impair Rab7 GTPase activity, and lead to constitutive activation (Spinosa et al., 2008). However, the finding of decreased hydrolysis in disease mutants was enigmatic given that the mutations are not localized near the catalytic site. Therefore, we set out to precisely define the impact of

disease-causing mutations on Rab7 structure and function in order to illuminate the mechanism of pathogenesis. We determined the crystal structure of GTP-bound L129F mutant Rab7 at 2.8 Å resolution revealing an alteration to the nucleotide binding pocket, but no impact on the catalytic region of Rab7. These findings guided biochemical analyses in which we determined that disease-causing mutations in Rab7 do not lead to an intrinsic GTPase defect, but instead result in decreased nucleotide affinity and permit unregulated nucleotide exchange. We report that misregulation of Rab7 activation results in an increase in the active fraction of Rab7 and abnormal retention on target membranes. However, we also show that the excessive activation of Rab7 mutants is counterbalanced by unregulated, GTP hydrolysis-independent cycling, thus ruling out constitutive activation of mutant Rab7 as a pathogenic mechanism for CMT2B. We also used an unbiased approach to interrogate the protein interactors of wild-type and mutant forms of Rab7. As predicted by our structural data, the complement of interactors in wild-type and mutant Rab7 is qualitatively identical, although there is significantly enhanced interaction of mutant Rab7 with a subset of effector proteins. This study reveals a pathogenic mechanism wherein disease mutations uncouple Rab7 from normal spatial and temporal regulatory restraints resulting in toxic misregulation of Rab7 activity.

Materials and Methods

Antibodies and Reagents

The following primary antibodies were used: HA rabbit Y-11 (Santa Cruz), HA mouse (Covance), HA mouse M2 (Sigma-Aldrich), GFP mouse (Roche), GFP rabbit (Santa Cruz 8334), LAMP2 Clone H4B4 (Developmental Studies Hybridoma Bank), GDI2 (Proteintech Group), VapB (Proteintech Group), SPG21 (Novus), Prohibitin (Proteintech Group), and Stomatin-like 2 (Proteintech Group). Secondary antibodies: goat anti-mouse IRDye 800CW, goat anti-rabbit IRDye 800CW, goat anti-mouse IRDye 680CW, goat anti-rabbit IRDye 680CW (LI-COR), and AlexaFluor 594 (Invitrogen). GTP and GDP were obtained from BioMol. All transfections were performed using Fugene6 (Roche) according to manufacturer protocols.

Constructs

Wild-type and L129F mutant HA-Rab7 in pcDNA3.1 expression vector were a generous gift from Vincent Timmerman. V162M, Q67L, and T22N mutations were introduced using the QuikChange Mutagenesis XLII kit (Stratagene). FLAG tag was substituted for the HA tag and subcloned into the EcoRI and XhoI sites of pcDNA3.1 by PCR. GFP-Rab7 was obtained from Addgene and GFP-Rab7 mutants were generated by mutagenesis. All Rab7 epitope tags were added to the N-terminus. The following constructs were generous gifts from various researchers: GFP-RILP from Jacques Neefjes, dsRED-RILP from Zakaria Hmama, HA-RILP from Cecilia Bucci, GST-RILP and GST from Aimee Edinger, RFP-LC3 from Craig Thompson, and PA-GFP from Jennifer Lippincott-Schwartz. PA-GFP Rab7 mutants were generated by mutagenesis.

Primers

Mutagenesis:

V162M Forward: GGAGGCCATCAACATGGAGCAGGCGTTCC

V162M Reverse: GGAACGCCTGCTCCATGTTGATGGCCTCC

Q67L Forward: GGGACACAGCAGGACTGGAACGGTTCCAG

Q67L Reverse: CTGGAACCGTTCCAGTCCTGCTGTGTCCC

T22N Forward: GATTCTGGAGTCGGGAAGAACTCACTCATGAACCAGTATG

T22N Reverse: CATACTGGTTCATGAGTGAGTTCTTCCCGACTCCAGAATC

Addition of FLAG tag to Rab7:

5'EcoFLAG:CGCCGAATTCATGGATTACAAGGATGACGACGATAAGACCTCTA

GGAAGAAAGTGTTGC

3'Xho: GGTCCTCGAGTCAACAACCTGCAGCTTTCTGCGGAGG

Expression and purification of Rab7 L129F protein for crystallization

The human full-length coding sequence of Rab7 was subcloned into pET-His-MBP vector (Novagen) using the NdeI and XhoI restriction sites. The L129F mutation was introduced by mutagenesis to generate His-MBP-Rab7 L129F. BL21-CodonPlus (DE3)-RIPL Competent Cells (Stratagene) were transformed with His-MBP-Rab7 L129F and grown in 6L 2YT media to O.D.₆₀₀ 0.4-0.5. Protein expression was induced with 0.1 mM IPTG for 3hr at 30°C. Cells were harvested by centrifugation and the cell pellet was resuspended in Buffer A (5 mM Tris-HCl, 0.5 M KCl, 30 μM benzamidine, 5 mM 2-mercaptoethanol, 10 mM imidazole, 10% glycerol, pH 7.5). Cells were lysed by

sonication and insoluble material was sedimented at 16,000 x g for 15 minutes. The supernatant was loaded onto Ni-NTA resin pre-equilibrated with Buffer A and the His-MBP-Rab7 L129F protein was isolated using an imidazole gradient (10-300 mM) at 4°C. The His-MBP tag was cleaved using TEV protease, and the Rab7 L129F-TEV mixture was passed over the Ni-NTA resin to remove the His-tagged products. The sample was further purified using anion exchange, cation exchange, and size exclusion columns. Purity of the protein was verified to be greater than 95% by SDS-PAGE and Coomassie stain.

Crystallization

The non-hydrolyzable GTP analog GppNHp (5 mM) (BioMol) and MgCl₂ (5 mM) were added to purified Rab7 L129F and crystals were grown by the sitting drop method.

Crystals appeared in 0.2 M sodium formate, 10mM trimethylamine hydrochloride, and 20% polyethylene glycol 3,350, pH 7.2 at 18°C in 3 days and grew to a maximum size of 100x10x10 μm in 2 weeks. Crystals were cryoprotected in 0.2 M sodium formate, 10 mM trimethylamine hydrochloride, 20% polyethylene glycol 3,350, pH 7.2 and 25% PEG400 and flash frozen in liquid N₂. X-ray diffraction data were collected at the National Synchrotron Light Source (NSLS) using the X6A beamline.

Determination of the structure of L129F Rab7

Phases were calculated by molecular replacement (MR) using PHASER (Potterton et al., 2003) as implemented in CCP4 suite of programs using the substrate-free structure of Rab7 (PDB ID 1VG8) as a search model. Maps calculated after one cycle of refinement

by REFMAC followed by solvent flattening and five-fold multidomain, non-crystallographic symmetry averaging using DM (Cowtan, 1994) revealed clear *fo-fc* density for the nucleotide substrate at 2.5 Å contour level. Model building was carried out in COOT (Emsley and Cowtan, 2004), and the model was refined using both CNS-SOLVE (Brunger et al., 1998) and REFMAC5 (Murshudov et al., 1997). The last cycles of refinement were carried out with TLS restraints as implemented in REFMAC5 and without NCS restraints (Table 1).

GTP/GDP dissociation assays

Wild-type, L129F, and V162M His-MBP-Rab7 fusion proteins were expressed and purified from bacteria as described above, but the His-MBP tag was not cleaved. Fusion proteins were bound to NiNTA beads (Sigma-Aldrich) for 30 minutes at 4°C in Buffer A (20 mM Tris-HCl, 100 mM NaCl, 5 mM MgCl₂, 1 mM NaH₂PO₄, 10 mM 2-mercaptoethanol, pH 7.8) followed by one wash with 1 M guanidine-HCl. Bound Rab7 proteins were then incubated in Buffer A containing 0.1 μM ³H-GTP or ³H-GDP for 30 minutes on ice and washed to remove unbound nucleotide. Proteins were incubated in Buffer A containing a 1000-fold excess of unlabeled GTP or GDP for 0, 15, 30, or 60 minutes at 37°C. Samples were washed to remove dissociated nucleotide. To elute nucleotides, 10 μl of elution buffer (0.2% SDS, 5 mM EDTA, 5 mM GTP, and 5 mM GDP) was added, and samples were incubated at 65°C for 2 minutes. Eluted nucleotides were quantified using scintillation counting, and the amount of ³H-GTP or ³H-GDP bound at 15, 30, and 60 minutes was compared to the initial amount bound (0 time point).

GTPase assays

His-MBP-Rab7 fusion proteins were bound to NiNTA beads as above followed by three washes with 1 M guanidine-HCl and three washes with Buffer A. Reactions were incubated with 30 μ l of Buffer A containing 32 P-GTP for 2 hours on ice to load GTP. Hydrolysis was initiated by moving the reactions to 37°C for 2 hours. In some reactions, 1000-fold excess unlabeled GTP was added to the reaction during hydrolysis (“+excess unlabeled GTP” condition). Following hydrolysis, nucleotides were eluted as above. Samples were spotted on PEI cellulose and resolved in NaH_2PO_4 (pH 3.4) for ~1 hour. Signals for GTP and GDP were calculated using a PhosphorImager. The percentage of 32 P-GTP hydrolyzed in each experiment was calculated by dividing the GDP signal by the total signal from GTP and GDP, taking into account that the specific activity of 32 P-GDP is 2/3 that of 32 P-GTP.

GTP exchange assays

For the cell-free exchange assay, recombinant MBP-His Rab7 proteins were bound, treated with guanidine HCl, and washed as above. To determine the maximum amount of 3 H-GTP that could be bound, His-MBP-Rab7 proteins were incubated in Buffer A containing 0.1 μ M 3 H-GTP for 30 minutes at 37°C. Following washes, bound 3 H-GTP was eluted and quantified as above. To determine the GTP exchange rate, His-MBP-Rab7 proteins were treated as above except incubated in Buffer A containing 0.2 mM unlabeled GDP before addition of 3 H-GTP. Following washes, Buffer A containing 3 H-GTP was added, and the proteins were incubated at 37°C for 10 or 30 minutes. Samples were washed and eluted nucleotide was quantified as above. The ratio of the amount of 3 H-

GTP bound at 10 or 30 minutes to the maximum amount bound without GDP pre-incubation was calculated for wild-type, L129F, and V162M Rab7. For the exchange assay from cell lysates, HEK293T cells were transfected with FLAG-Rab7, and cells were harvested 48 hour post-transfection and lysed in IP buffer (20 mM HEPES, 10% glycerol, 0.5% Triton-X100, 150 mM NaCl, 2 mM MgCl₂, 1 mM DTT, and Complete Mini Protease Inhibitor Cocktail EDTA-free (Roche)). Rab7 proteins were immunopurified using FLAG-M2 agarose (Sigma-Aldrich) and washed several times in IP buffer. Immunopurified Rab7 proteins were then incubated in IP buffer containing 0.1 μ M ³H-GTP for 10 minutes at 37°C. Following several washes, bound nucleotides were eluted and quantified as above.

Coimmunoprecipitation

HEK293T cells were transfected with FLAG-Rab7, HA-Rab7, or cotransfected with HA-Rab7 and GFP-RILP. Cells were collected and lysed 48 hours post-transfection in IP Buffer (20mM HEPES, 10% glycerol, 0.5% Triton-X100, 150mM NaCl, 2 mM MgCl₂, 1 mM DTT, and Complete Mini Protease Inhibitor Cocktail EDTA-free (Roche)). Lysates were incubated with HA-agarose or FLAG-M2 agarose (Sigma-Aldrich) for 3 hours at 4°C. After washing the beads four times with IP Buffer, bound proteins were eluted with 200 μ g/ml HA or FLAG peptide (Sigma-Aldrich). Immunoprecipitated proteins were separated by SDS-PAGE and transferred to nitrocellulose membranes (Invitrogen) for Western blotting. Signal was detected using fluorescent secondary antibodies (LI-COR) and the LI-COR Odyssey imaging system.

GST-RILP pulldown

The protocol was performed as previously described (Romero Rosales et al., 2009). Briefly, the Rab7-binding region of murine RILP (amino acids 220-299) fused to GST was expressed in bacteria and purified. HEK293T cells were transfected with GFP alone or GFP-Rab7, lysed, and incubated with GST-RILP overnight at 4°C. After extensive washing, bound proteins were eluted and separated by SDS-PAGE followed by Western blotting.

LC-MS/MS protein identification

Enzymatic Digest of Proteins: HEK293T cells were transfected with FLAG-Rab7 constructs and immunoprecipitated as described above. Immunoprecipitated proteins were separated by SDS-PAGE and stained with SYPRO Ruby (Sigma-Aldrich). The protein bands of interest were excised from a 1D gel manually. In-gel digestion was then performed with sequencing-grade, modified trypsin supplied frozen (Promega). The protein band was excised, cut into small plugs, washed with 50% acetonitrile, and destained by several incubations in 100mM ammonium bicarbonate pH 8 containing 50% acetonitrile. After reduction (10 mM, DTT for 1 hour at 37°C) and alkylation (50 mM iodoacetamide for 45 minutes at room temperature in the dark), the gel plugs were washed again with 50% acetonitrile in 50 mM ammonium bicarbonate followed by a second wash in 50% acetonitrile in 10 mM ammonium bicarbonate. The gel plugs were then dried using a speedvac (Savant) and rehydrated in 10 µl of 0.2 µg trypsin. After 10 minutes, 25 µL of 25 mM ammonium bicarbonate pH 8 was added to the tube. The enzymatic reaction was carried out overnight (approximately 12 hours) at 37°C, followed

by peptide elution from the gel plugs using 20 to 30 μL of 0.2% formic acid. The solution was then transferred to a sample vial for LC-MS/MS analysis.

Electrospray Ionization Ion Trap Mass Spectrometry Analysis: LC-MS/MS analysis was carried out using a ThermoFisher LTQ XL linear ion trap mass spectrometer in line with a nanoAcquity ultra performance LC system (Waters Corporation). Tryptic peptides were loaded onto a “precolum” (Symmetry C18, 180 μm i.d X 20 mm, 5 μm particle) (Waters Corporation) which was connected through a zero dead volume union to the analytical column (BEH C18, 75 μm i.d X 100 mm, 1.7 μm particle) (Waters Corporation). Tryptic peptides were eluted over a gradient (0-70% B in 60 minutes, 70-100% B in 10 minutes, where B = 70% Acetonitrile, 0.2% formic acid) at a flow rate of 250 nL/min and introduced online into a linear ion trap mass spectrometer (ThermoFisher) using electrospray ionization (ESI). Data dependent scanning was incorporated to select abundant precursor ions for fragmentation by acquisition of a full-scan mass spectrum followed by MS/MS on the 10 most abundant ions (one microscan per spectra; precursor $m/z \pm 1.5\text{Da}$, 35% collision energy, 30ms ion activation, 35s dynamic exclusion, repeat count 2).

Database Searching: Product ions generated by fragmentation along the peptide backbone by collision activated dissociation (CAD) (b/y-type ions) were used in an automated database search against the NCBIInr_20090524 (selected for Homo sapiens, 222,717 entries) database using the Mascot search routine (Perkins et al., 1999) assuming the digestion enzyme trypsin (2 missed cleavages) with following residue modifications

being allowed: carbamidomethylation on cysteine and oxidation on methionine. Mascot was searched with a fragment ion tolerance of 0.6 Da and a parent ion tolerance of 1.5 Da. The identifications from the automated search were further validated through Scaffold (Proteome Software) and manual inspection of the raw data. Peptide identifications were accepted if they could be established at greater than 95% probability as specified by the Peptide Prophet algorithm (Keller et al., 2002). Protein identifications were accepted if they could be established at greater than 99% probability and contained at least 2 identified peptides. Protein probabilities were assigned by the Protein Prophet algorithm (Nesvizhskii et al., 2003).

Immunofluorescence

HeLa cells were plated on 4-well chamber slides (Lab-Tek) and transfected with GFP-Rab7. Cells were fixed 24 hours post-transfection with 4% paraformaldehyde for 10 minutes and blocked with 5% normal goat serum for 1 hour. Cells were permeabilized using 0.2% saponin for 10 minutes. For LAMP2 staining, permeabilized cells were incubated in LAMP2 antibody (1:500) overnight at 4°C. Following washes, cells were incubated in AlexaFluor594 (1:500) for 1 hour. Vectashield + DAPI (Vector Laboratories) was added and cells were cover-slipped. Cells were visualized using a Leica DMIRE2 compound microscope under the 63x oil immersion lens, and images were acquired using SlideBook software.

Quantification of Rab7 subcellular localization

HeLa cells were transfected with GFP-Rab7 and fixed 24 hours later. Random adjacent fields were imaged at 63x as described above, and individual GFP-Rab7 positive cells were cropped to new files using SlideBook software. The individual cell images were randomly ordered and presented to a blinded scorer. The predominant morphology and localization of GFP-Rab7 for each cell was characterized as “diffuse, small,” “diffuse, few enlarged,” “some clustering, many enlarged,” or “highly clustered, many enlarged” (see Supplementary Fig. S3.6 for scoring examples). The percentages of phenotypes for each Rab7 construct were calculated and graphed using Microsoft Excel.

FRAP

For Figure 5, HeLa cells were plated in 35 mm cover slip-bottom dishes (MatTek) and transfected with GFP-Rab7 constructs. Live-cell imaging was performed 24 hours post-transfection using a FluoView FV1000 Olympus laser scanning confocal microscope under 60x oil immersion. Cells were imaged every 3 seconds for 15 seconds total using the Argon ion 488nm laser (30mW) at 1% excitation power to record the pre-bleach fluorescence levels. Small regions of the cytosol containing GFP-Rab7 vesicles were then bleached using the 488nm laser at 100% power for 2 seconds. Recovery of fluorescence was monitored every 3 seconds for 225 seconds using the 488nm laser at 1% power. Regions of interest (ROIs) were drawn around bleached Rab7 vesicles and the fluorescence intensity at each time point was calculated using Metamorph software. Fluorescence intensity values were exported to Microsoft Excel and fluorescence recovery curves from each condition were averaged and plotted. Pre-bleach fluorescence

was set to 1 and the first post-bleach time point was set to 0 for each ROI. For FRAP of compound mutants (Fig. 6), cells were plated and transfected as above, and imaged using a Nikon TE2000 microscope with a C1Si confocal using the 60x oil immersion objective. Pre- and post-bleach excitation was performed with a 488nm diode laser at 2% power every 3 seconds for 5 frames and 50 frames, respectively. Photobleaching was performed at 100% laser power for 10 seconds. Data were analyzed using EZC1 software, then exported to Microsoft Excel and graphed as above.

FLAP

HeLa cells were plated as in FRAP assays and transfected with PA-GFP-Rab7 constructs. Live-cell imaging was performed 24 hours post-transfection using a FluoView FV1000 Olympus laser scanning confocal microscope. Regions of cytosol containing PA-GFP-Rab7 vesicles were identified using the 488nm laser at 10% power. Small regions were then activated by a 2-second pulse with the violet diode 405nm laser (25mW) at 50% power. Loss of fluorescence was monitored every 3 seconds for 150 seconds using the 488nm laser at 1% power (at this power, unactivated PA-GFP fluorescence is undetectable). ROIs were drawn around activated Rab7 vesicles and the fluorescence intensity was plotted over time as in FRAP assays. The first post-bleach time point was set to 1 for each ROI. Fluorescence loss curves from each condition were averaged and plotted.

Statistical analysis

Two-tailed student's t-tests (two sample equal variance) were used to determine p-values for GTPase, GTP exchange, and nucleotide dissociation experimental data. For FRAP and FLAP data, the baseline fluorescence measurement was fitted to the genotype and time point of measurement using conventional linear models. The p-values for the F-statistic with measurement fitting to protein were calculated. P-values of less than 0.05 were considered statistically significant.

Results

The L129F mutation alters the nucleotide binding pocket of Rab7

Rab GTPases cycle between activated, GTP-bound, membrane-associated states and inactive, GDP-bound, cytosolic states. Mutations in Rab7 that cause CMT2B cluster near the highly conserved G-loops that are involved in nucleotide binding. A previous study demonstrated decreased GTP hydrolysis in disease mutants (Spinosa et al., 2008).

However, as residues mutated in CMT2B are not near the catalytic glutamine (Q67) or the hydrolyzed γ -phosphate of GTP, it was unclear how disease mutations could impair GTPase activity. To resolve this issue and provide mechanistic insight into CMT2B, we solved the crystal structure of the L129F Rab7 mutant in its active, GTP-bound form. The structure of full-length L129F Rab7 bound to the non-hydrolyzable GTP analog GppNHp was solved to 2.8 Å by molecular replacement using wild-type Rab7 as a search model (Table 2.1). The L129F substitution does not alter the overall structure of the molecule as compared to the published structure of wild-type Rab7 bound to GppNHp (PDB 1VG8) (Fig. 2.1A-C, Supplementary Fig. S2.1 for stereo views) (Rak et al., 2004). Notably, the conformation of the effector binding switch region of the protein closely approximates that of wild-type Rab7 and is therefore not predicted to alter effector binding.

Furthermore, the catalytic glutamine (Q67) and the position of the γ -phosphate group of GppNHp were not significantly altered, providing no structural basis to predict decreased intrinsic GTPase activity (Fig. 2.1D, Supplementary Fig. S2.2 for an omit map of the nucleotide binding pocket). However, L129F substitution enlarges the hydrophobic group that lies adjacent to the guanine ring of GTP and leads to steric hindrance and subtle

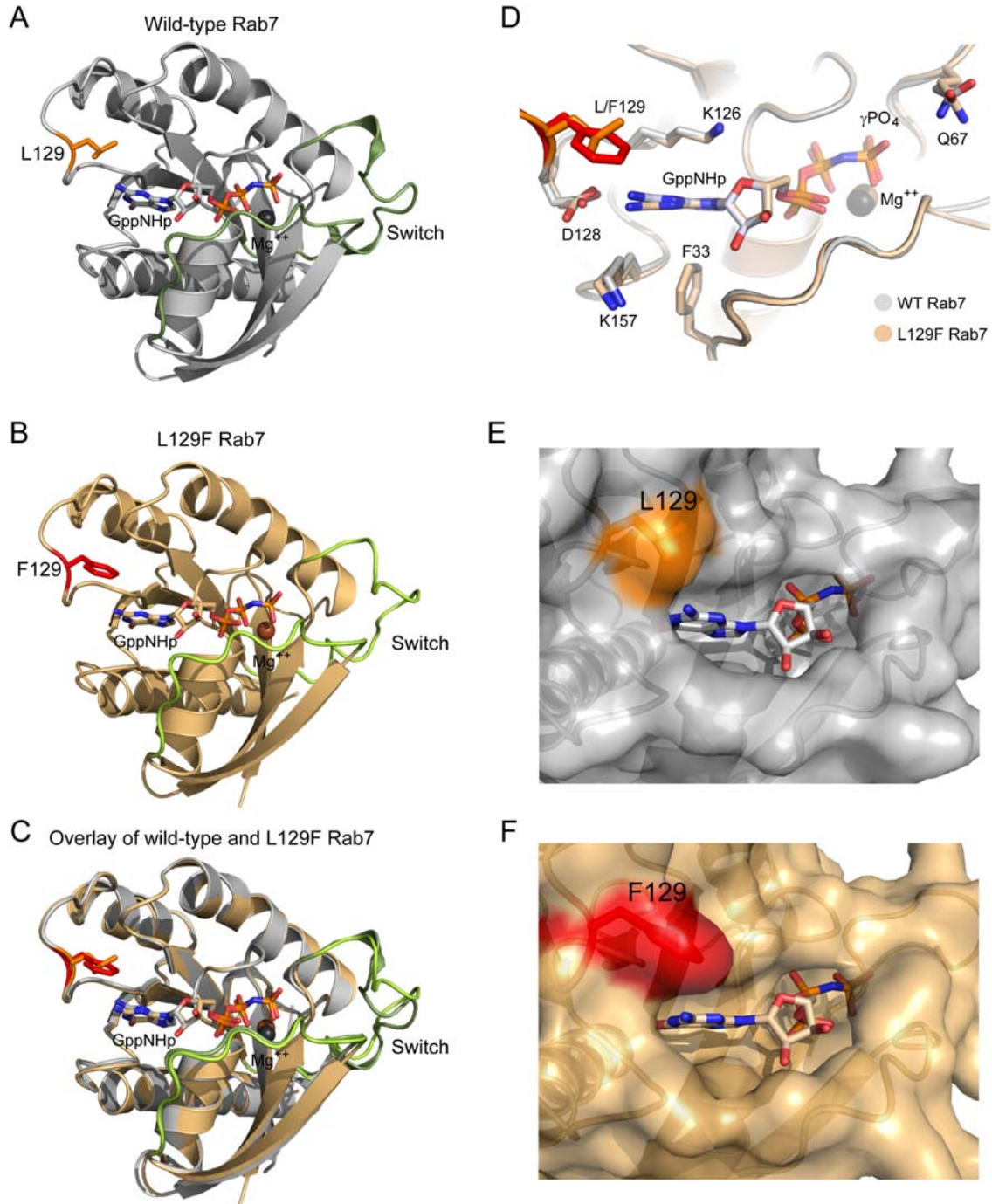


Figure 2.1. Structural insights into the disease-causing Rab7 L129F mutant. (A) Structure of wild-type Rab7 bound to the non-hydrolyzable GTP analog GppNHp (PDB 1VG8) (Rak et al., 2004). Switch regions are shown in dark green, L129 in orange, and Mg^{++} in black. (B) Structure of Rab7 L129F. Switch regions are shown in light green, F129 in red, and Mg^{++} in dark brown. (C) Overlay of wild-type and L129F Rab7 demonstrates that the F129 mutation does not alter the overall structure of the protein.

Note the normal conformation of the switch regions in the L129F mutant. **(D)** Close-up, overlaid views of the binding pockets of wild-type (grey) and the F129 mutant (brown). The positions of the γ -phosphate group of GTP and the catalytic residue Q67 are unaltered by the F129 mutation. Note the shift of the guanine ring of GppNHp in F129 and the displacement of the K157 and D128 residues. These changes suggest alterations in nucleotide binding affinity. **(E)** Detailed surface representation of the wild-type guanine nucleotide binding pocket showing GppNHp in ball and stick representation and L129 in orange. **(F)** Detailed surface representation of the F129 guanine nucleotide binding pocket showing GppNHp in ball and stick representation and F129 in red. Note the slight change in position of the guanine ring of the nucleotide and the altered conformation of the opening to the binding pocket.

repositioning (~ 0.6 Å) of the guanine ring away from F129 (Fig. 2.1D-F, Supplementary Fig. S2.3 for stereo views). This also slightly modifies the position of the invariant D128 and K157 residues that are directly involved in nucleotide binding (Fig. 2.1D). Of particular note is the repositioning of the carboxylate group of D128, which in the wild-type Rab7 makes pseudo Watson-Crick pairing interactions with the guanine base of the nucleotide. In L129F this interaction appears to be partially altered leading to longer hydrogen bonds and in some cases (we have five molecules in the asymmetric unit and therefore five independent observations) complete disruption of one of the two hydrogen bonds. We predicted that these changes would alter affinity for guanine nucleotides and affect the rates of dissociation for GTP and/or GDP. Interestingly, K157, which is also directly involved in nucleotide binding and is shifted in the L129F mutant structure, is mutated to asparagine in a patient with CMT2B (Meggouh et al., 2006).

Mutant Rab7 has decreased nucleotide affinity, but no intrinsic GTPase defect

To determine how the steric hindrance imposed by the L129F mutation affects guanine nucleotide binding, we performed GTP and GDP dissociation assays using purified

recombinant wild-type and L129F Rab7. We also analyzed the V162M mutant to determine whether there are consistent biochemical alterations among different disease-causing Rab7 mutants. Recombinant Rab7 proteins were loaded with $^3\text{H-GTP}$ or $^3\text{H-GDP}$ and the dissociation of nucleotide was followed over time. We found that Rab7 mutants have an increased rate of GTP dissociation relative to wild-type (Fig. 2.2A), and an even more rapid rate of GDP dissociation with almost complete dissociation within 15 minutes (Fig. 2B). These results are consistent with previous work showing increased dissociation of guanine nucleotides in Rab7 disease mutants (Spinosa et al., 2008). In Rab7 mutants, approximately 70% of initially-bound GTP dissociated over the course of 60 minutes.

While Rab7 disease mutants were previously reported to have nearly complete loss of GTPase activity (Spinosa et al., 2008), we found no structural basis for altered GTP hydrolysis in the L129F mutant. To account for this discrepancy, we hypothesized that reduced hydrolysis might reflect increased rates of GTP dissociation rather than an intrinsic catalytic defect. To test this idea, we first performed GTPase assays using purified recombinant Rab7 as previously described (Spinosa et al., 2008). When Rab7 was loaded with $^{32}\text{P-GTP}$ and hydrolysis was initiated in the presence of excess unlabeled GTP, we saw a marked decrease in GTP hydrolysis in the L129F mutant that was similar to the Q67L mutant (which contains a targeted disruption of the catalytic residue; Fig. 2.2C-D, left). However, this assay specifically measures the rate of GTP hydrolysis *per GTP binding event* since re-association of $^{32}\text{P-GTP}$ is effectively precluded by the excess unlabeled GTP. We predicted that if we performed the assay with excess $^{32}\text{P-GTP}$ and no unlabeled GTP, we could counteract the effect of decreased nucleotide affinity by

allowing for dissociation and re-association of radiolabeled GTP. Indeed, we found that the apparent GTPase defect in the L129F mutant could be partially rescued by omitting excess unlabeled GTP from the reaction, whereas this modification had no effect on the Q67L mutant (Fig. 2.2C, right and Fig. 2.2D). Furthermore, increasing the concentration of ^{32}P -GTP further restored catalytic activity (Fig. 2.2E), indicating that dissociation and re-association of GTP happens rapidly in disease mutants and that catalytic activity of L129F Rab7 approaches that of wild-type Rab7. Thus, when GTP is in constant supply (as is the case *in vivo*), catalytic activity in disease mutants is not significantly impaired, and decreased GTP hydrolysis cannot account for the defects seen in mutant Rab7.

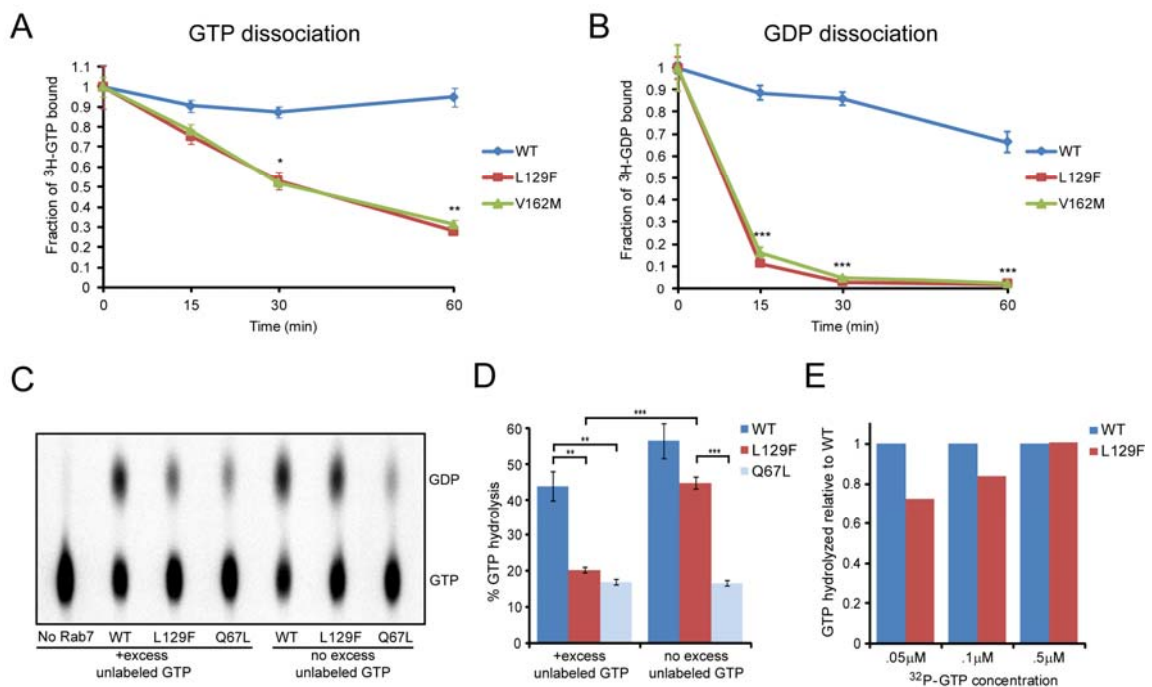


Figure 2.2. Rab7 disease-causing mutants have increased guanine nucleotide dissociation, but nearly normal GTPase activity. (A-B) GTP (A) and GDP (B) dissociation rates of recombinant Rab7 proteins. Rab7 mutants were loaded with ^3H -GTP or ^3H -GDP, then washed and incubated with excess unlabeled GTP or GDP at 37°C for 0, 15, 30, or 60 minutes. The remaining bound ^3H -GTP or ^3H -GDP was then eluted and quantified by scintillation counting. (C) Representative GTPase assay of wild-type, L129F, and Q67L Rab7. His-MBP-Rab7 proteins were loaded with $0.1 \mu\text{M}$ ^{32}P -GTP on

ice, then moved to 37°C for 2 hour to allow for hydrolysis. Nucleotides were eluted and separated by thin layer chromatography. GTPase assays performed with excess unlabeled GTP during hydrolysis (left) reveal a marked reduction in hydrolysis in the L129F mutant. However, assays performed without excess unlabeled GTP during hydrolysis (right) demonstrate that catalytic activity in the L129F mutant is restored by a constant supply of ³²P-GTP. Hydrolysis is virtually undetectable when no Rab7 is added to the reaction (left). **(D)** Quantification of GTPase assays demonstrates nearly complete restoration of catalytic activity in the L129F mutant when ³²P-GTP is provided in constant supply. As expected, the GTPase-deficient Q67L mutant shows a marked hydrolysis defect in both conditions. **(E)** GTPase assays were performed with varying concentrations of ³²P-GTP, and without excess unlabeled GTP. Increasing the GTP concentration restores the catalytic activity of the L129F mutant. This suggests that there is no intrinsic GTPase defect in disease mutants when GTP is in constant supply. Values plotted for A-D represent the average of at least three independent experiments. Error bars represent standard error of the mean. (*p<0.05, **p<0.01, ***p<0.001)

Mutant Rab7 undergoes GEF-independent nucleotide exchange and excessive activation

Normally, GDP is tightly bound by Rab GTPases, and the low intrinsic rate of GDP dissociation makes GDP release the rate-limiting step of nucleotide exchange and Rab activation. GEF proteins have evolved to facilitate GDP dissociation and the subsequent GTP loading of Rab proteins. Given the rapid rate of GDP dissociation in the Rab7 disease mutants, we hypothesized that nucleotide exchange might be misregulated and occur independent of GEF activity. To test this hypothesis, we interrogated GTP exchange rates using purified, recombinant Rab7 proteins in the absence of any GEF activity. First, we determined that Rab7 wild-type and disease mutants bound roughly the same amount of GTP following stripping of endogenous bound nucleotide (Fig. 2.3A). Next, we tested GTP exchange by stripping endogenous nucleotide, then pre-loading the Rab7 proteins with GDP before incubation with ³H-GTP. In this assay, ³H-GTP binding requires dissociation of the pre-loaded GDP and thus represents the rate of GTP

exchange. The amount of ^3H -GTP bound was compared to the maximum amount that could be bound without GDP pre-incubation. As expected, wild-type Rab7 showed a slow rate of GTP exchange in the absence of GEF activity (only 10-20% of maximal binding). However, disease-causing Rab7 mutants underwent GTP exchange significantly faster, achieving nearly 60% of maximal binding over 30 minutes (Fig. 2.3B). This suggests that GTP exchange in Rab7 mutants can occur in an unregulated, GEF-independent manner. To determine if GTP exchange is also misregulated in a cellular context, we tested the ability of immunopurified Rab7 complexes to undergo guanine nucleotide exchange. FLAG-Rab7 was immunopurified from HEK293T cell lysates and then incubated with ^3H -GTP. As in the cell-free system, Rab7 mutants were able to undergo nucleotide exchange more readily than wild-type Rab7 despite equal immunoprecipitation of Rab7 in each condition (Fig. 2.3C). These results indicate that the structural changes imposed by the L129F and V162M mutations lead to misregulation of GTP exchange and inappropriate activation of Rab7 mutants.

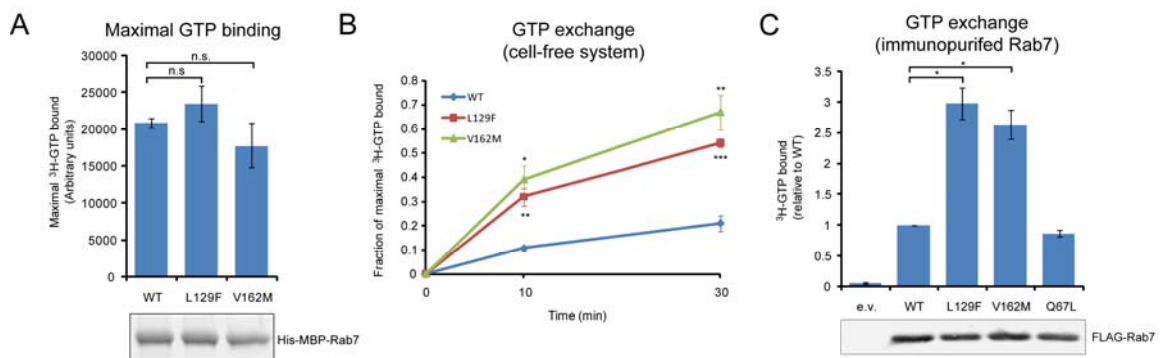


Figure 2.3. Rab7 disease mutants lead to GEF-independent nucleotide exchange. (A)

Top: Purified His-MBP-Rab7 proteins were stripped of endogenous nucleotide and then incubated with ^3H -GTP for 30 minutes at 37°C to demonstrate equivalent maximal GTP binding. Bottom: Loading control shows equivalent amount of Rab7 protein in each condition. (B) Quantification of GTP exchange of Rab7 proteins. His-MBP-Rab7 proteins were stripped, loaded with GDP, and then incubated with ^3H -GTP for 10 or 30

minutes at 37°C. Disease mutants exchanged GTP for GDP much faster than wild-type Rab7 (*p<0.05, **p<0.01, ***p<0.005). (C) Top: GTP exchange assay using immunopurified FLAG-Rab7. FLAG-Rab7 proteins were immunopurified from HEK293T cells followed by incubation with ³H-GTP for 10 minutes at 37°C. Rab7 disease mutants undergo greater nucleotide exchange compared to wild-type (*p<0.005). Bottom: Control immunoprecipitation performed in parallel demonstrates equal immunoprecipitation of FLAG-Rab7 constructs.

Augmented GTP exchange in the disease mutants would be predicted to shift the ratio of the GTP and GDP-bound fractions of Rab7 in cells. To test this, we performed pulldown assays using an immobilized Rab7 binding region of the Rab7 effector Rab-interacting lysosomal protein (RILP) and lysates from HEK293T cells expressing GFP-Rab7 (Romero Rosales et al., 2009). Since RILP specifically binds GTP-bound Rab7, the amount of Rab7 associated with RILP in this assay represents the GTP-bound fraction. GST-RILP showed increased interaction with the predominantly GTP-bound, GTPase deficient Q67L mutant and no interaction with the GTP-binding deficient T22N mutant, indicating that this experiment accurately reflects changes in the active pool of Rab7 (Fig. 2.4A). The amount of Rab7 disease-causing mutants pulled down by GST-RILP was significantly increased compared to wild-type Rab7 (Fig. 2.4A-B). This finding indicates that accelerated GTP exchange in disease mutants leads to an increase in the active, GTP-bound fraction of Rab7.

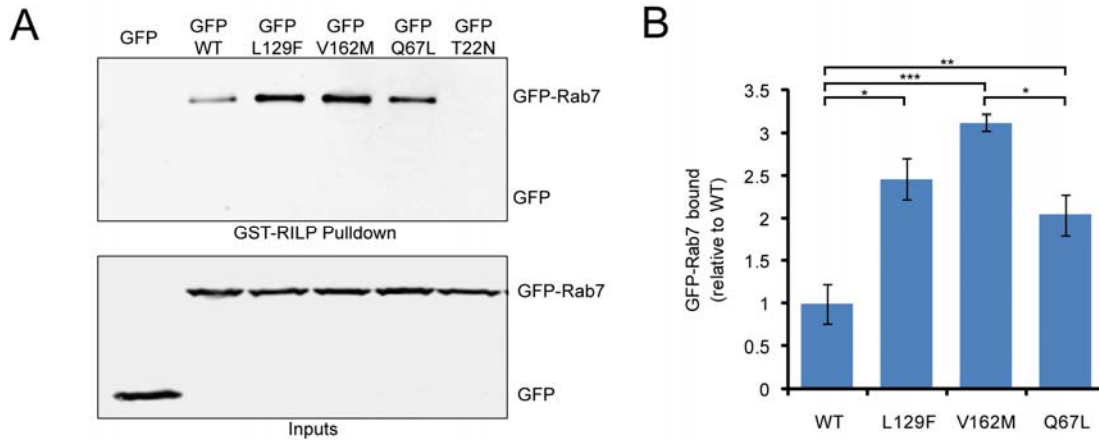


Figure 2.4. Rab7 disease mutants lead to an increase in the GTP-bound, active fraction. (A) Top: Representative immunoblot of GST-RILP pull-down from HEK293T lysates containing GFP-Rab7. GST-RILP pulls down more Rab7 disease mutant protein indicating an increase in the GTP-bound form. As expected, there is increased binding of Q67L and no binding of T22N Rab7. Bottom: Immunoblot of 2% of the pull-down input demonstrates equivalent expression of GFP-Rab7 in each condition. (B) Quantification of GST-RILP pull-down replicates (* $p < 0.02$, ** $p < 0.05$, *** $p < 0.002$). All values plotted represent the average of three independent experiments. Error bars represent standard error of the mean. e.v. = empty vector.

Disease-causing mutations cause quantitative changes in Rab7 interactions

To more broadly address the impact of disease-causing Rab7 mutations on interaction with binding partners, we used an unbiased proteomics approach to examine the protein-protein interactions in wild-type and mutant Rab7. Rab7 effectors specifically recognize the switch regions when Rab GTPases are in the GTP-bound conformation. Based on the crystal structure, we predicted that the L129F Rab7 mutant would interact normally with Rab7 effectors. However, since Rab7 mutations increase the fraction of Rab7 in the active conformation and cause misregulation of the Rab7 activity cycle, we predicted that there may be quantitative differences in the type of Rab7 complexes that are formed. A number of Rab7-interacting proteins have been described, including RILP, Oxysterol binding protein-related protein 1L (ORP1L), Rabring7, Rab escort protein-1 (REP-1),

Rab GDI, the Vps34 subunit of PI3 kinase, and members of the retromer complex (Regazzi et al., 1992; Andres et al., 1993; Cantalupo et al., 2001; Mizuno et al., 2003; Stein et al., 2003; Johansson et al., 2005; Rojas et al., 2008).

To examine Rab7 interactors, FLAG-Rab7 complexes were immunopurified from HEK293T cell lysates, separated by SDS-PAGE, and interacting proteins were then identified by mass spectrometry. The profiles of proteins identified in wild-type and mutant Rab7 were qualitatively identical suggesting that Rab7 mutants bind to the same complement of interactors as wild-type Rab7 (Fig. 2.5A-B, Supplementary Fig. S2.4). We identified several putative novel Rab7 interacting proteins as well as previously known Rab7 interactors (Table 2.2). To verify the specificity of our mass spectrometry protein identification, interactions with the known effectors RILP and GDI2 and the novel interactors VapB, SPG21, PHB, and stomatin-like 2 were confirmed by coimmunoprecipitation followed by Western blotting (Supplementary Fig. S2.5).

Although the complement of effectors is largely unchanged by disease-causing mutations, we were able to detect quantitative differences in the amount of specific effectors coimmunoprecipitated with wild-type and mutant Rab7 (Fig. 2.5B and C). Specifically, Rab7 disease mutants L129F and V162M and the constitutively active mutant Q67L showed increased interaction with Vps13C and ORP1L, whereas only the disease mutants showed increased interaction with clathrin heavy chain, and all constructs interacted equally with REP-1 (Fig. 2.5C). These results suggest that the misregulation of the Rab7 activity cycle in disease mutants leads to augmentation of

specific effector interactions. Furthermore, the increased interaction with Vps13C and the GTP-dependent interactor ORP1L seen in disease mutants and in the Q67L mutant provides additional support for an increase in the active fraction of mutant Rab7.

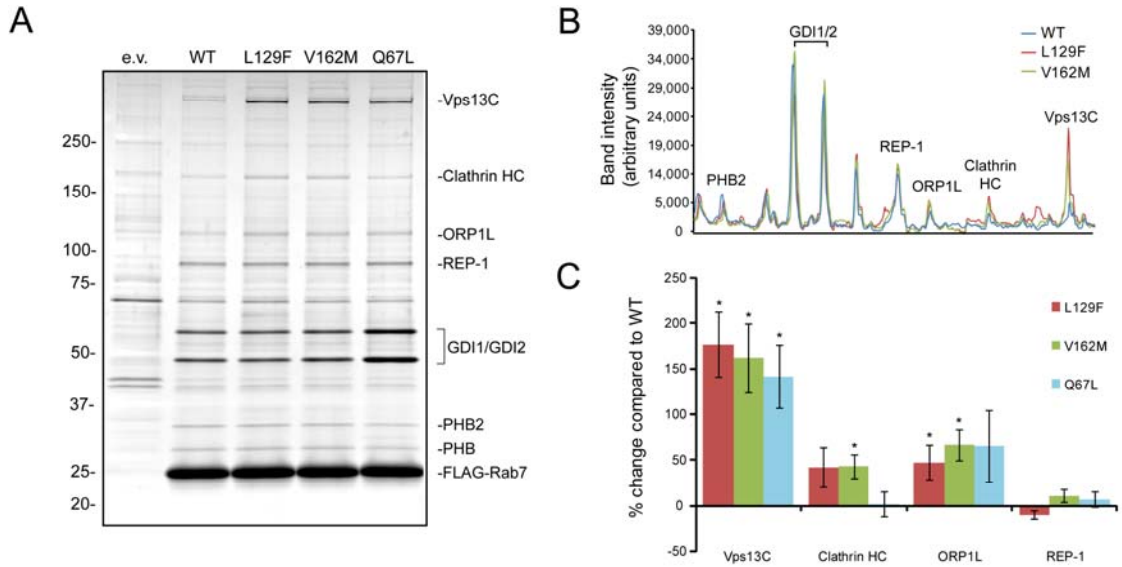


Figure 2.5. Rab7 disease mutants demonstrate quantitative changes in effector interactions. (A) FLAG-Rab7 was immunoprecipitated from HEK293T cells followed by SDS-PAGE and SYPRO Ruby protein stain. Interacting proteins were identified by LCMS/MS. (B) Rab7 wild-type and disease mutants have roughly similar band intensity profiles, although a subset of protein interactors show differential binding (compare intensity profiles for Vps13C and ORP1L). (C) Quantification of FLAG-Rab7 coimmunoprecipitation replicates demonstrates increased interaction of Rab7 disease mutants with Vps13C, clathrin heavy chain, and ORP1L, and normal interaction with REP-1 (* $p < 0.05$). Values plotted represent the average of five or six independent experiments. Error bars represent standard error of the mean. e.v. = empty vector

Rab7 disease mutant localization is distinct from constitutively active Rab7

We next assessed the consequences of the structural and biochemical alterations in mutant Rab7 on membrane targeting and exchange dynamics. To determine if disease mutations affect Rab7 subcellular localization, we analyzed the distribution of GFP-tagged Rab7 in HeLa cells. Wild-type Rab7 reversibly associates with the cytosolic face

of late endosomes, lysosomes, and autophagosomes and shows a diffuse vesicular pattern that largely overlaps with the late-endosomal/lysosomal marker LAMP2 (Fig. 2.6A, top) and the acidotropic dye LysoTracker Red (data not shown) as expected (Bucci et al., 2000). The dominant negative T22N mutant has a diffuse, reticular localization and leads to dispersal and altered morphology of late endosomes and lysosomes (Fig. 2.6A, bottom). In contrast, the constitutively active Q67L mutant Rab7 colocalizes with LAMP2, but leads to prominent accumulation of enlarged vesicles that cluster adjacent to the nucleus (Fig. 2.6A, middle). Surprisingly, despite evidence of unregulated activation, Rab7 disease mutants have normal subcellular localization and associate normally with LAMP2 (Fig. 2.6B) and LysoTracker Red (data not shown). Quantification of the cellular phenotypes verified our observation that disease mutants are similar to wild-type Rab7 and distinct from the Q67L mutant (Fig. 2.6C, see Supplementary Fig. S2.6 for scoring examples). We also demonstrated that Rab7 disease mutations do not impair targeting to autophagosomes or flux through the autophagic pathway (Supplementary Fig. S2.7). Thus, even though Rab7 disease mutants show a marked increase in the active fraction, the cellular phenotype of disease mutants is clearly distinct from the Q67L mutant (Fig. 2.6A-C), providing further evidence that a GTPase defect alone cannot account for the phenotype in Rab7 disease mutants.

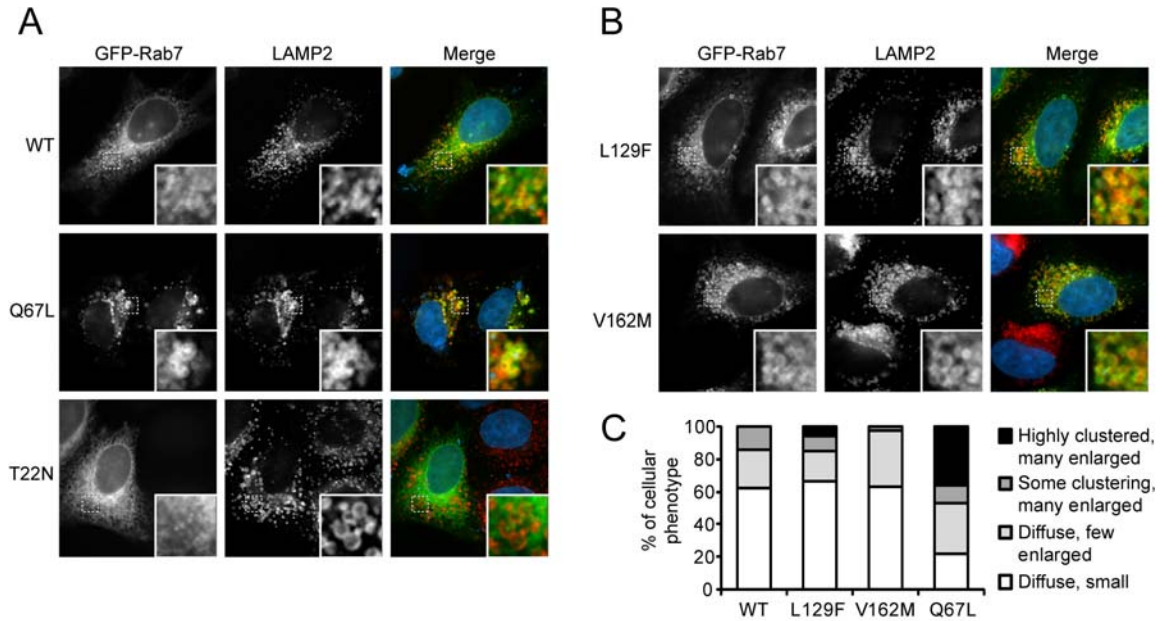


Figure 2.6. Rab7 disease mutants have grossly normal subcellular localization. (A-B) HeLa cells transfected with GFP-Rab7 constructs were fixed and stained with anti-LAMP2 antibody. Wild-type Rab7 and disease mutants colocalize with LAMP2-positive vesicles and do not cause any alteration in their morphology or localization. In contrast, constitutively active Q67L Rab7 causes clustering of LAMP2-positive vesicles, while dominant negative T22N Rab7 leads to their dispersal and enlargement. **(C)** Quantification of vesicular phenotypes in GFP-Rab7-expressing cells demonstrates that disease mutants are similar to wild-type and distinct from Q67L Rab7. Approximately 40 cells were blindly scored for each Rab7 construct (see Supplementary Materials Fig. S6 for scoring examples).

Mutant Rab7 is abnormally retained on vesicular membranes

Rab GTPases switch between the GTP-bound state in which they are active and membrane-associated and the GDP-bound state in which they are inactive and cytosolic.

Our results suggest increased activation of Rab7 disease mutants which would be predicted to correlate with alterations in the activity cycle. To assess the net impact of Rab7 mutations on membrane cycling, we used dynamic live-cell imaging to characterize wild-type and mutant GFP-Rab7 in living cells. Time-lapse images demonstrate that disease-causing mutants of Rab7 associate with vesicular structures that are highly motile

and undergo multiple fusion and fission events similar to wild-type (Supplementary Movies S2.1-4). We next used dynamic live-cell imaging and a fluorescence recovery after photobleaching (FRAP) approach to examine how disease-causing mutations of Rab7 affect membrane cycling activity. HeLa cells were transfected with GFP-Rab7 and regions of cytosol containing GFP-Rab7 positive vesicles were bleached with a high intensity laser. Since recovery of fluorescence requires that the bleached GFP-Rab7 molecules dissociate from the membrane to allow insertion of unbleached Rab7 from the surrounding cytosol, the rate of fluorescence recovery represents flux through the Rab7 activity cycle (Jordens et al., 2001). Rab7 disease mutants L129F and V162M showed a small but significant decrease in the rate of fluorescence recovery compared to wild-type, whereas the constitutively active Q67L mutant showed a nearly complete loss of fluorescence recovery due to the inability to hydrolyze GTP (Fig. 2.7A-B). These results indicate that disease-causing mutations in Rab7 cause a subtle decrease in the rate of membrane exchange.

Decreased FRAP could result from decreased membrane extraction or from impaired recruitment of unbleached Rab7 onto target membranes. To distinguish between these possibilities, we developed a complementary approach utilizing a photoactivatable GFP variant (PA-GFP) (Patterson and Lippincott-Schwartz, 2002) fused to Rab7. Since PA-GFP fluorescence is low until activation by brief high intensity laser stimulation, this construct permits selective activation of small regions of cytosol containing Rab7-positive vesicles. In activated regions of the cell, a majority of the activated Rab7 is

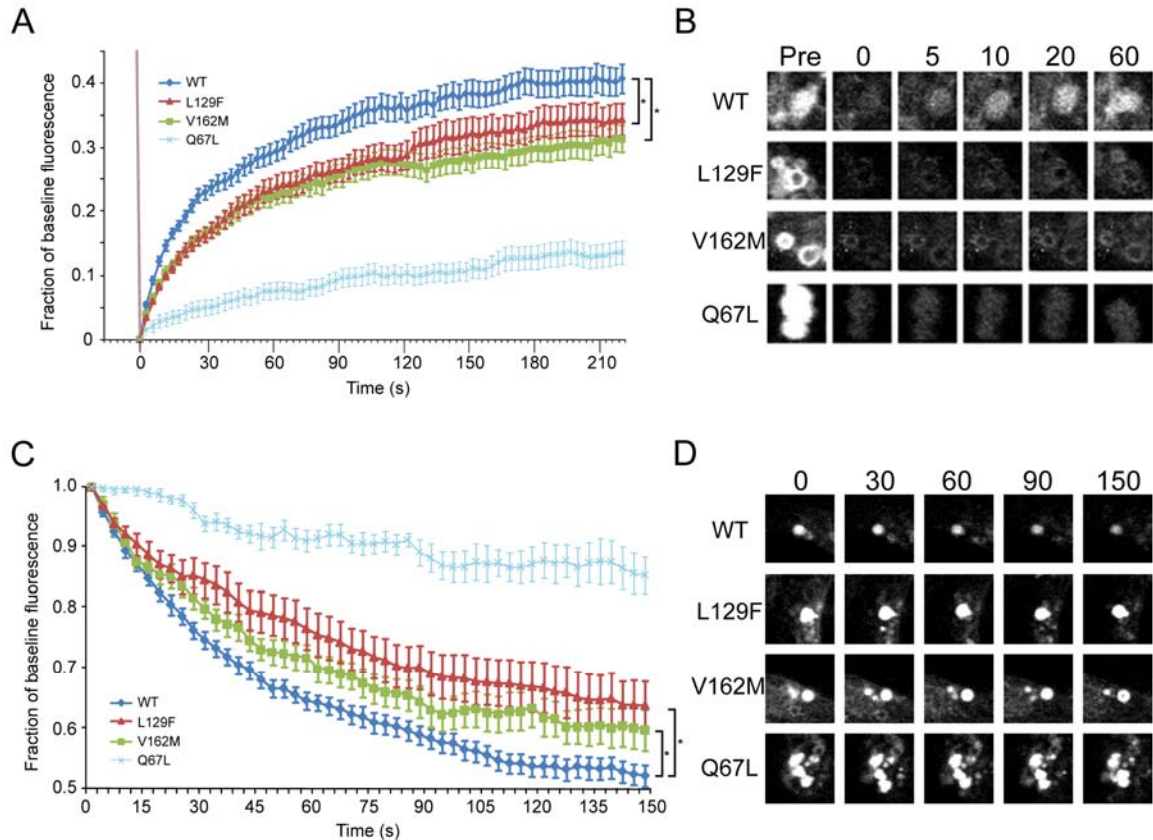


Figure 2.7. Rab7 disease mutants have decreased membrane cycling. (A) FRAP of GFP-Rab7-positive vesicles in HeLa cells demonstrates that Rab7 disease mutants have a decreased rate of fluorescence recovery compared to wild-type. As expected, constitutively active Rab7 (Q67L) shows minimal fluorescence recovery due to the inability to hydrolyze GTP. (B) Representative time lapse images of GFP-Rab7 vesicles before and after photobleaching. (C) FLAP of photoactivatable-GFP (PA-GFP)-Rab7-positive vesicles demonstrates that Rab7 disease mutants have a decreased rate of fluorescence loss compared to wild-type. As expected, constitutively active Rab7 (Q67L) shows minimal fluorescence loss due to the inability to hydrolyze GTP. (D) Representative time lapse images of PA-GFP-Rab7 vesicles after photoactivation. Values indicate average fluorescence for at least 20 ROIs in at least 10 cells for each condition (* $p=1 \times 10^{-15}$). Error bars represent standard error of the mean.

membrane-bound and thus the fluorescence loss after photoactivation (FLAP)

specifically measures the rate of extraction of Rab7 from its target vesicle membranes.

Rab7 disease mutants L129F and V162M showed a decreased rate of fluorescence loss compared to wild-type Rab7, suggesting delayed membrane extraction (Fig. 2.7C-D). As

expected, constitutively active Rab7 (Q67L) showed a markedly decreased rate of fluorescence loss due to the inability to hydrolyze GTP. Taken together, the FRAP and FLAP data suggest that Rab7 disease-causing mutants are impaired in membrane exchange specifically due to slowed extraction from their target membranes. Notably, the decreased rate of FRAP and FLAP in disease mutants was much less pronounced than in the Q67L mutant (Fig. 2.7A-D). Thus, despite a profound increase in the active fraction similar to that seen in the Q67L mutant, the net impact of disease-causing mutations *in vivo* is surprisingly subtle.

GTP dissociation inactivates mutant Rab7

Our data demonstrate that despite accelerated nucleotide exchange and a marked increase in the active fraction similar to the Q67L mutant (Fig. 2.3-2.4), Rab7 disease mutants have normal subcellular localization and only subtle defects in membrane extraction (Fig. 2.7). To reconcile these observations, we hypothesized that the excessive activation in mutant Rab7 is counterbalanced by unregulated, hydrolysis-independent termination of activity mediated by accelerated GTP dissociation (Fig. 2.2A). To test this, we generated compound mutants containing both the Q67L mutation (which inactivates the catalytic site) and a disease-causing mutation (either L129F or V162M). We predicted that conversion from GTP-bound, active Rab7 to inactive Rab7 through GTP dissociation would rescue the function of these catalytically dead mutants. While transfected GFP-Rab7 Q67L showed vesicular clustering in the majority of cells, the phenotype was largely reversed by introducing the disease-causing mutations to the Q67L background (Fig. 2.8A-B, See Supplementary Fig. S2.6 for scoring examples). To further demonstrate

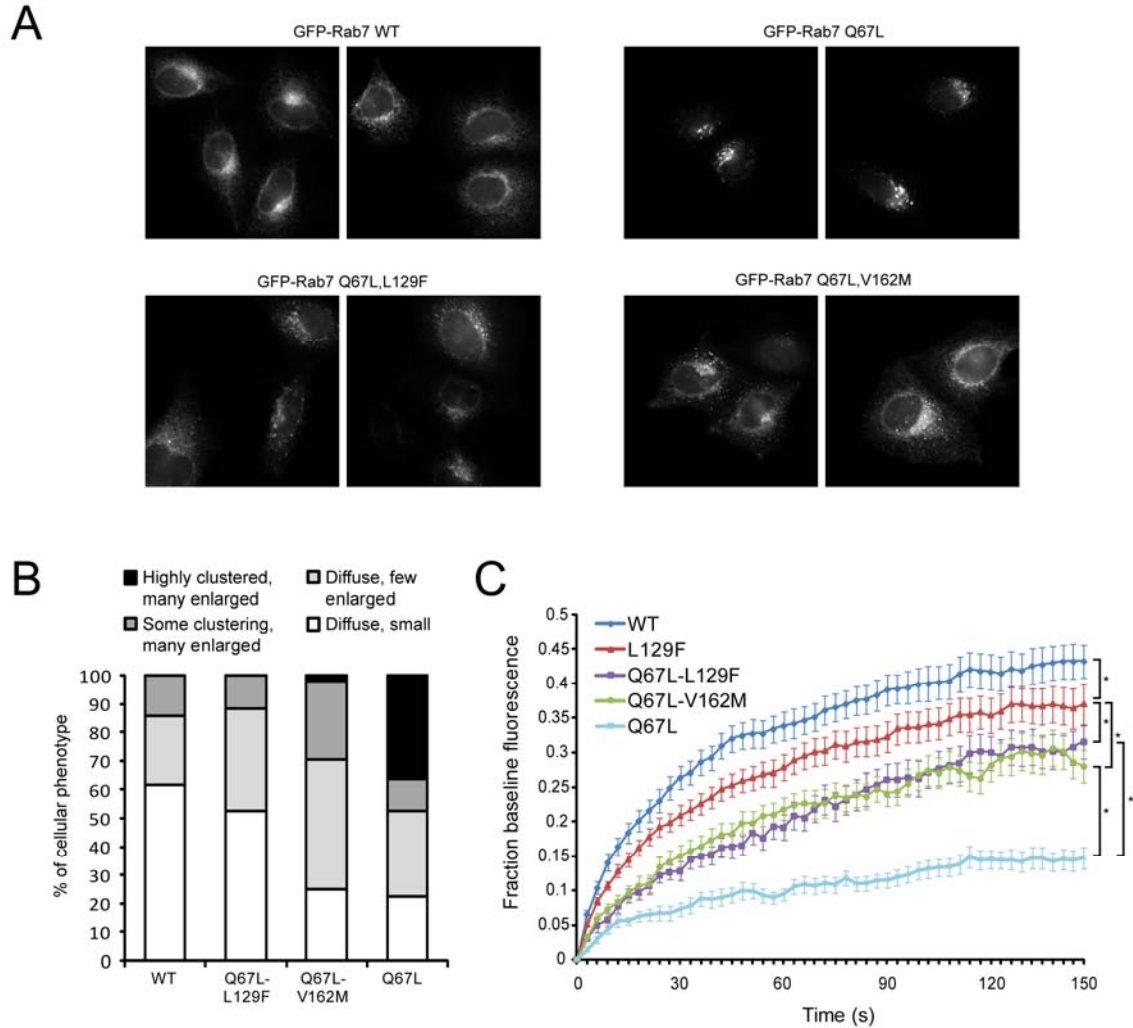


Figure 2.8. Rab7 disease mutants lead to GTPase-independent membrane cycling. (A) HeLa cells transfected with GFP-Rab7 were fixed and imaged. Rab7 Q67L,L129F or Q67L,V162M compound mutants largely rescue the abnormal vesicular clustering seen in the GTPase-deficient Q67L mutant. (B) Quantification of vesicular phenotypes in GFP-Rab7-expressing cells. Approximately 40 cells were blindly scored for each Rab7 construct (see Supplementary Materials Fig. S6 for scoring examples). (C) Compound mutants rescue the FRAP defect seen in the constitutively active Q67L mutant. Rab7 Q67L shows minimal fluorescence loss due to the inability to hydrolyze GTP. Membrane release and fluorescence recovery is restored by combining the Q67L mutation with the L129F or V162M disease mutations. Values indicate average fluorescence for at least 30 ROIs in at least 15 cells for each condition ($*p < 1 \times 10^{-15}$). Error bars represent standard error of the mean.

reversal of the Q67L phenotype in compound mutants, we performed FRAP assays to follow the extraction of the compound mutants from membranes. We found that the Rab7 compound mutants largely rescued the FRAP defect seen in the Q67L mutant alone, suggesting that the Rab7 disease-causing mutations increase GTP dissociation and lead to GTPase-independent membrane cycling of Rab7 *in vivo* (Fig. 2.8C). These results further indicate that GTPase deficiency cannot account for the defects in disease mutants since these mutations are able to reverse the phenotype associated with a pure GTPase defect. Furthermore, these data demonstrate that disease mutants are not dependent on GTP hydrolysis for inactivation as is the case for nearly all Rab GTPases. Together with our GTP exchange assays, our results indicate that Rab7 mutations lead to misregulation of both activation of Rab7 by nucleotide exchange and inactivation of Rab7 by GTP dissociation. Therefore, GTP binding and membrane cycling of Rab7 mutants occur independent of the action of the normal regulatory controls that provide spatial and temporal specificity to Rab7 function.

Tables

Table 2.1: Data collection and refinement statistics

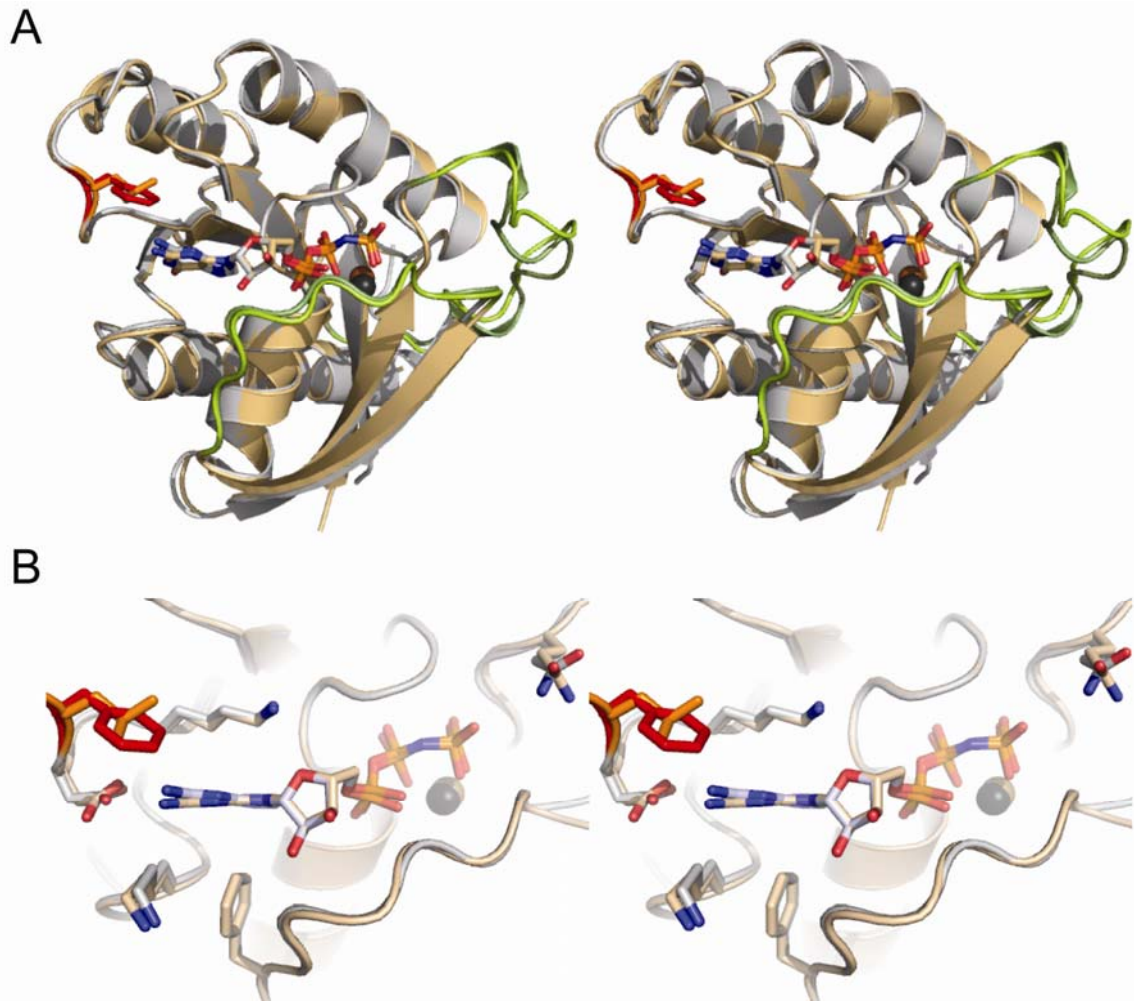
Data collection	
Space group	P1
Cell dimensions (a, b, c in Å)	35.6, 89.33, 89.38
Resolution (Å)	20-2.8 (2.9-2.8)*
Rsym or Rmerge	10.0 (41.7)
<i>I</i> / σ <i>I</i>	7.7 (1.7)
Completeness (%)	98.7 (98.2)
Redundancy	2 (2)
Refinement	
Resolution (Å)	20-2.8
No. Unique reflections	27713
<i>R</i> _{work} / <i>R</i> _{free}	25.5/27.1
No. atoms	
Protein	6925
Ligands	155
Ions	5
Water	45
R.m.s. deviations	
Bond lengths (Å)	0.011
Bond angles (°)	1.16
Ramachandran plot (%)	
Most favored	87.6
Allowed	10.9
Generously allowed	1.2
Disallowed	0.2

*Highest resolution shell shown in parentheses.

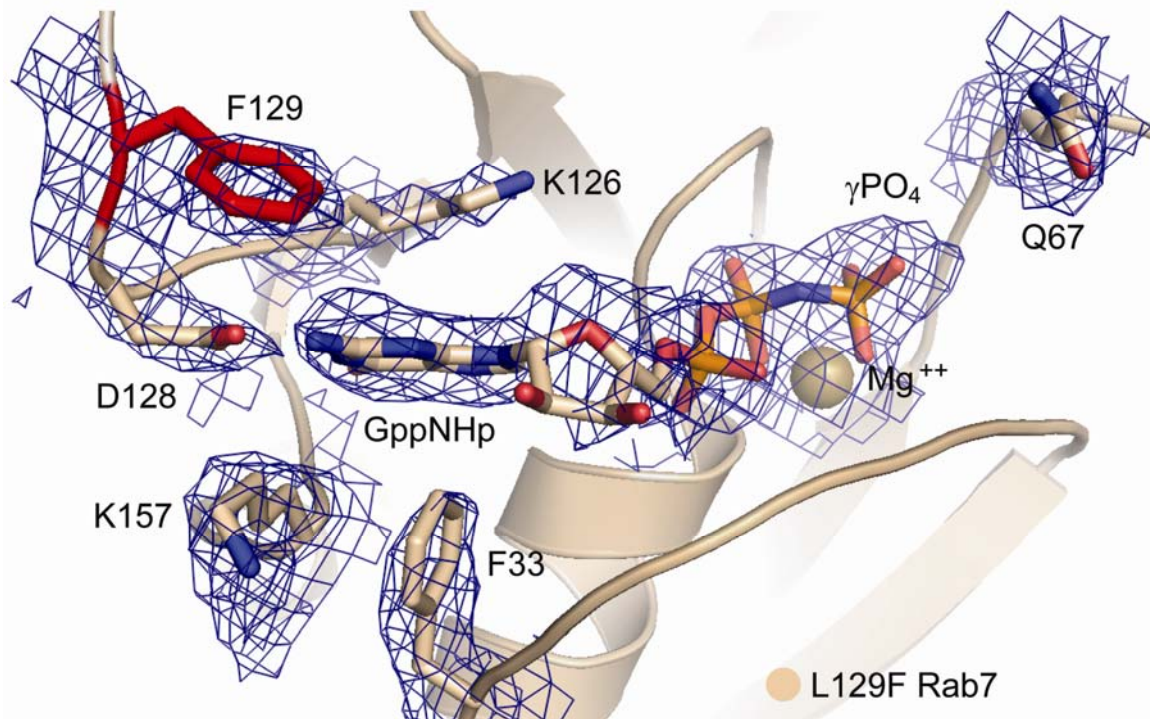
Table 2.2: Proteomics summary and statistics

Protein name	MW (Da)	Sequence count	Coverage (%)	Novelty
GDI2	51,088	370	76	
GDI1	51,177	255	70	
Prohibitin 2 (PHB2)	33,276	115	51	*
Prohibitin (PHB)	29,843	84	51	*
REP-1 (CHM)	74,740	77	39	
Vps13C	419,351	217	34	*
ORP1L	109,739	71	29	
VapB (ALS8)	27,365	6	25	*
Stomatin-like 2 (EPB72)	38,518	23	25	*
Clathrin HC	193,703	44	24	*
GNB2L1 (RACK1)	40,193	7	18	*
ATP6V0A1	96,487	10	13	*
Spastic paraplegia 21 (maspardin)	35,223	7	12	*
IMMT (Mitofilin)	83,669	10	9	*
RILP	44,375	3	8	
ANKFY1	128,489	4	4	*

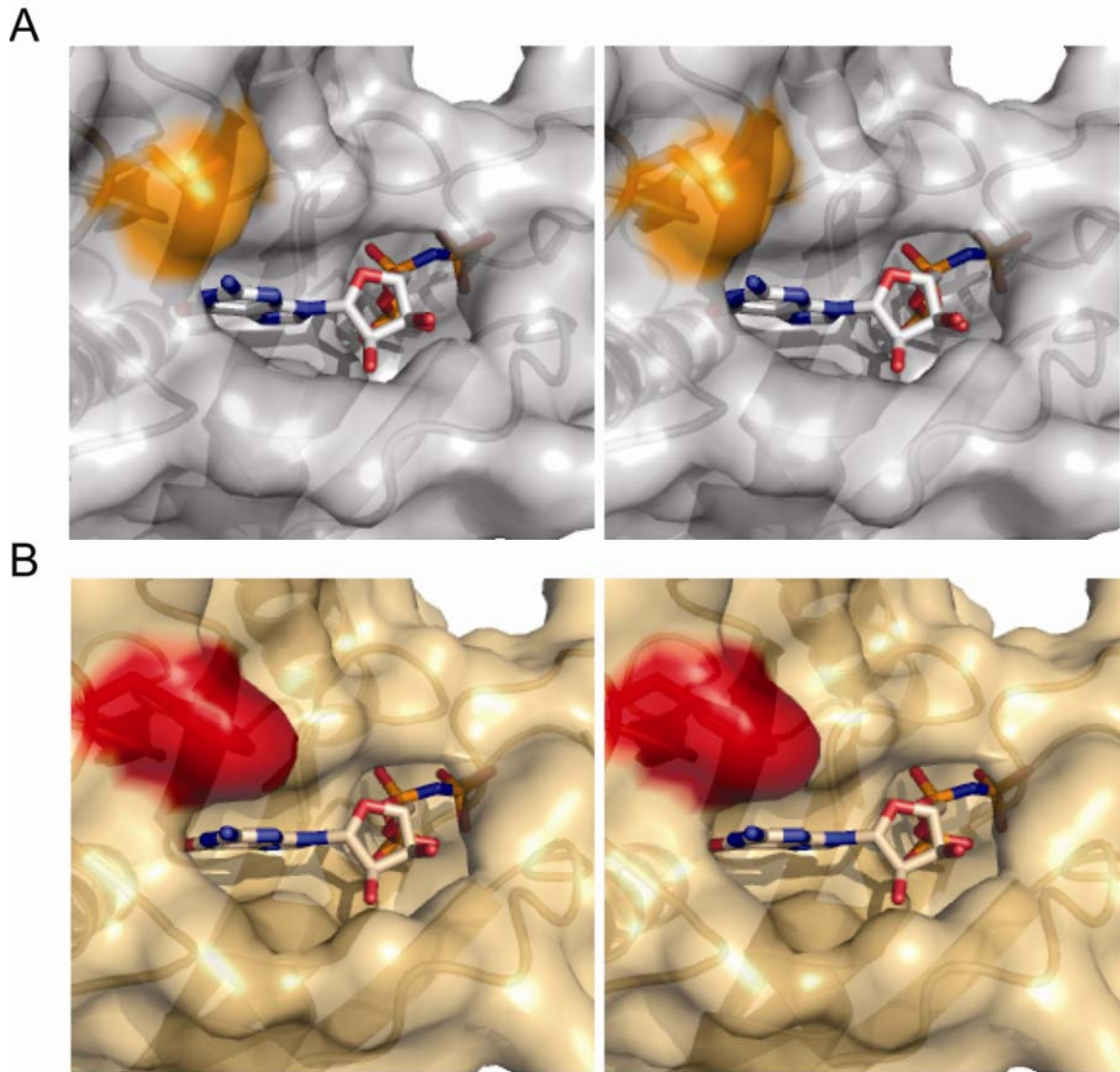
Supplementary data



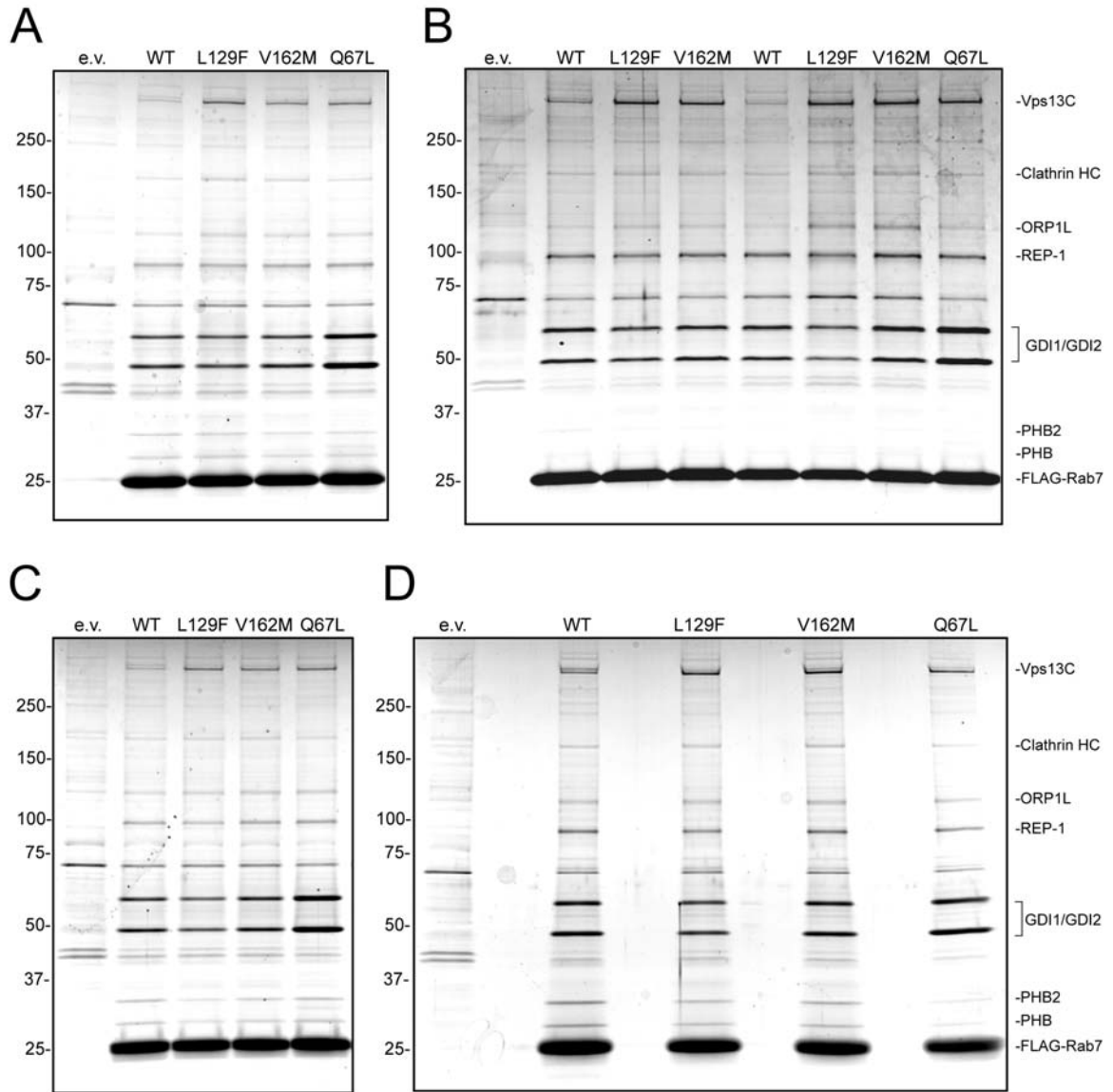
Supplementary Figure S2.1. Stereo views of wild-type and L129F Rab7. (A) Overlay of wild-type Rab7 (grey) and L129F Rab7 (brown) bound to the GTP analog GppNHp. **(B)** Overlay of wild-type (grey) and L129F Rab7 (brown) GTP binding pockets. See Figure 1D for amino acid side chain identities.



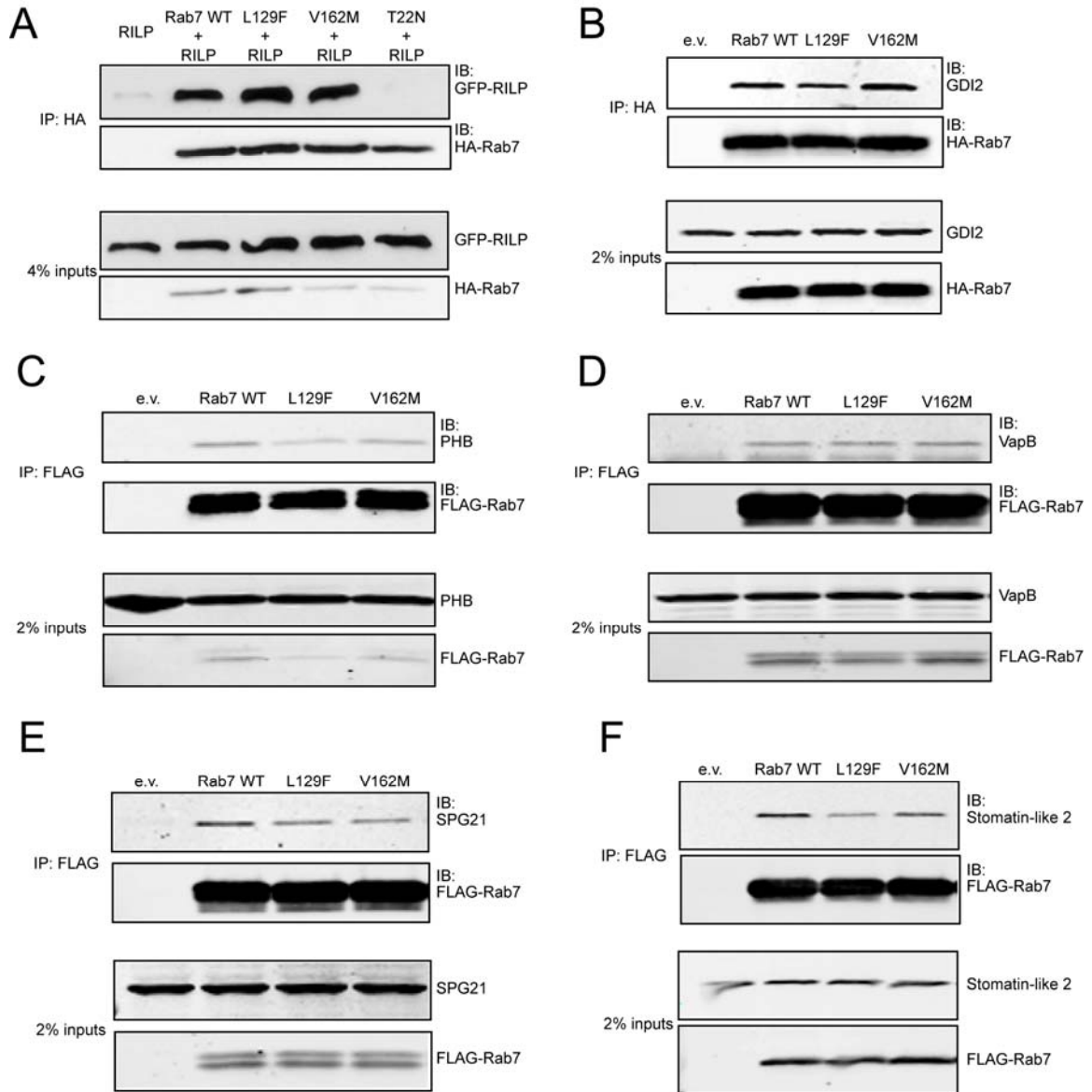
Supplementary Figure S2.2. L129F Rab7 omit map. Simulated annealed omit map of the nucleotide GppNHp and active site residues (stick) at 1.0 sigma contour level. F129 side chain is shown in red, and Mg⁺⁺ is shown in dark brown.



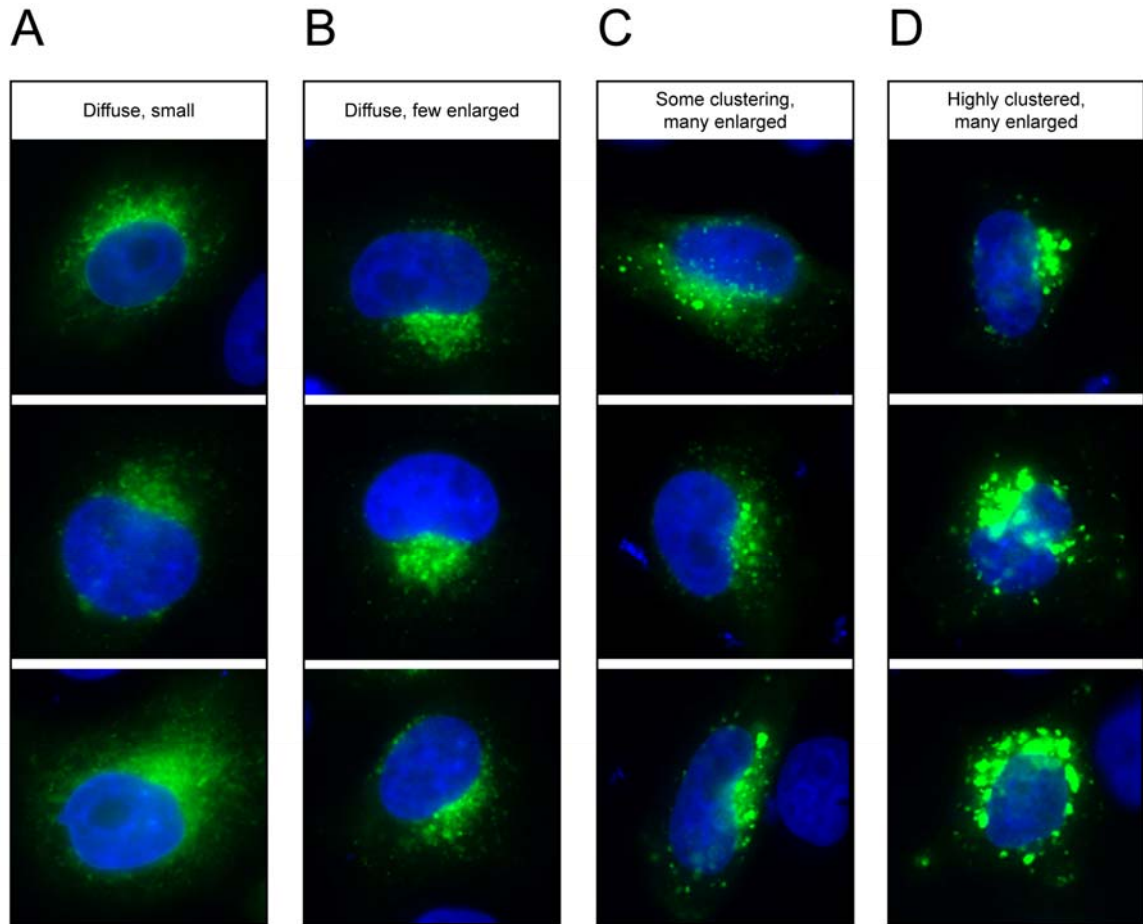
Supplementary Figure S2.3. Stereo views of the wild-type and L129F Rab7 GTP binding pocket. (A) Surface view of wild-type Rab7 nucleotide binding pocket. L129 is shown in orange. (B) Surface view of L129F Rab7 nucleotide binding pocket. F129 is shown in red.



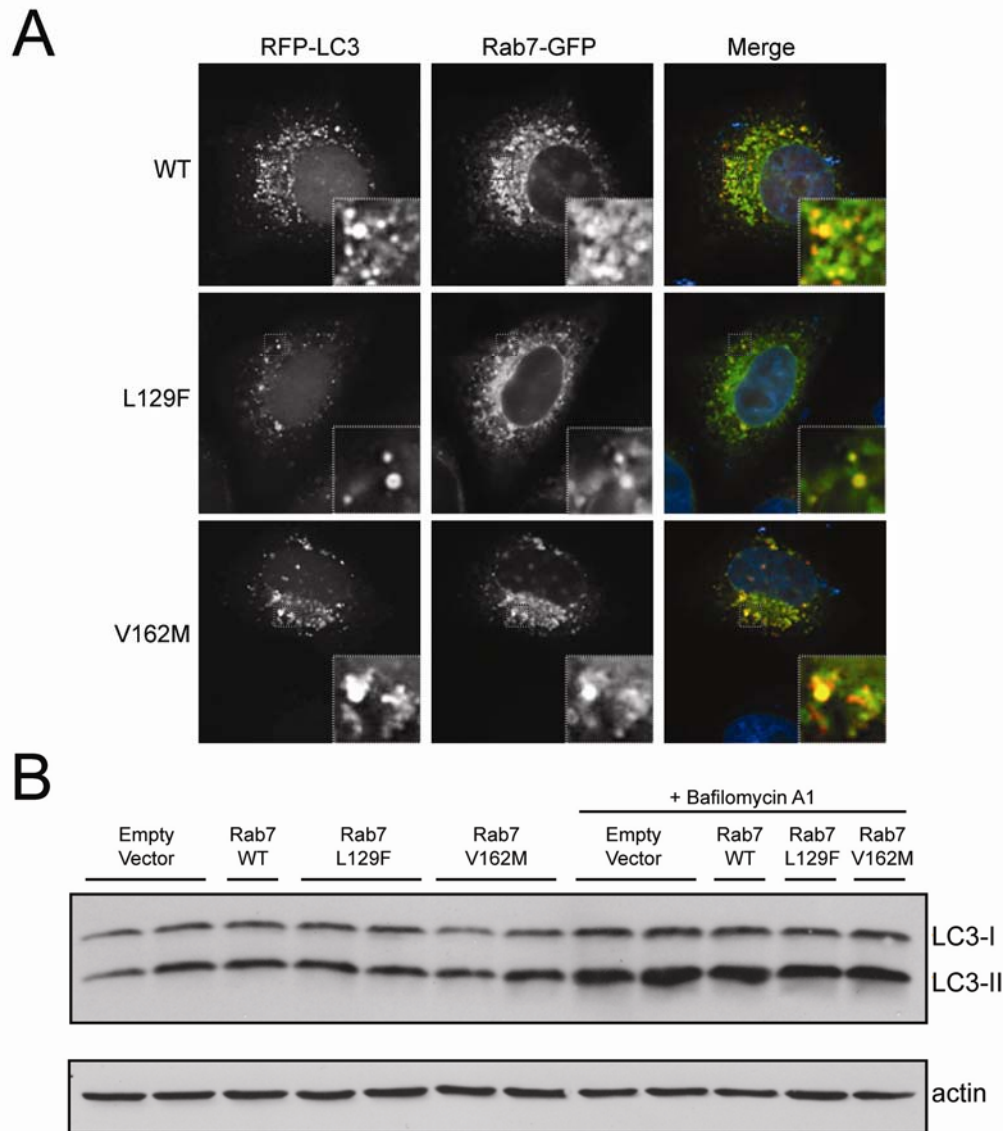
Supplementary Figure S2.4. Analysis of Rab7 interacting proteins. HEK293T cells transfected with FLAG-Rab7 were collected and lysed 48 hours post-transfection and immunoprecipitated with FLAG-agarose. Proteins were separated by SDS-PAGE and stained with SYPRO Ruby. (**A-D**) Five replicates of the experiment shown in Figure 4A. Protein identities were determined by LC-MS/MS as described in Supplementary Methods. e.v. = empty vector



Supplementary Figure S2.5. Verification of interaction with proteins identified by LC-MS/MS. HEK293T cells were transfected with epitope-tagged Rab7 (HA or FLAG) or cotransfected with HA-Rab7 and GFP-RILP. Cells were collected and lysed 48 hours post-transfection and immunoprecipitated with HA-agarose or FLAG-agarose. Rab7 wild-type and disease mutants interact normally with overexpressed GFP-RILP (**A**), endogenous GDI2 (**B**), and the novel interactors PHB (**C**), VapB (**D**), SPG21 (**E**), and Stomatin-like 2 (**F**). e.v. = empty vector



Supplementary Figure S2.6. Examples of vesicular phenotypes in cells expressing GFP-Rab7 constructs. (A) Examples of cells with a “diffuse, small” phenotype which display mostly diffuse and discrete small vesicles. (B) Examples of cells with a “diffuse, few enlarged” phenotype which display mostly small vesicles with a small number of enlarged vesicles. (C) Examples of cells with a “some clustering, many enlarged” phenotype which display many enlarged, clustered vesicles, but also many small vesicles. (D) Examples of cells with a “highly clustered, many enlarged” phenotype which display many prominent, large clusters of vesicles. Green = GFP-Rab7, Blue = DAPI.



Supplementary Figure S2.7. Rab7 mutants associate with autophagosomes and do not alter autophagic flux. (A) HeLa cells were transfected with GFP-Rab7 constructs and RFP-LC3, a specific marker of autophagic vacuoles (Kabeya et al., 2000). To stabilize autophagolysosomes, cells were treated for 2 hours prior to fixation with the vacuolar proton pump inhibitor Bafilomycin A1 which prevents acidification and degradation of autophagolysosome contents (Klionsky et al., 2008). Wild-type Rab7 and disease mutants colocalize with RFP-LC3-positive vesicles and do not cause any significant alteration in their morphology or localization. (B) HeLa cells were transfected with Rab7-HA constructs and endogenous LC3-I and LC3-II levels were assessed by Western blot. Cells were also treated with Bafilomycin A1 for 2 hours prior to lysis to stabilize autophagolysosomes. Rab7 disease mutants do not cause an increase in LC3-II accumulation, suggesting that autophagy is neither induced nor inhibited by

overexpression of Rab7 disease mutants. Red = RFP-LC3, Green = GFP-Rab7, Blue = DAPI.

Discussion

In this study we characterized the structural, biochemical, and cell biological consequences of mutations in the small GTPase Rab7 that cause the dominantly inherited axonal degeneration CMT2B. Examination of the crystal structure of the L129F Rab7 mutant revealed alteration of the nucleotide binding pocket but no significant alteration to the catalytic site. We demonstrated that despite rapid GTP dissociation and re-association, GTPase activity in disease mutants is not significantly reduced. We showed that disease mutations result in an increase in the active fraction of Rab7 and a corresponding increase in binding to a subset of effector proteins. In addition, we demonstrated that increased activation in disease mutants is due to unregulated nucleotide exchange and not due to a hydrolysis defect. Surprisingly, the cellular phenotype of mutant Rab7 is milder than expected given the prominent, unregulated GTP exchange and marked increase in the active fraction. To account for this, we documented that unregulated activation of Rab7 disease mutants is mitigated by unregulated inactivation. Thus, our data reveal how misregulation of multiple steps of the Rab7 activity cycle leads to alteration of Rab7 activity. A previous publication suggested that Rab7 disease mutants lead to constitutive activation and a nearly complete loss of catalytic activity (Spinosa et al., 2008). However, such a severe alteration of activity would be predicted to have far-reaching effects on Rab7-dependent pathways. Indeed, overexpression of constitutively active Rab7 leads to developmental defects in *Drosophila* (Entchev et al., 2000; Wilkin et al., 2008). Although Rab7 is ubiquitously expressed, disease mutations cause adult-onset, slowly progressive disease that is restricted to the neurons with the

longest axonal projections. Our findings of subtle changes in Rab7 activity are consistent with this pattern of disease in which a slight underlying defect becomes pathological only in a subset of vulnerable neurons.

Unregulated Rab7 cycling and accumulation of activated Rab7

Almost all Rab GTPases share two physiological properties, slow GDP dissociation and low intrinsic GTPase activity. These properties render Rabs, including Rab7, dependent on the positive and negative influences of regulatory GEF and GAP proteins. In Rab7 disease mutants, these two critical properties are absent, and Rab7 mutants are able to circumvent normal regulatory controls (Fig. 2.9). Specifically, we provide evidence that Rab7 mutants are able to become activated independent of GEF activity due to rapid, unregulated GTP exchange, but this activation is counterbalanced by unregulated, GTPase-independent termination of activity (Fig. 2.8). The net effect of unregulated activation and inactivation is a subtle increase in the duration of association of active Rab7 with target membranes and an increase in the GTP-bound, active fraction.

Membrane cycling in mutant Rab7 is uncoupled from GTP hydrolysis

Although a previous report concluded that disease mutants have a GTPase defect (Spinosa et al., 2008), we demonstrate that this apparent defect is largely a reflection of increased GTP dissociation. Under conditions where GTP is provided in excess, the hydrolysis rate of disease mutants approaches that of wild-type Rab7 (Fig. 2.2C-E). As the physiologic concentration of GTP (~500uM) is higher than the concentrations we used in our assays (Traut, 1994), we predict that *in vivo*, dissociation of GTP would be

followed by re-association and subsequent hydrolysis. Indeed, the observation that the phenotype of disease mutants is somewhat altered by adding the Q67L mutation (Fig. 2.8A-C) provides indirect evidence that a modest amount of GTP hydrolysis does occur in disease mutants *in vivo*. Otherwise, adding the GTPase mutation to the disease mutant background would have no effect on their cellular phenotype. In addition, disease mutations are also able to rescue membrane cycling in the GTPase-deficient mutant (Fig. 2.8C), suggesting hydrolysis-independent inactivation as a result of disease mutations. Based on these results, we propose that Rab7 disease mutants are able to become inactivated by two routes: 1) rapid dissociation and re-association of GTP with eventual GTP hydrolysis, and 2) dissociation of GTP and association of GDP. Both of these mechanisms of inactivation are distinct from inactivation in wild-type Rab7 and highlight how disease mutations lead to misregulation of Rab7 activity.

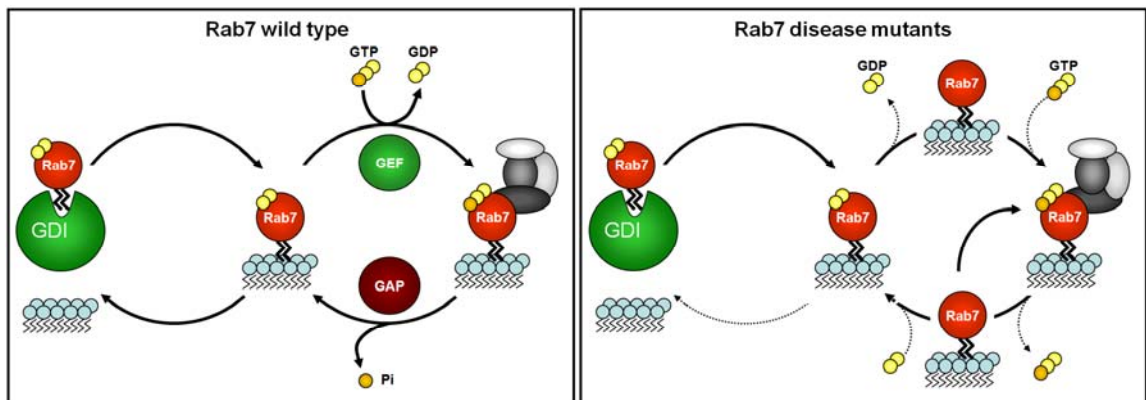


Figure 2.9. Model of how Rab7 disease mutants cause misregulation of the activation cycle. Activation of membrane-associated Rab7 normally requires GEF activity due to very slow dissociation of GDP. Following GTP binding, GAP-catalyzed hydrolysis inactivates Rab7 and allows extraction from the membrane by GDI. In Rab7 disease mutants, the regulation of the activity cycle is disrupted. Decreased affinity for GDP allows GTP exchange to occur independent of GEF activity, and GTP dissociation allows hydrolysis-independent inactivation of Rab7. Following GTP dissociation, Rab7 mutants can either become reactivated by binding GTP, or can bind GDP and become extracted by GDI. Since the relative affinity for GTP is greater than for GDP, Rab7

mutants are more likely to rebind GTP and undergo multiple activation cycles on target membranes before they are extracted. Thus, disease mutants cause misregulation of activation and inactivation of Rab7 resulting in alteration of the GTP-GDP ratio and a subtle increase in residence on target membranes. In the GTP-bound state, we predict that Rab7 disease mutants are largely bound to effectors, although it is possible that some fraction is not associated with effector proteins.

Rab7 mutations cause a quantitative but not qualitative change in interaction with effector proteins

Using LC-MS/MS, we demonstrate that disease-causing mutations do not qualitatively alter the complement of Rab7 interactors but cause quantitative changes in specific interactions (Fig. 2.5). This observation is consistent with our structural studies that reveal that the overall structure of mutant Rab7, and in particular the effector binding region, is unchanged from wild-type (Fig. 2.1). Specifically, we demonstrate significantly increased interaction of both Rab7 disease mutants with ORP1L, a well-characterized effector of active Rab7 that facilitates retrograde trafficking of late endosomes (Johansson et al., 2007), and Vps13C, which also shows increased binding to the Q67L mutant and is likely a mediator of active Rab7 function. Vps13C is an as yet uncharacterized protein whose yeast homolog regulates trafficking to the vacuole (Brickner and Fuller, 1997). Our analysis also identified several previously unidentified potential interactors of Rab7 (Table 2.2). Of particular note are VapB, the FYVE containing-protein ANKFY1, and SPG21, which localize to membranes and potentially play a role in vesicular transport (Soussan et al., 1999; Kuriyama et al., 2000; Hanna and Blackstone, 2009). A recent study elegantly demonstrated a role for VapB and VapA in regulating the cholesterol-dependent microtubule trafficking of Rab7-positive late endosomes (Rocha et al., 2009). High cholesterol levels on the cytosolic face of vesicles

activate ORP1L leading to stable recruitment of dynein, whereas low cholesterol levels allow the extraction of motor proteins from Rab7-RILP complexes by VapA and B. Our data suggest that misregulation of the Rab7 activity cycle in disease mutants may perturb such carefully orchestrated vesicular trafficking pathways.

Notably, two of the novel Rab7 interacting proteins we identified have been implicated in human diseases affecting the nervous system. VapB mutations cause a familial type of amyotrophic lateral sclerosis (ALS8) (Nishimura et al., 2004), and SPG21/maspardin mutations cause spastic paraplegia 21 (Simpson et al., 2003). In addition, mutations in previously known Rab7 interactors have been implicated in multiple neurological diseases: REP-1 in choroideremia (van den Hurk et al., 1992; Seabra et al., 1993), GDI in X-linked mental retardation (D'Adamo et al., 1998), p150^{glued} in distal spinobulbar muscular atrophy (Puls et al., 2003), β III spectrin in spinocerebellar ataxia 5 (Ikeda et al., 2006), and RILP as a gene deleted in Miller-Dieker syndrome (Cardoso et al., 2003). These results reveal a nexus of Rab7-associated proteins involved in human neurological disease and suggest that neurons are particularly vulnerable to mutations that impair protein trafficking through the endo-lysosomal system. Furthermore, the frequency with which function of the endo-lysosomal system is disrupted in familial and sporadic neurodegenerative diseases suggests overlapping mechanisms of pathogenesis, as has been suggested previously (Nixon et al., 2008).

Functional consequences of Rab7 mutations

Dominantly inherited neurodegenerative diseases are typically attributed to gain-of-function mechanisms. At present, prevailing hypotheses suggest that disease results from gain of a *novel* toxic function that is unrelated to the normal function of the mutant protein. For example, many neurodegenerative diseases are caused by mutations that disrupt protein folding leading to the formation of aggregates that are potentially neurotoxic. In other cases a dominant-negative mechanism leads to loss of function of the mutant protein and its associated complexes. Our elucidation of the molecular defect caused by mutations in Rab7 illustrates an alternative mechanism: toxic misregulation of *native* function. While there is precedent for this mechanism underlying tumorigenesis, to our knowledge, this is the first example of this type of mechanism underlying neurodegenerative disease.

How might misregulation of Rab7 lead to axonal degeneration? Rab7 specifically regulates transport, docking, and fusion of late endosomes, autophagosomes, and lysosomes. As such, Rab7 plays an important role in determining the fate of endocytic vesicles by regulating their fusion and subsequent degradation by lysosomes. In cultured neurons, over-expression of dominant-negative Rab7 reduces the degradation of TrkA-containing signaling endosomes leading to increased trophic signaling and excessive neurite outgrowth (Saxena et al., 2005). Misregulation of Rab7 function as seen in CMT2B may have the opposite effect, resulting in premature lysosomal degradation of endocytic vesicles. CMT2B is characterized by length-dependent axonal degeneration that most prominently affects pain sensation. Notably, there is significant clinical overlap between CMT2B and familial insensitivity to pain (HSAN5, OMIM 608654) caused by

loss-of-function mutations in nerve growth factor beta (NGFB) and also congenital insensitivity to pain with anhydrosis (CIPA, OMIM 256800), which is caused by loss-of-function mutations in the NGFB receptor TrkA (Indo et al., 1996; Einarsdottir et al., 2004). The phenotypic similarity of CMT2B to these syndromes leads us to speculate that Rab7 mutations may cause premature degradation of TrkA-containing signaling endosomes with resulting attenuation of neurotrophic support and selective axonal degeneration in a length-dependent manner. Our results provide a framework for future work examining how Rab7 mutants influence signaling endosome dynamics and vesicular trafficking in cultured neurons and animal models.

Chapter 3: Conclusions and Future Directions

Work presented in this chapter was performed by Brett McCray, Eran Perlson from Erika Holzbaur's laboratory (University of Pennsylvania), and Christopher Deppmann from David Ginty's laboratory (Johns Hopkins University). The chapter was written by Brett McCray.

CMT2B disease mutations and misregulation of the Rab7 activity cycle

As described in Chapter 1, Rab GTPases undergo a cycle of activation and inactivation that is coupled to reversible membrane association. In the active state, Rabs bind GTP, associate with membranes, and recruit effector complexes that exert diverse biological functions. Multiple proteins regulate the localization, membrane targeting, nucleotide exchange, and catalytic activity of Rab GTPases. As Rabs are master regulators of vesicular trafficking, they play a critical role in multiple regulated cellular processes from secretion of bioactive molecules, to protein degradation, to trophic signaling. Appropriate vesicular trafficking requires precise spatial and temporal coordination of Rab GTPase activity. As such, it is no wonder that Rab GTPases have evolved complex and multifactorial regulatory mechanisms. Highlighting the importance of these regulatory pathways, mutations that affect Rab regulatory proteins have been found to underlie various human diseases. For example, mutations in the GDP-dependent Rab chaperone Rab GDI lead to mental retardation (D'Adamo et al., 1998), and mutations in the Rab5 GEF protein Alsin cause a form of amyotrophic lateral sclerosis (Hadano et al., 2001; Yang et al., 2001).

While the mechanisms of targeting of Rab GTPases to specific vesicular compartments are rather poorly understood, targeting likely depends on a complex interplay of phosphoinositide and regulatory protein concentrations within vesicle membranes. In particular, the presence of factors such as the specific GDF and GEF proteins for a given Rab GTPase likely aid in the membrane recruitment and stable activation of Rabs. Once targeted to the appropriate membrane, other accessory proteins regulate activation and

inactivation of Rabs. Nearly all characterized Rab GTPases demonstrate intrinsically low rates of spontaneous nucleotide exchange and low rates of GTP hydrolysis. Thus, uncatalyzed activation and deactivation of Rabs occurs with slow kinetics. This property allows Rab activity to be exquisitely sensitive to both GEF activity that regulates GDP-GTP exchange and GAP activity that regulates GTP hydrolysis. Our results presented in Chapter 3 highlight how CMT2B mutations cause misregulation of these critical steps in the Rab7 activity cycle.

As GEF activity is likely to be critical for the specific and temporally appropriate recruitment of Rabs onto target membranes, misregulation of Rab7 activation is likely to lead to inappropriate membrane targeting. In the absence of GEF activity, membrane targeted Rabs are rapidly extracted by the action of GDI, which recognizes the GDP-bound conformation. Thus, delivery of Rabs to a target membrane is normally insufficient for their activation and stable association. In the CMT2B disease mutants, we demonstrate a marked decrease in GDP affinity that favors GEF-independent GTP exchange. Thus, by eliminating the normally slow rate of GDP dissociation, disease mutations lead to unregulated and inappropriate activation of Rab7 that effectively eliminates the role of GEF activity in providing regulation of membrane recruitment. Disrupted regulation of membrane recruitment and activation could potentially lead to temporally or spatially inappropriate accumulation of Rab7 on target membranes. Indeed, we show that excessive activation directly leads to an increase in the membrane-bound fraction and shifts in effector binding.

The interval between GTP binding and hydrolysis represents the window of time during which Rabs are active and able to exert specific biological activity. While the kinetics of GTP hydrolysis on membranes are still relatively poorly understood, it is clear that GTP hydrolysis is tightly regulated by GAP proteins in order to limit the biological activity of membrane-bound Rabs. In Rab7 disease mutants, rapid GTP dissociation provides an alternative route to GTP hydrolysis for inactivation and membrane release. Thus, disease mutations partially negate the regulatory action of GAP proteins and cause uncoupling of GTP hydrolysis and membrane extraction. Particularly in situations where sustained Rab7 activity is required, such misregulation in Rab7 disease mutants could lead to premature and inappropriate silencing that interferes with proper Rab7 function.

Together, our data indicate that disease-associated mutations in Rab7 lead to misregulation of activation and inactivation and likely circumvent regulatory mechanisms responsible for specifying the spatial and temporal pattern of Rab7 activity. Such misregulation could have a profound impact on endo-lysosomal dynamics, especially in the axons of peripheral neurons.

Rab7 disease mutations and trafficking of signaling endosomes

The misregulation of the Rab7 activity cycle in disease mutants suggests that the precise regulatory controls normally imposed on Rab7 are critical for neuronal health and maintenance. However, the question remains of how such misregulation leads to the specific pattern of axonal degeneration seen in CMT2B patients. As previously described, Rab7 has been implicated in the long-range axonal trafficking of Trk receptors, both in motor and sensory neurons (Deinhardt et al., 2006). Thus, it is possible that misregulation

of Rab7 activity leads to a defect in the transport of signaling endosomes that compromises the fidelity of neurotrophic signaling. Inappropriate, GTPase-independent inactivation of Rab7 disease mutants could lead to premature dissociation of Rab7 effector complexes that are required for efficient retrograde transport of signaling endosomes. Preliminary evidence from cultured hippocampal neurons suggests generalized transport defects with an increase in the number of stationary vesicles in neurons expressing Rab7 disease mutants (work done in collaboration with Eran Perelson and Erika Holzbaur, U. of Pennsylvania, Fig. 3.1). This observation raises the possibility that disease mutations may lead to slowing of axonal trafficking. Specifically, a transport defect could result in length-dependent decreases in effective delivery of Trk signaling endosomes to the cell body and could thereby account for the specific pattern of degeneration in CMT2B. However, additional work characterizing the transport of Rab7-positive vesicles in neurons will be needed to support this claim.

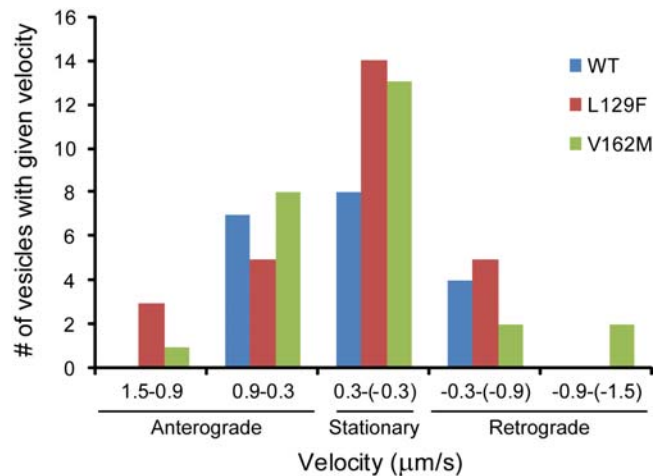


Figure 3.1. Rab7 disease mutants disrupt axonal trafficking. Primary hippocampal neurons were transfected with GFP-Rab7 constructs, and vesicular movement was followed using phase contrast dynamic live-cell imaging. Images were acquired every 3s for a total of 120s. Vesicle movements were tracked using the manual tracking plugin for ImageJ. The average velocities for all vesicles over the course of the experiment were calculated, and vesicle velocities were grouped into 0.6 μm/s bins. The histogram

demonstrates an increase in slow moving and stationary vesicles (velocities from 0.3 to - 0.3) in neurons expressing Rab7 disease mutants. These results are consistent with a generalized trafficking defect caused by Rab7 mutations.

The hypothesis presented above regarding Rab7 mutants and axonal trafficking follows from the assumption that Rab7 is the primary Rab GTPase responsible for the delivery of signaling endosomes from distal neuronal processes back to the cell body. While evidence of such a role for Rab7 exists (Deinhardt et al., 2006), other experimental results suggest that signaling endosomes are primarily transported by Rab5 rather than Rab7 (Delcroix et al., 2003; Ye et al., 2003; Cui et al., 2007). If Rab5 were the primary signaling endosome-related GTPase, then we envision an alternative explanation for how Rab7 disease mutations lead to axonal degeneration. In this scenario, Rab7 localization to signaling endosomes may represent a degradative signal that diverts endosomes from trophic support to a lysosomal fate (Fig. 3.2, top). In fact, Rab7 activity in PC12 cells has been shown to regulate the duration of signaling of NGF-TrkA receptor complexes by controlling their rate of degradation (Saxena et al., 2005). In this system, inhibition of Rab7 activity prolonged TrkA signaling in response to low dose NGF, and constitutively active Rab7 led to more rapid silencing of signaling (Saxena et al., 2005). Thus, the specific function of Rab7 in the signaling endosome pathway may be to facilitate lysosomal targeting and degradation. This raises the question of how signaling endosomes are normally targeted for degradation, and where in the axon this normally occurs.

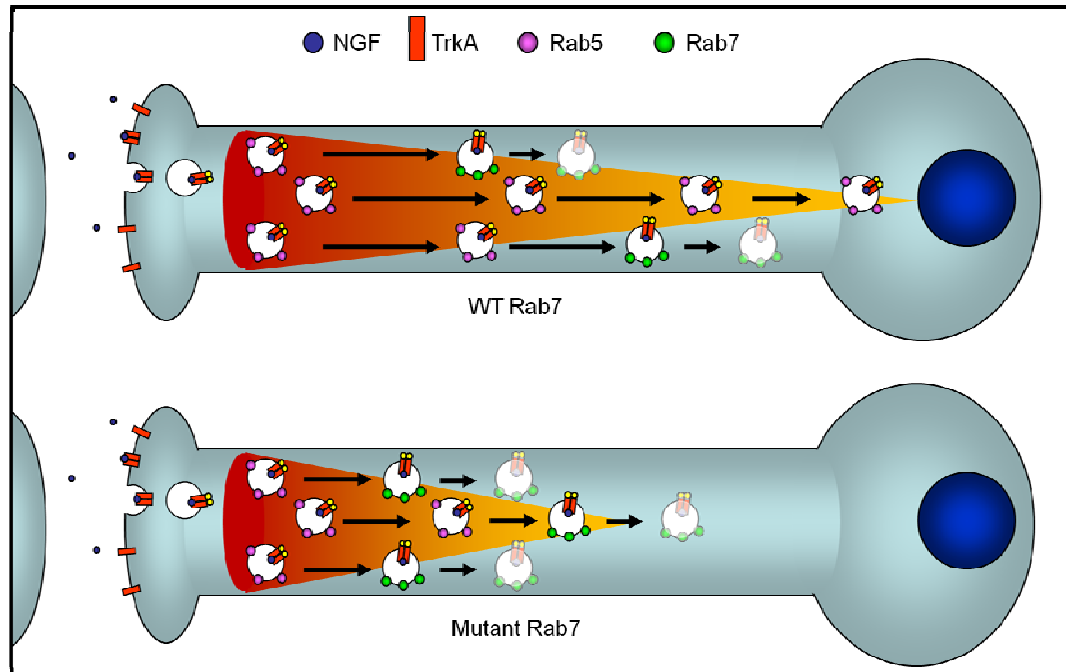


Figure 3.2. Model of disruption of TrkA signaling in Rab7 disease mutants. Normally, NGF binds TrkA receptors at the synapse and leads to dimerization, internalization, and transport of activated receptors to the cell body. Such transport is proposed to be Rab5-dependent, although this is controversial. In this scenario, recruitment of Rab7 to signaling endosomes leads to their degradation, but such recruitment is largely inhibited until the vesicles have successfully trafficked to the soma. In Rab7 disease mutants however, misregulation of activity could lead to premature recruitment of Rab7 to signaling endosomes, inappropriate degradation, and attenuation of trophic support.

Ultrastructural examination of NGF localization in cell bodies of cultured sympathetic neurons revealed that the majority of NGF resides within degradative organelles such as lysosomes and MVBs, thus indicating that signaling endosomes are ultimately targeted to acidic degradative vesicles (Claude et al., 1982). However, degradation of NGF-TrkA complexes within axonal process is virtually undetectable (Ure and Campenot, 1997), suggesting that most signaling endosomes evade lysosomal targeting until they reach the cell body. There is a continuous presence of acidified vesicles throughout axonal processes, although the concentration increases from distal to proximal (Overly and

Hollenbeck, 1996). Thus, the fact that signaling endosomes largely avoid degradation in the axons cannot be accounted for a lack of degradative vesicles within axons. Instead, these results suggest that signaling endosome degradation is tightly regulated and initiated only once signaling endosomes have successfully trafficked from the distal axonal processes back to the soma. If Rab7 targeting to signaling endosomes serves as a degradation signal, Rab7 recruitment to signaling endosomes must be actively inhibited prior to delivery to the cell body.

As described above, GEF proteins play a critical role in the stable activation of Rabs on target membranes. In Rab7 disease mutants, however, unregulated, GEF-independent activation might lead to improper targeting of active Rab7 to signaling endosomes within axons and premature lysosomal degradation rather than long-range trafficking (Fig. 3.2, bottom). Thus, misregulation of Rab7 activation could lead to attenuation of neurotrophic signaling. One might predict that such premature degradation of signaling endosome would be a stochastic event, and therefore the cumulative probability of mistargeting of signaling endosomes to lysosomes would increase in longer axonal processes. Therefore, reduction in trophic signaling would be directly correlated to axon length and could presumably lead to a pattern of disease consistent with that seen in CMT2B. We have begun to address this question using cultures of primary sympathetic neurons transfected with wild-type or disease mutant Rab7. In these neurons, overexpression of Rab7 disease mutants leads to prominent accumulation of large, LysoTracker Red-containing vesicles in the cell body (work done in collaboration with Chris Deppmann, U. of Virginia, and David Ginty, Johns Hopkins, Fig. 3.3). This finding is consistent with the previously

presented model and could indicate excessive targeting of vesicles for degradation in neurons expressing Rab7 disease mutants.

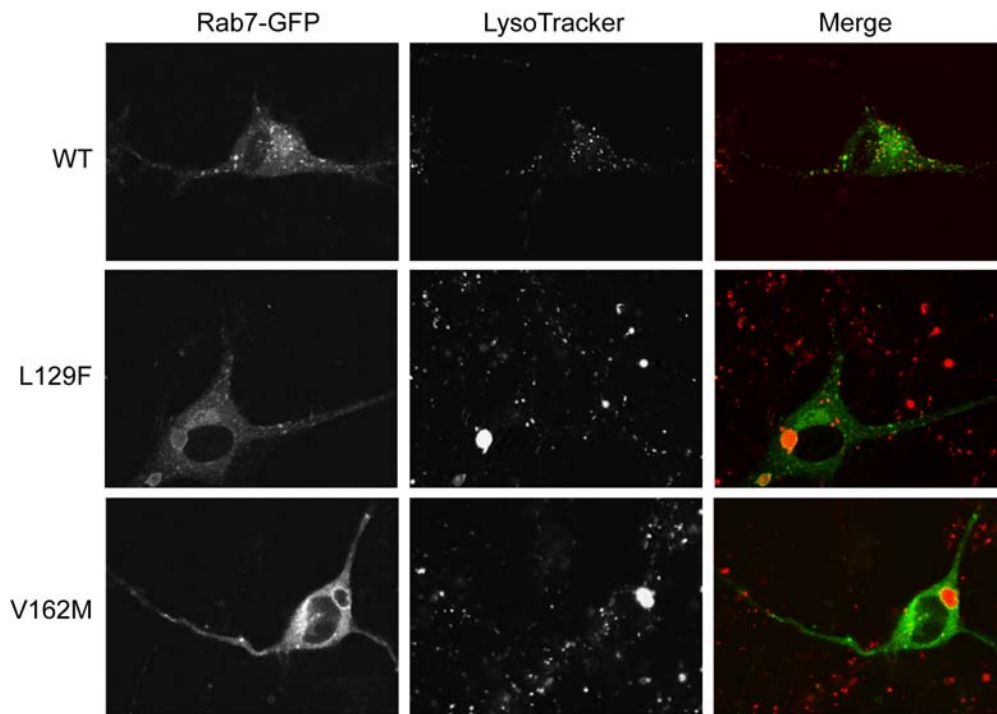


Figure 3.3. Rab7 disease mutants cause accumulation of enlarged acidic vesicles in sympathetic neurons. Primary mouse sympathetic neurons were transfected with GFP-Rab7 constructs and imaged 48hr post-transfection. LysoTracker Red DND-99 (Invitrogen) was added to visualize acidic vesicles. L129F and V162M Rab7 mutants induce the abnormal formation of enlarged, LysoTracker-positive vesicles in the soma. These structures were never seen in cells expressing wild-type Rab7.

Characterization of Rab7-effector interactions in neurons

To test whether misregulation of Rab7 disease mutants led to changes in protein-protein interactions, we performed an unbiased proteomic characterization of interactions in wild-type and mutant Rab7. Using extracts from HEK293T cells, we identified several previously known Rab7 interacting proteins as well as several novel putative interactors (Chapter 2, Fig. 3.5). In addition, we saw quantitative differences in the amounts of

specific effectors that were immunoprecipitated by wild-type Rab7 and Rab7 disease mutants. It is possible that some of these altered interactions could play an important role in the pathogenesis of CMT2B, and future studies will address the functional impact of these Rab7-effector interactions. The mutation-dependent association of Rab7 with the endo-lysosomal protein Vps13C is particularly intriguing, and it will be important to determine the function of Vps13C in Rab7-dependent pathways and to assess whether Vps13C activity is related to CMT2B pathogenesis. The membrane trafficking protein VapB was also identified as an interactor of Rab7 and will be discussed separately.

There are two caveats to our proteomic characterization of Rab7 that deserve mention. First, our original choice to use HEK293T cells for expression of Rab7 constructs was made primarily because of the high transfectability of these cells. However, while strong expression of Rab7 was optimal for producing large amounts of immunoprecipitated protein, dramatic overexpression of Rab7 could have led to non-physiologic interactions. Thus, verification of interactions done under more physiologic conditions would increase the reliability of our results. Second, it is important to note that despite ubiquitous expression of Rab7, CMT2B disease mutations cause disease that is entirely restricted to peripheral neurons. This pattern of vulnerability indicates that neurons are uniquely sensitive to the specific defects imposed by Rab7 disease mutations. Thus, it is possible that the biological basis of CMT2B is related to neuron-specific Rab7-effector interactions that would not have been detected in our experiments using non-neuronal cells. We have now produced GFP-Rab7 lentivirus which will allow high-efficiency infection of various neuronal cell types and allow assessment of Rab7 interactions in

neuronal cells. A neuronal proteomics approach using differentiated PC12 cells, or primary sensory, motor, or sympathetic neurons might uncover tissue-specific changes in effector interactions that are particularly relevant to CMT2B pathogenesis.

Functional characterization of the Rab7-VapB interaction

We originally identified VapB (VAMP (vesicle associated membrane protein)-associated protein B and C) as a potential interactor of Rab7 through an unbiased proteomics screen (Chapter 3, Table 3.2, Fig 3.5, and Fig. S3.5). A P56S mutation in VapB leads to a familial, autosomal-dominant form of amyotrophic lateral sclerosis (ALS) designated ALS8 (Nishimura et al., 2004). ALS8 patients display the hallmark ALS signs of upper and lower motor neuron involvement associated with weakness, fasciculations, muscle wasting, spasticity, and hyperreflexia (Nishimura et al., 2004; Landers et al., 2008). The mechanisms by which mutations in VapB lead to motor neuron degeneration are currently unknown.

VapB is a ubiquitously expressed 33kD type II integral membrane protein that localizes to multiple intracellular membranes (Weir et al., 1998). VapB was originally identified in *Aplysia* as a specific interacting protein of VAMP, also known as synaptobrevin, and this interaction was shown to be important for neurotransmitter release at the synapse (Skehel et al., 1995). VapB is highly conserved in eukaryotes and exhibits 63% sequence identity with the functionally and structurally related protein VapA (Lev et al., 2008). The functional domains of Vap proteins include a major sperm protein (MSP) domain at the N-terminus, a coiled-coil domain, and a transmembrane domain at the extreme C-

terminus. The MSP is an immunoglobulin-like domain that interacts with FFAT (two phenylalanines in an acid tract) motifs found within various membrane interacting proteins, particularly oxysterol binding proteins (OBPs), OBP-related proteins (ORPs), and SNAREs (Loewen et al., 2003). The transmembrane domain anchors VapB within specific membranes and also mediates homodimerization and VapA-VapB heterodimerization (Nishimura et al., 1999). VapB is primarily localized to the ER and Golgi, although localization within synaptic vesicles, the plasma membrane, and endocytic vesicles has been suggested (Lapierre et al., 1999; Pennetta et al., 2002; Nishimura et al., 2004). Evidence suggests that VapB has diverse functions including regulation of membrane trafficking, membrane fusion, and lipid transport and metabolism (Lev et al., 2008).

The function of VapB has been most extensively characterized using the *Drosophila* homolog Vap-33. Levels of Vap-33 regulate bouton number and size at the *Drosophila* neuromuscular junction (NMJ), possibly through the cleavage and secretion of the MSP domain (Pennetta et al., 2002; Chai et al., 2008; Tsuda et al., 2008). The ALS-causing P56S mutation in VapB localizes to the MSP domain and induces aggregation of VapB (Nishimura et al., 2004). In addition, the P56S mutant suppresses cleavage and secretion of Vap-33 and leads to the formation of inclusions in the ER and in motor neuron axons (Chai et al., 2008; Tsuda et al., 2008). These inclusions sequester wild-type Vap-33 and may lead to Vap-33 loss of function and subsequent interference with BMP signaling at the NMJ (Chai et al., 2008; Ratnaparkhi et al., 2008). Thus, mutations in VapB may lead

to a toxic gain of function through misfolding and aggregation, or a loss of function through sequestration of wild-type VapB.

To follow up our initial identification of VapB as a potential interactor of Rab7, we sought to confirm this interaction using coimmunoprecipitation. FLAG-Rab7 coimmunoprecipitated endogenous VapB from HEK293T cells, and this reaction was specific in that no immunoprecipitation of VapB was evident in control lysates (Fig. 3.4A). To determine whether VapB is a general Rab GTPase binding protein, we examined VapB interactions in cells expressing FLAG-Rab7 or FLAG-Rab4. Rab4 is a Rab GTPase that regulates trafficking from recycling endosomes to the plasma membrane and shares significant homology with Rab7 (van der Sluijs et al., 1992). However, despite partially overlapping distributions and similar three dimensional structures, Rab4 and Rab7 interact with distinct sets of effector proteins. While FLAG-Rab7 was again able to coimmunoprecipitate endogenous VapB, no interaction of VapB with FLAG-Rab4 was detected (Fig. 3.4B). We also saw no interaction with Rab11-FLAG, another early endosomal Rab protein (data not shown). We next determined whether the interaction with Rab7 was altered in CMT2B Rab7 disease mutants. Rab7 L129F and V162M disease mutants interacted normally with VapB and at roughly the same level as wild-type Rab7 (Fig. 3.4C). However, the predominantly GTP-bound mutant Q67L showed somewhat augmented interaction with VapB, and the GDP-locked, dominant-negative Rab7 mutant T22N failed to coimmunoprecipitate VapB. These results suggest that the Rab7 interaction with VapB is nucleotide-dependent and indicate that VapB is a *bona fide* Rab7 effector protein.

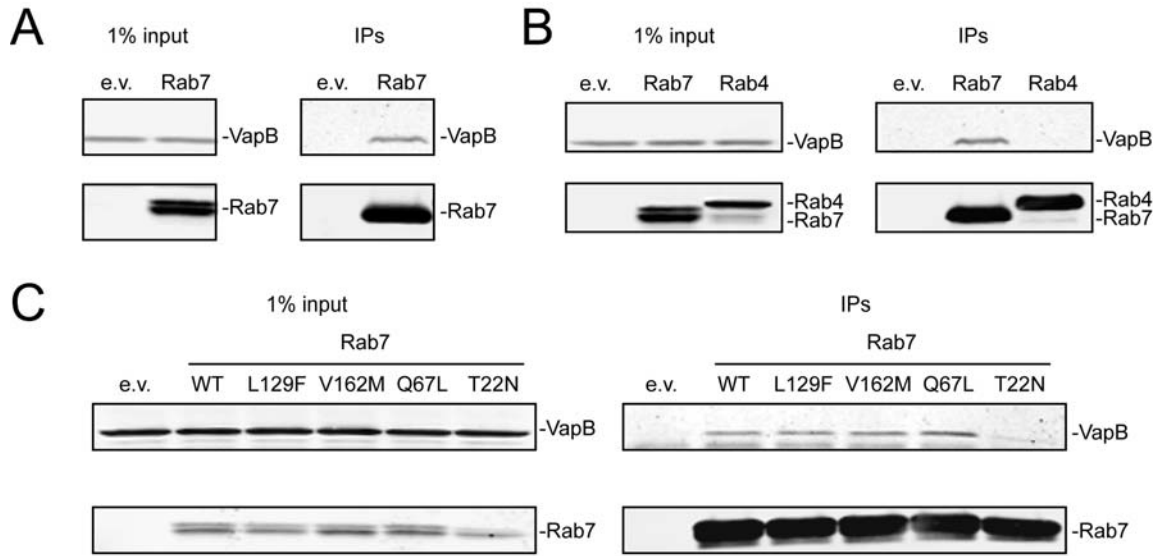


Figure 3.4. Rab7 specifically interacts with VapB. (A-C) HEK293T cells were transfected with FLAG-tagged constructs and subjected to immunoprecipitation with FLAG-agarose (Sigma). (A) VapB is specifically coimmunoprecipitated from cell lysates expressing FLAG-Rab7 and not from cells transfected with empty vector. (B) VapB is coimmunoprecipitated by FLAG-Rab7, but not by FLAG-Rab4, indicating that VapB is a specific interactor of Rab7 and not a general interactor of Rab GTPases. (C) VapB interacts with wild-type and disease mutant Rab7 and shows somewhat enhanced interaction with the constitutively active Q67L mutant. In contrast, VapB does not interact with the dominant-negative, GDP-locked T22N Rab7 mutant.

A recent study identified VapA and VapB as regulators of the Rab7-RILP-ORP1L retrograde vesicular trafficking complex (Rocha et al., 2009). ER-resident Vap proteins were found to facilitate the dissociation of RILP from Rab7 under conditions of low cholesterol content. Thus, it is possible that the interaction of Rab7 and VapB we describe occurs in the context of cholesterol-dependent vesicular trafficking. Further work will be needed to elucidate the functional and structural details of the interaction between Rab7 and VapB.

Concluding remarks

Our results demonstrate that disease-causing mutations in Rab7 lead to misregulation of the activity cycle. Furthermore, we document that such misregulation has multiple effects including an increase in the active fraction of Rab7, prolonged interaction with target membranes, and shifts in effector protein binding. Given that Rab7 mutations lead to a length dependent neuropathy of sensory and motor neurons, future experiments will be needed to elucidate how the general defects we describe in Rab7 mutants translate to the specific pattern of neuronal pathology seen in CMT2B.

The basis of tissue specificity is a fundamental and difficult question not only in CMT2B, but in the field of neurodegeneration in general. As the genetic bases for more and more neurologic diseases are uncovered, it is becoming apparent that neurons are particularly vulnerable to disruption of trafficking through the endo-lysosomal and autophagic pathways (Fig. 3.5). Defects in vesicular transport and biogenesis underlie a variety of diseases, and these diseases display heterogeneous patterns of degeneration of neurons within the brain, spinal cord, or periphery leading to symptoms that range from cognitive decline to ataxia, weakness, and numbness. Notably, the causative proteins in many of these diseases are widely expressed, but the pattern of degeneration is often highly restricted and distinct across different diseases. While in some cases this reflects that mutations perturb very specific pathways, mutations in various proteins in the same pathway can lead to distinct diseases with non-overlapping patterns of neuronal degeneration. For example, Rab7, p150^{glued}, and β III spectrin are part of a common complex that regulates retrograde transport of late endosomes and lysosomes. However,

mutations in these proteins cause degeneration in specific patterns and therefore cause distinct clinical syndromes: CMT2B with length-dependent degeneration of motor and sensory neurons, distal SBMA with loss of motor neurons and prominent vocal cord paresis, and spinocerebellar ataxia 5 with loss of deep cerebellar nuclei. Such heterogeneity and variable tissue specificity have puzzled neuroscientists and suggest that a simple, generalized transport defect is insufficient to explain the diverse pathological features among neurodegenerative diseases.

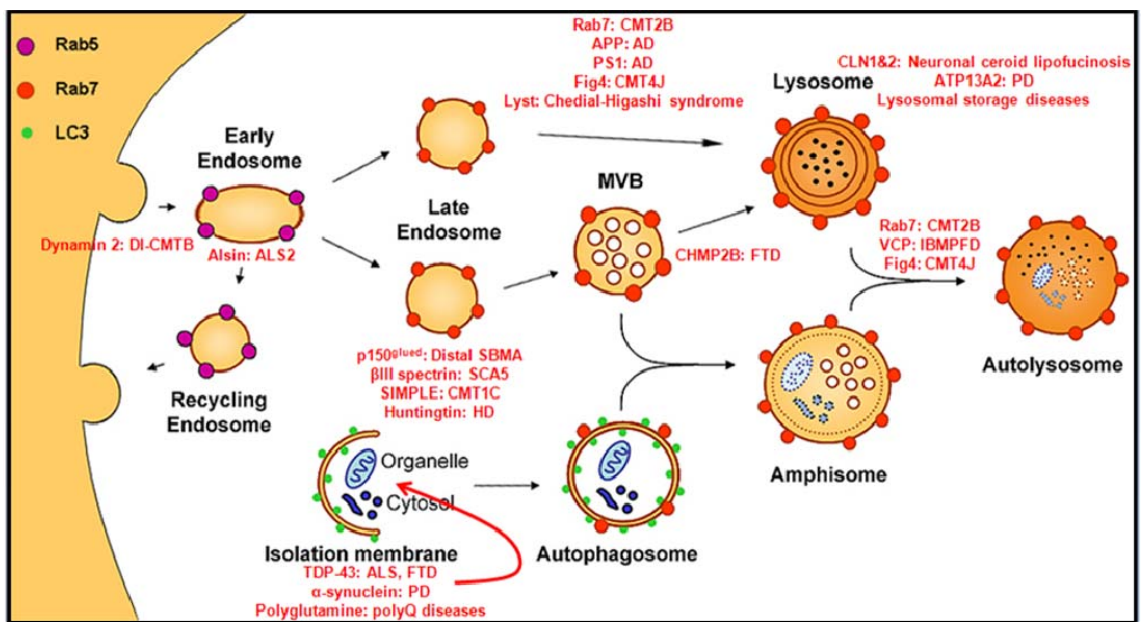


Figure 3.5. The vesicular transport pathway is a hotspot for genetic neurologic diseases. Multiple neurological diseases are caused by mutations in proteins involved in endocytic, autophagic, and lysosomal transport pathways. Shown in red are specific proteins and the disease associated with mutant forms of the protein. DI-CMTB, dominant intermediate Charcot-Marie Tooth (CMT) disease type B; CMT, Charcot-Marie-Tooth disease; SCA5, spinocerebellar ataxia 5; HD, Huntington's disease; AD, Alzheimer's disease; IBMPFD, inclusion body myopathy with Paget's disease of bone and frontotemporal dementia; FTD, frontotemporal dementia; PD, Parkinson's disease; ALS, amyotrophic lateral sclerosis; SBMA, spinobulbar muscular atrophy

Instead, the phenotypic heterogeneity in neurodegeneration suggests that disease-causing mutations perturb very specific pathways that lead to selective degeneration of specific neuron subsets. Perhaps tissue specific pathology reflects the dependence of specific neurons on pathways that are either non-existent or are less central to homeostasis and survival in other neuron subtypes. For example, perturbation of signaling molecules necessary for proprioceptive neuron development would be predicted to cause specific loss of proprioception with sparing of touch and pain sensation. While this concept makes intuitive sense, such obvious mutation-phenotype correlations are rarely seen in neurological diseases.

While it is clear that several common pathways are required for neuronal survival regardless of the neuron subtype, clues to the question of specific neuronal degeneration will likely come from a better understanding of the unique pathways that govern developmental and survival signaling in various neuron subtypes. While the molecular and proteomic characterization of signaling endosome regulatory proteins and cargos is in its infancy, it has already become clear that there is tremendous complexity in the regulation of retrograde axonal transport and downstream endosomal signaling events. Sensory, motor, and autonomic neurons have distinct developmental programs, respond to unique trophic signals, and rely on signaling through distinct protein complexes (Zweifel et al., 2005). In addition, while all neurons undergo directed transport of vesicles and signaling complexes, the cargos transported are likely to be highly heterogeneous in space, time, and among different neuronal types. Indeed, retrogradely

transported vesicles can carry cargos that initiate pro-survival signaling or apoptotic signaling depending on the circumstance (Perlson et al., 2009).

Other potential mechanisms for defining specific neuronal vulnerabilities will likely be uncovered by future studies. For example, competition among neurons for limited trophic support might make certain neuronal subtypes more sensitive to subtle defects in signaling endosome trafficking (Deppmann et al., 2008). Alternatively, differential neuron-specific expression levels of antagonistic proteins could shift the balance of transport and degradation of certain endosomes and their cargo. For example, Rab5 and Rab7 may subserve opposing roles in regulating the targeting of signaling endosomes to degradative compartments, and variations in expression levels or activity in different cell types could influence endosomal degradation rates (Bucci et al., 2000). It is also likely that multiple transport-related protein complexes exist with unique stoichiometries and components, and tissue-specific heterogeneity of such complexes could lead to unique transport properties among different neurons. Finally, neuronal heterogeneity could arise from different combinations and concentrations of neurotrophin receptors expressed within synapses. Thus, neurons could be intrinsically tuned to be sensitive to variations in specific neurotrophin concentrations, and subtle disruption of such pathways could be uniquely toxic to a subset of neurons. Further investigation into the molecular details of signaling endosome transport and the pathogenic mechanisms of specific neurodegenerative diseases will likely reveal multiple potential mechanisms that could account for neuron-specific vulnerabilities.

We believe that our work characterizing the structural, biochemical, and cell biological properties of Rab7 disease mutants provides a framework for future work assessing the consequences of Rab7 mutations for axonal trafficking and the pathogenesis of CMT2B. Furthermore, elucidating the precise defects underlying CMT2B could lead to fundamental advances in our understanding of neuronal homeostasis and the well-documented connection between trafficking defects and human neurological disease. Based on our work, we hypothesize that Rab7 mutations might specifically disrupt proper trafficking and signaling of endosomes containing activated TrkA receptors, and such disruption could account for length-dependent degeneration of sensory neurons that are dependent on NGF-TrkA signaling for survival. The subtle nature of the mutations in CMT2B likely allows for proper development of sensory neurons, but leads to an insidious process of axonal degeneration that occurs progressively with aging. An interesting implication of our results and our working hypothesis regarding CMT2B is that pharmacologic augmentation of NGF-TrkA signaling might provide therapeutic benefit in affected patients. Trials have been conducted to test whether exogenous NGF could improve symptoms in a number of neurological diseases, including diabetic neuropathy, but these trials have uniformly shown no significant benefit in these patient populations (Schulte-Herbruggen et al., 2007). However, in the diseases tested, there was no apparent link between the disease pathogenesis and decreased NGF-TrkA signaling. In contrast, we believe that a primary feature of CMT2B may be decreased transport of active TrkA to cell bodies in sensory neurons, and administration of exogenous NGF could potentially compensate for Rab7 mutation-dependent attenuation of trophic support. No animal models of CMT2B currently exist, but generation of transgenic mice

expressing mutant Rab7 in sensory and motor neurons could allow for more direct characterization of the pathological features of the disease. It will also be interesting to determine whether exogenous administration of NGF can diminish axonal loss in animal models of CMT2B, or whether patients with the disease will respond to such therapy.

Appendix 1: The role of autophagy in age-related neurodegeneration

This section includes the following published review with some modifications:

McCray, B.A., and Taylor, J.P. The role of autophagy in age-related neurodegeneration.

Neurosignals **16**, 75-84 (2008).

Abstract

Most age-related neurodegenerative diseases are characterized by accumulation of aberrant protein aggregates in affected brain regions. In many cases, these proteinaceous deposits are composed of ubiquitin conjugates, suggesting a failure in the clearance of proteins targeted for degradation. The two principle routes of intracellular protein degradation are the ubiquitin-proteasome system (UPS) and the autophagy-lysosome system (autophagy), and both of these degradation pathways have been implicated in the pathogenesis of neurodegenerative disease. Converging evidence now suggests that impairment of autophagy contributes to the initiation or progression of age-related neurodegeneration. Moreover, many misfolded neurodegenerative proteins can be specifically degraded by autophagy, indicating that autophagic degradation may be exploited to remove toxic protein species. These observations suggests that manipulation of autophagy may provide novel strategies for therapeutic intervention for a class of diseases for which no effective treatments presently exist.

Living may be hazardous to your health

Attendant to the process of protein synthesis is the risk of producing defective polypeptides that are prone to misfolding and aggregation. Indeed, it has been estimated that in excess of 25% of nascent peptides are faulty and rapidly removed by proteasomal degradation (Schubert et al., 2000). Even with correctly synthesized proteins there is competition between alternative folding pathways, some terminating in kinetically trapped and incorrectly folded conformers. Post-synthetic damage, cleavage events, or an imbalance of necessary co-factors or components of multimeric complexes also contribute to the burden of misfolded proteins (Taylor et al., 2002). More than simply being functionally deficient, misfolded proteins are prone to aberrant interactions, the formation of insoluble protein aggregates, and the acquisition of toxic properties. Thus, the importance of a vigilant quality control system to prevent the cytotoxic accumulation of misfolded proteins. This may be of particular importance to neurons, which are post-mitotic and unable to dilute cytotoxic misfolded proteins through cell division. Protein quality surveillance takes place at many levels in the synthetic and folding processes (Muchowski and Wacker, 2005).

In many cases, the ultimate fate of defective proteins identified by quality control systems is degradation by either of two intracellular catabolic pathways, the ubiquitin proteasome system (UPS) or the autophagy-lysosome system (Rubinsztein, 2006). The UPS accomplishes selective degradation of short-lived proteins. Degradation by the proteasome is spatially and temporally controlled largely by highly specific targeting of proteins by conjugation with polyubiquitin chains (Ciechanover, 2005). As such,

proteasomal degradation contributes to fine tuning the expression levels of select proteins and participates in the regulation of diverse cellular functions including cell cycling, signal transduction, and transcription regulation. The UPS also plays an important role in clearance of defective or misfolded proteins. Many neurodegenerative diseases are characterized pathologically by the accumulation of ubiquitin conjugates in affected neurons, suggesting that a defect in UPS function contributes to pathogenesis. This hypothesis has been bolstered by the identification of disease-causing mutations in several UPS components, but remains controversial (Ciechanover and Brundin, 2003).

By contrast with the UPS, autophagy is a less selective, bulk degradation process that is largely responsible for the turnover of longer lived proteins (Levine and Klionsky, 2004). Autophagy plays a vital role in neuronal homeostasis by removing aged and potentially damaged proteins and providing a steady supply of macromolecules for further synthesis. Increasingly, defects in autophagy have been implicated as contributing to the initiation or progression of neurodegenerative disease. Here we will (i) describe the process of autophagy, (ii) review the evidence implicating a role for autophagy in neurodegenerative disease, (iii) address the controversy of whether autophagy is helpful or harmful in the context of neurodegenerative disease, and (iv) discuss the prospects of harnessing autophagy for therapeutic benefit.

The autophagy-lysosome system

The term “autophagy” describes a catabolic process in which cytoplasmic components such as organelles and proteins are delivered to the lysosomal compartment for

degradation. Several specialized forms of autophagy exist, and they are distinguished by the way in which cytosolic constituents reach lysosomes (Fig. A1.1). Microautophagy

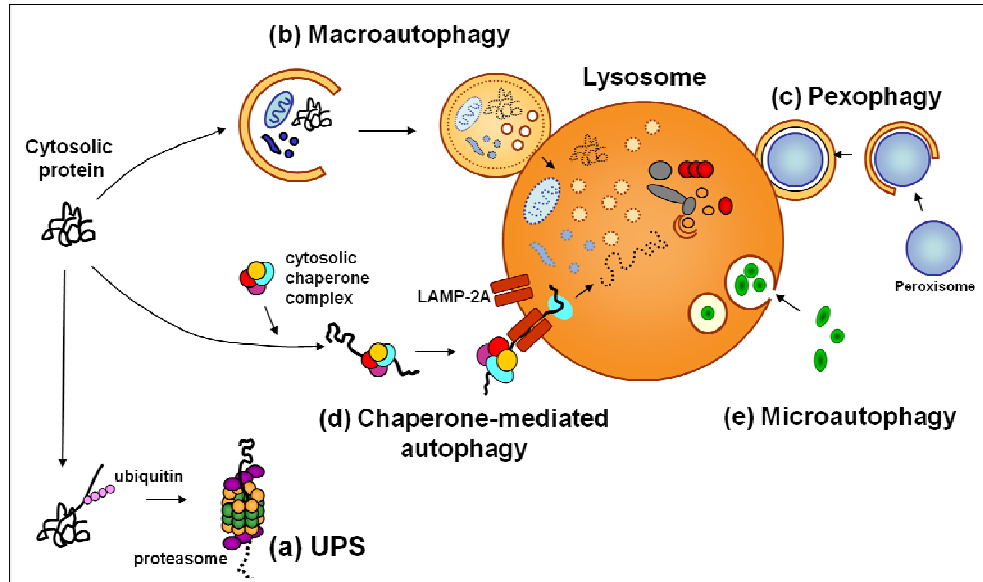


Figure A1.1. Intracellular protein degradation pathways. Cytosolic proteins can be degraded by the UPS or autophagy-lysosome system. Multiple forms of autophagy involve distinct routes by which cytoplasmic components are delivered for lysosome-mediated degradation. **(a)** Proteasome-mediated degradation involves covalent addition of ubiquitin chains to target proteins followed by proteolytic cleavage within the catalytic barrel of the proteasome. **(b)** Macroautophagy is a multistep process by which cytosolic components are engulfed by an isolation membrane to form autophagosomes that are delivered to lysosomes. **(c)** In pexophagy, peroxisomes are surrounded by autophagic membranes and delivered to lysosomes. **(d)** Chaperone-mediated autophagy involves recognition of a peptide signal that induces receptor-mediated translocation into the lysosome. **(e)** In microautophagy, cytosolic contents are directly engulfed by lysosomes.

involves direct engulfment of small volumes of cytosol by lysosomes (Ahlberg et al., 1982). Pexophagy is a specialized form of autophagy for selective degradation of peroxisomes (Dunn et al., 2005). Chaperone-mediated autophagy is a regulated process in which proteins harboring a pentapeptide motif are specifically targeted for receptor-mediated translocation into the lysosome, and is a significant catabolic pathway that may

account for degradation of up to 30% of all cytosolic proteins (Dice, 1990; Cuervo and Dice, 1996). These processes are distinguished from macroautophagy (hereafter referred to as autophagy), in which a membranous structure termed the isolation membrane or phagophore expands as a cup-shaped organelle to engulf a portion of cytoplasm, eventually fusing to form a new vacuole known as an autophagosome that compartmentalizes the cytosolic components (Arstila and Trump, 1968). In mammals, newly formed autophagosomes undergo a stepwise maturation process involving fusion with late endosomes and multivesicular bodies to form a structure termed an amphisome (Berg et al., 1998). Autolysosomes are formed when amphisomes ultimately fuse with lysosomes to deliver their contents for degradation by lysosomal hydrolases (Fig. A1.2). Finally, the breakdown products from the autolysosome are translocated back across the lysosomal membrane for reuse in metabolic processes.

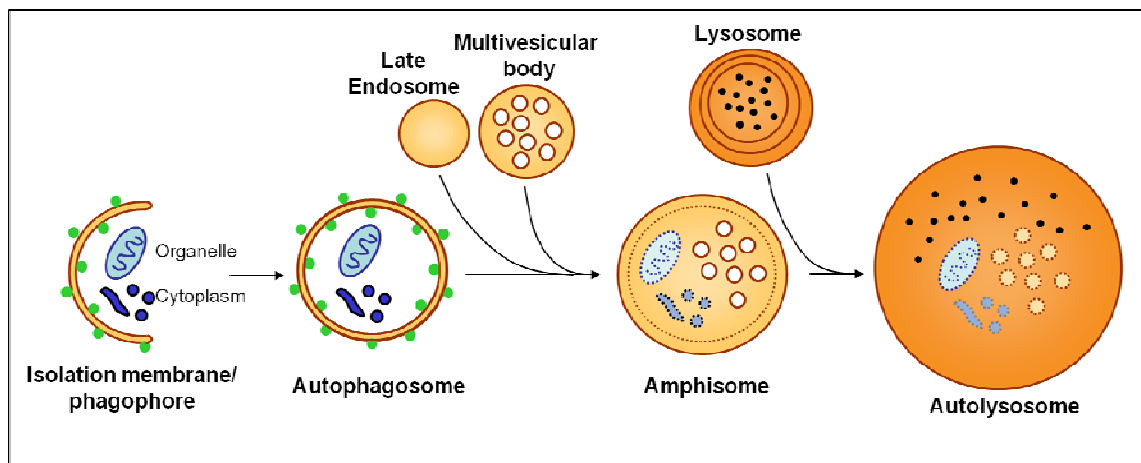


Figure A1.2. The process of macroautophagy. Macroautophagy begins with the formation of an isolation membrane (phagophore) that surrounds cytoplasmic constituents. This membrane elongates and then fuses with itself to create a sealed vesicle, termed the autophagosome, which encloses a portion of cytosol. In mammalian cells, autophagosomes undergo a maturation process that involves fusion events with late endosomes and multivesicular bodies. The products of these fusions are termed amphisomes. Finally, amphisomes fuse with lysosomes to generate degradative autolysosomes which complete the digestion of amphisome contents.

Induction and maturation of autophagosomes

Autophagosome formation involves the coordinated activity of a large number of autophagy-related genes (Atg genes). Initially identified in yeast, the Atg genes are highly conserved in metazoans, including mammals (Wang and Klionsky, 2003). These genes function in two independent ubiquitin-like conjugation systems that each culminate in the formation of membrane-associated complexes that carry out the process of autophagosome formation (Fig. A1.3) (Ohsumi, 2001). In one arm of the conjugation system, sequential action of an E1 ligase-like protein (Atg7) and an E2 ligase-like protein (Atg10) generate a covalent isopeptide linkage of the C-terminal glycine of a ubiquitin-like protein (Atg12) with a lysine residue of Atg5. Multiple Atg5-Atg12 conjugates are then cross-linked by Atg16 to form large Atg5-Atg12-Atg16 that contributes to phagophore membrane elongation. In the other arm of the conjugation pathway, Atg8 is proteolytically processed by Atg4 before interacting with the E1-like enzyme Atg7. Next, Atg8 is transferred to the E2-like protein Atg3 which ultimately catalyzes the conjugation of Atg8 to the lipid phosphatidylethanolamine (PE). This lipidation reaction allows Atg8-PE to associate with both the outer and inner membranes of the forming autophagosome (Kabeya et al., 2000). The mammalian homolog of Atg8 is known as microtubule associated protein 1 light chain 3, or LC3. During activation of autophagy in mammals, a processed form of LC3, denoted LC3-I, is further cleaved to generate LC3-II, which is conjugated to PE and inserted into the phagophore (Kabeya et al., 2000). LC3 is the only protein in higher eukaryotes that is known to remain associated with the completed autophagosome, and consequently LC3 staining is used extensively as a histological marker of autophagosomes, and accumulation of LC3-II as an index of autophagic

activity and/or flux (Klionsky et al., 2007). In addition, increased LC3-II levels correlate with induction of autophagosome formation, a defect in their maturation, or both.

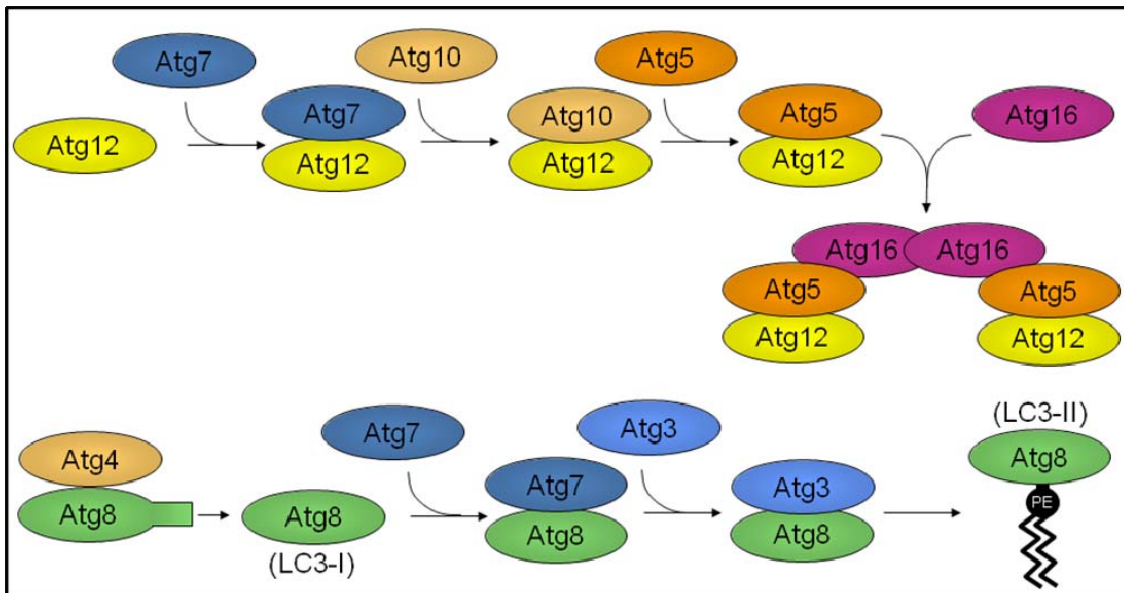


Figure A1.3. Ubiquitin-like conjugation systems in autophagosome formation.

Formation of autophagosome membranes occurs through two ubiquitin-like systems. In the first conjugation cascade, Atg7 and Atg10 coordinate the covalent binding of Atg5, Atg12, and Atg16. In the second arm, Atg8 is cleaved to generate LC3-I, which is then conjugated to the lipid PE by the action of Atg7 and Atg3. The lipid-bound form of Atg8 is known as LC3-II.

Regulation of autophagy

Autophagy is an evolutionarily conserved process whose primary task in lower organisms is the maintenance of metabolic homeostasis in the face of changing nutrient availability. Induction of autophagy leads to the degradation of non-essential cytoplasmic constituents into basic materials that can be reused for anabolism or energy production. As such, autophagy is tightly regulated by the nutrient supply via nutrient signaling pathways. In yeast, autophagy is situated downstream of the nutrient sensor phosphatidylinositol 3-kinase (PI3K), and its downstream effector Akt controls the activity of the kinase TOR

(target of rapamycin), a negative regulator of autophagy (Petiot et al., 2000; Arico et al., 2001). Thus, activation of insulin-like receptors and PI3K leads to stimulation of TOR activity and suppression of autophagy. Conversely, autophagy is induced by signals that indicate decreased nutrients such as growth factor removal, serum starvation, and amino acid depletion. Inhibition of TOR, either through decreased signaling through PI3K and Akt, or pharmacologically by the macrolide antibiotic rapamycin, also leads to up-regulation of autophagy (Noda and Ohsumi, 1998). In multicellular organisms, this general arrangement is conserved and nutrient sensing is subserved by PI3K Class I, although additional modes of regulation have also evolved, including activation by Class III PI3K which likely induces autophagy through interaction with Atg6 (Petiot et al., 2000).

Multiple roles for autophagy: matters of life and death

In yeast, the primary function of autophagy is to maintain viability during times of starvation. In multicellular organisms, autophagy is also critical to maintaining metabolic homeostasis, but has taken on additional, pleiotropic cellular functions. Autophagy is protective in stressful conditions such as nutrient or growth factor depletion, and also defends cells from invasion by certain pathogenic bacteria and viruses (Kirkegaard et al., 2004). Constitutive clearance of cytosolic proteins by low-level basal autophagy is an additional important cytoprotective function, particularly to neurons, as evidenced by accumulation of ubiquitinated proteinaceous deposits and the development of neurodegeneration in mice deficient for basal autophagy (Hara et al., 2006; Komatsu et al., 2006). Autophagy also plays a vital role in protecting cells from oxidative stress by

selectively eliminating damaged mitochondria, the most important source of free radicals in the cell (Kim et al., 2007).

In addition to this cytoprotective role, induction of autophagy can be detrimental. For example, some cancer cells use autophagy for protection against radiation therapy (Kondo et al., 2005), and various pathogens have evolved mechanisms to subvert autophagy for their own purposes (Kirkegaard et al., 2004). In some paradigms, activation of autophagy has been associated with non-apoptotic cell death, termed type II programmed cell death (Bursch, 2001; Gozuacik and Kimchi, 2004; Yu et al., 2004). Autophagy was initially implicated in cell death by work demonstrating a role for beclin-1 (a positive regulator of autophagy that is homologous to yeast ATG6) as a potential tumor suppressor. Beclin-1 directly associates with the anti-apoptotic protein Bcl-2 (Liang et al., 1998), and loss of beclin-1 activity predisposes to malignant transformation in animal models (Qu et al., 2003; Yue et al., 2003). Furthermore, beclin-1 mutations have been identified in human breast cancers (Aita et al., 1999). However, the precise relationship of beclin-1, induction of autophagy, and cell death remains obscure.

Neuronal cell death is frequently accompanied by autophagic features (Florez-McClure et al., 2004), although evidence of a role for autophagy in mediating cell death is limited to a few studies. In the nematode *C. elegans*, gain-of-function mutations in genes that encode specific ion channel subunits such as the degenerins DEG-1 and MEC-4, and the acetylcholine receptor subunit DEG-3 lead to a necrotic-like degeneration of a subset of neurons which is suppressed by genetic inhibition of autophagy genes (Toth et al., 2007). Similarly, in the Lurcher mouse model of cerebellar degeneration, autophagic neuronal

death was implicated as mediating the pathological effects of mutations in the GluR2^{Lc} glutamate receptor (Yue et al., 2002). The observation in Lurcher pathogenesis may have broad implications regarding the possibility that autophagy may be a common mediator of cell death initiated by excitotoxicity (Orr, 2002), but this remains to be established. However, a general role for autophagy in neuronal death remains speculative. In most instances in which autophagic morphology has been found to accompany neuronal cell death, it remains indeterminate whether autophagy is the culprit, whether autophagy was induced secondarily to facilitate the removal of cellular components, or whether autophagy was induced as a cytoprotective response to cellular stress. It is quite possible that autophagic induction has the potential to be either protective or destructive, and the influence of autophagy depends on the type, degree, and duration of the inciting cellular stress.

Decline of autophagy with aging

The autophagy-lysosome system undergoes striking changes in aging cells. Aging leads to reductions in autophagosome formation and autophagosome-lysosome fusion, both of which are consistent with decreased macroautophagy (Terman, 1995). There are also notable changes in lysosomes themselves, including increased lysosome volume, decreased lysosomal stability, altered activity of hydrolases, and intra-lysosomal accumulation of the indigestible material lipofuscin (Terman and Brunk, 2004). The precise molecular defects remain unknown, but these changes correlate with a decrease in the total capacity for degradation of long-lived proteins in many tissues of aged animals (Terman, 1995; Donati et al., 2001). Studies in aged rodents and senescent cells in culture

have revealed that aging is also associated with reduced rates of translocation of substrate proteins into lysosomes through chaperone-mediated autophagy (Cuervo and Dice, 2000). This reduction is caused by age-related changes including increased degradation of the lysosomal membrane protein LAMP-2A and reduced ability of LAMP-2A to reinsert into the lysosomal membrane (Dice, 2007).

The consequence of age-related decline in autophagy is diminished turnover of intracellular components and the reduced ability of cells to adapt to changes in the extracellular environment (Ward, 2002). Compromised clearance of old and/or damaged mitochondria by macroautophagy coupled with reduced turnover of long-lived proteins likely contribute to the intracellular accumulation of oxidized proteins in aged organisms (Kim et al., 2007). Age-related decline in autophagy may be particularly detrimental to the nervous system as post-mitotic cells such as neurons are vulnerable to the accumulation of undegraded metabolic products over the lifetime of the organism (Terman et al., 1999). Neuronal homeostasis uniquely depends on balanced, bidirectional trafficking of intracellular constituents between distal neurites and the cell soma. In neurons, autophagosomes and endosomes that fuse in the distal axon must be retrogradely transported, often over great distances, to the soma in order to fuse with lysosomes and degrade their contents (Hollenbeck, 1993; Yue, 2007). Thus, subtle disruptions of autophagosome formation, maturation, or trafficking would be predicted to have dire consequences for autophagic flux and neuronal homeostasis. Indeed, evidence is mounting that autophagic pathways are vitally important for the maintenance of neuronal health, particularly in the context of degenerative disease states.

Accumulation of autophagic vacuoles in patients and models of neurodegenerative disease

Autophagic vacuoles are rare in neurons of the normal adult brain (Nixon et al., 2005). Increasingly, however, accumulation of autophagic vacuoles has been appreciated in the affected brain regions of a wide variety of neurodegenerative diseases. In Alzheimer's disease, autophagic vacuoles appear in neocortical and hippocampal pyramidal neurons and accumulate markedly within the dendritic arbors of these affected cells (Nixon et al., 2005) (See Fig. A1.4 for images and additional description of altered autophagy in Alzheimer's disease). Autophagic vacuoles have also been described in melanized neurons of the substantia nigra in Parkinson's disease (Anglade et al., 1997), and in affected brain regions in a variety of prion diseases including Creutzfeldt-Jakob disease, Gerstmann-Straussler-Scheinker disease, and fatal familial insomnia, where prominent changes in axon terminals include the accumulation of autophagic vacuoles and features consistent with axonal degeneration (Sikorska et al., 2004). Accumulation of autophagic vacuoles has also been described in pathological evaluation of tissue from polyglutamine disease patients. For example, cathepsin D immunopositive autophagic vacuoles that contain remnants of polyglutamine-expanded huntingtin protein are found in lymphoblasts derived from Huntington's disease patients, while examination of cortical neurons by immunoelectron microscopy shows huntingtin-immunoreactive bodies that resemble multivesicular bodies, but are also cathepsin D positive and may be amphisomes or autolysosomes (Sapp et al., 1997).

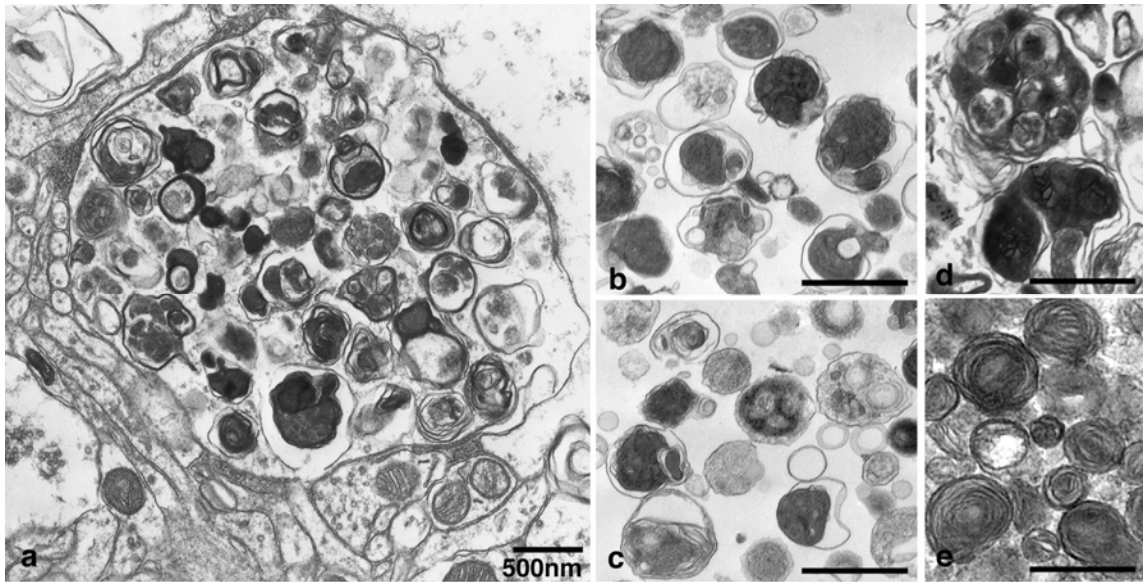


Figure A1.4. Accumulation of autophagic structures in Alzheimer's disease brain. (a) Ultrastructural appearance of dystrophic neurites from Alzheimer's disease brain demonstrating autophagic structures that are similar to autophagic structures from highly purified subcellular fractions from mouse liver (b, c). Autophagic structures morphologies in Alzheimer's brain include large double-membrane-limited vesicles containing multiple smaller double-membrane vesicles exhibiting heterogeneous intraluminal contents (d). Multilamellar bodies, another variant of autophagic structures, are also common in dystrophic neurites (e). This figure is adapted with permission from Nixon et al., 2005.

In many cases, the accumulation of autophagic vacuoles observed in patients with neurodegeneration has been recapitulated in respective disease models. For example, exogenous expression of a variety of polyglutamine-expanded disease proteins leads to an increase in biochemical and morphological markers of autophagy *in vitro* (Kegel et al., 2000; Taylor et al., 2003; Ravikumar et al., 2004; Iwata et al., 2005a) as well as in fly (Pandey et al., 2007) and mouse (Petersen et al., 2001; Skinner et al., 2001) models of polyglutamine diseases. However, from these descriptive studies it is not possible to distinguish whether accumulation of autophagic vacuoles is due to induction of autophagosome formation or a defect in clearance of autophagic vacuoles, such as might

occur with failure of autophagosome-lysosome fusion. If the accumulation of autophagic vacuoles observed in neurodegenerative disease is due to autophagy induction, descriptive studies also do not permit determination whether increased autophagy is helpful (e.g., an adaptive response to misfolded protein stress) or harmful (e.g., autophagic cell death). Of course, autophagy is not necessarily performing the same function in all diseases or at all stages within a single disease. Nevertheless, recognition of morphological features of altered autophagy in neurodegeneration set the stage for experimental studies of the functional role of autophagy in neurodegenerative diseases. Substantial progress has been made in sorting among these possibilities from studies of model systems of disease.

Autophagy is neuroprotective

Evidence suggesting a protective role for autophagy in the context of disease was initially provided by a series of *in vitro* studies demonstrating that disease-causing proteins are frequently degraded by autophagy. For example, pharmacological induction or inhibition of macroautophagy alters the rate of turnover of a polyglutamine-expanded protein, polyalanine-expanded protein, as well as wild type and mutant forms of α -synuclein (Ravikumar et al., 2002; Kabuta et al., 2006). Moreover, ultrastructural analysis by immuno-electron microscopy has demonstrated delivery of polyglutamine-expanded proteins to autophagic vacuoles (Kegel et al., 2000; Taylor et al., 2003). Chaperone-mediated autophagy has also been found to contribute to the degradation of α -synuclein, a process that is impaired by disease-causing mutations (Cuervo et al., 2004). An interesting observation is the recruitment of Atg proteins including LC3, Atg5, Atg12,

and Atg16 into mutant huntingtin aggregates, suggesting autophagic activity in the vicinity of protein inclusions (Iwata et al., 2005b; Yamamoto et al., 2006). However, as protein aggregates have recently been found to nonspecifically sequester autophagy components, these particular results should be interpreted with caution (Kuma et al., 2007). Collectively, these studies suggested that autophagy contributes to the degradation of multiple disease proteins and raised the possibility that induction of autophagy could be a protective pathway in the context of misfolded protein accumulation.

Compelling evidence that autophagy is neuroprotective was provided by a series of animal studies in which impairment of the autophagy-lysosomal system was consistently found to induce neurodegeneration. Knockout of cathepsin D, a lysosomal protease highly expressed in the nervous system, in mice caused accumulation of autophagosomes and lysosomes with accompanying neural dysfunction and degeneration (Koike et al., 2000; Koike et al., 2005; Shacka et al., 2007). Interestingly, signs of autophagic stress occur at very early ages in these mice and precede cell death (Koike et al., 2000). A *Drosophila* cathepsin D mutant also shows accumulation of indigestible pigments and modest neurodegeneration (Myllykangas et al., 2005). The importance of autophagy in neurodegeneration was further underscored by two studies examining conditional CNS knockout of autophagy in mice. Deficiency of Atg5 or Atg7, both critical genes for autophagosome formation, caused neurodegeneration characterized by ubiquitin-positive neuropathology (Hara et al., 2006; Komatsu et al., 2006). No evidence of proteasome impairment was detected, suggesting that loss of basal autophagy alone leads to ubiquitinated protein accumulation even in the context of normal UPS function. In

addition to highlighting the importance of autophagy in protecting neurons from toxic protein accumulation, these studies suggested the possibility of functional cross talk between autophagy and the UPS. Subsequent studies using *Drosophila* genetics provided direct evidence of a compensatory relationship between autophagy and the UPS (Pandey et al., 2007).

But what of autophagy in the context of neurodegenerative disease *in vivo*? In all of the studies published to date, autophagy has been found to be neuroprotective in the context of disease. In several different *Drosophila* models of neurodegeneration based on misexpression of disease related proteins, genetic inhibition of autophagy is detrimental while pharmacologic induction of autophagy with rapamycin is protective (Ravikumar et al., 2004; Ravikumar et al., 2006; Pandey et al., 2007). While the effect of TOR inhibition by rapamycin is pleiotropic, in two of these studies it was verified that the beneficial effect of rapamycin was autophagy-dependent (Ravikumar et al., 2005; Pandey et al., 2007). Consistent results were obtained in a *C. elegans* model expressing a pathologic huntingtin fragment, in which degeneration was enhanced by genetic inhibition of autophagy (Jia et al., 2007). Perhaps the most exciting result was the finding that treatment of a transgenic mouse model with CCI-779, an analog of rapamycin, ameliorated several metrics of neurodegeneration including tremor prevalence, grip strength, body and brain weight, and rotarod performance, thus extending observations to mammals (Ravikumar et al., 2004).

Can autophagy be co-opted for therapeutic benefit?

The evidence indicating that induction of autophagy is cytoprotective in neurodegenerative disease models raises the tantalizing possibility that this intracellular catabolic pathway may be exploited to clear toxic disease proteins and provide therapeutic benefit for patients. While rapamycin is an FDA-approved drug that has been used extensively in renal transplant patients, it is a less than optimal choice for therapeutic induction of autophagy as it is associated with serious adverse effects, most of which are related to long-term immunosuppression. Consequently, novel approaches to manipulating autophagy in human patients are desirable. Using a yeast screen, one recent study identified several small molecules capable of augmenting autophagy in mammalian cells and further demonstrated therapeutic benefit of these compounds in a *Drosophila* model of neurodegeneration (Sarkar et al., 2007). However, it remains to be seen whether any of these compounds will have clinical benefit and a favorable adverse effect profile in mammalian neurodegeneration models. Recently, overexpression of histone deacetylase 6 (HDAC6), a cytoplasmic deacetylase containing a ubiquitin binding domain, was found to suppress neurodegeneration in a model of polyglutamine disease and to compensate for defects in the UPS by facilitating autophagic protein degradation (Pandey et al., 2007). These results suggest that HDAC6 functions at the intersection of the UPS and autophagy and identify HDAC6 as a promising target for pharmacologic manipulation in neurodegeneration. Future studies defining the molecular details of autophagic degradation of misfolded proteins will likely provide additional targets for therapeutic intervention in neurodegenerative diseases.

Unanswered questions and future directions

While we now know that misfolded protein accumulation induces autophagy, and that autophagy suppresses neurodegeneration by assisting in the clearance of toxic protein species, unresolved questions remain. For instance, why is endogenous upregulation of autophagy insufficient to protect against the accumulation of proteotoxic species? Studies of autophagy and degeneration also underscore larger questions relating to fundamental issues in neurodegenerative disease. For instance, why do mutations that affect often ubiquitously expressed proteins specifically cause the demise of specific subpopulations of neurons? And finally, why is the onset of many neurodegenerative diseases age-dependent in spite of expression of toxic protein species throughout the lifespan? While the answers to these questions are sure to be multifactorial and complex, perhaps some of the answers are related to the changing nature of autophagy with age. It is possible that upregulation of autophagy is sufficient to effectively clear misfolded proteins and forestall neurodegeneration early in life, but that diminished autophagic protein degradation with age might allow toxic protein accumulation and late-onset development of neurodegenerative pathology. Postmitotic cells such as neurons are likely to be particularly vulnerable to subtle disruptions in protein degradation pathways and membrane homeostasis as they require massive coordination of long-distance trafficking of vesicles and trophic factors. Therefore, a neuronal age-related decline in autophagy combined with the unique homeostatic demands of neurons might largely contribute to the selective sensitivity of neurons to the accumulation of proteotoxins. Support for these notions has come from manipulation of aging pathways in model organisms. Inhibition of insulin signaling pathways prolongs lifespan in multiple species (Kenyon, 2005).

Strikingly, these pathways involve repression of PI3K and Akt signaling, manipulations which lead to upregulation of autophagy. Furthermore, autophagy is required for extension of lifespan in worms that are deficient in insulin-like signaling pathways, suggesting that mutations that extend lifespan might work by activating autophagy (Melendez et al., 2003). Recent evidence has now directly linked neurodegeneration to aging by demonstrating that aging pathways strongly influence the onset of disease in *C. elegans* models of neurodegeneration. Expression of A β in muscle causes the progressive development of motor degeneration, but by delaying the aging process, aggregation of A β and the onset of symptoms is also delayed (Cohen et al., 2006). In addition, knockdown of autophagy blocks the protective effects of delayed aging, suggesting that neuroprotection associated with manipulation of aging pathways is autophagy-dependent (Florez-McClure et al., 2007). These results are consistent with the notion that protein aggregation and accompanying neuronal dysfunction might occur coincident with age-related decline in cellular mechanisms to deal with misfolded protein species. Thus, the age-related onset of pathology in neurodegenerative conditions might be correlated with a decline in autophagic capacity beyond a critical threshold. However, additional studies will be required to define the precise relationship of aging, autophagy, and neurodegeneration.

The result suggesting that autophagy contributes to basal turnover of ubiquitinated proteins is a fascinating finding that provokes additional questions. Presently, it is not known whether autophagy contributes nonspecifically to bulk degradation of ubiquitinated proteins, whether a certain subset of ubiquitinated proteins is selectively

identified for autophagic degradation, or whether undigested autophagy substrates are futilely ubiquitinated after deposition. And how precisely does CNS knockout of autophagy lead to degeneration? Defects in basal autophagy could lead to altered neuronal homeostasis and degeneration through impaired utilization of nutrients or an imbalance of vesicular biogenesis and turnover. Alternatively, neuronal dysfunction might be a more direct result of failed protein degradation with resultant accumulation of ubiquitinated protein aggregates. A final question: is autophagy universally protective in the context of neurodegenerative disease? A recent provocative study has implicated autophagy as a contributor to the production of toxic A β species in Alzheimer's disease suggests that this is not necessarily so (Yu et al., 2005). Perhaps in the case of some diseases autophagy is initially induced as a neuroprotective response in stressed or injured neurons but is subsequently overwhelmed or impaired by disease-related factors. This could partly account for evidence that autophagy seems to be both induced and impaired in several major neurodegenerative diseases. Interestingly, mutations in Fig4, a protein which regulates levels of PI(3,5)P, have been found to cause an autosomal recessive form of Charcot-Marie-Tooth disease known as CMT4J (Chow et al., 2007). These mutations were subsequently shown to inhibit autophagy within axons, suggesting that defects in the autophagy-lysosomal pathway might underlie peripheral neuropathy in addition to loss of neurons in the brain and spinal cord (Ferguson et al., 2009). Future experiments will be needed to address whether such disruption of autophagy leads to the pathological accumulation of toxic, misfolded proteins, or whether blockage of autophagic flux causes disease through an as yet unidentified mechanism.

Appendix 2: HDAC6 regulates the steady-state levels and turnover of polyglutamine-expanded androgen receptor

This section summarizes work that was included as part of the following publication:

Pandey, U.B., Nie, Z., Batlevi, Y., McCray, B.A., Ritson, G.P., Nedelsky, N.B., Schwartz, S.L., DiProspero, N.A., Knight, M.A., Schuldiner, O., Padmanabhan, R., Hild, M., Berry, D.L., Garza, D., Hubbert, C.C., Yao, T.P., Baehrecke, E.H., and Taylor, J.P. HDAC6 rescues neurodegeneration and provides an essential link between autophagy and the UPS. *Nature* **447**, 859-63 (2007).

Abstract

A prominent feature of late-onset neurodegenerative diseases is accumulation of misfolded protein in vulnerable neurons (Taylor et al., 2002). When levels of misfolded protein overwhelm degradative pathways, the result is cellular toxicity and neurodegeneration (Trojanowski and Lee, 2000). Cellular mechanisms for degrading misfolded protein include the ubiquitin-proteasome system (UPS), the main non-lysosomal degradative pathway for ubiquitinated proteins, and autophagy, a lysosome-mediated degradative pathway (Rubinsztein, 2006). The UPS and autophagy have long been viewed as complementary degradation systems with no point of intersection (Ciechanover et al., 1984; Pickart, 2004). This view has been challenged by two observations suggesting an apparent interaction: impairment of the UPS induces autophagy *in vitro*, and conditional knockout of autophagy in the mouse brain leads to neurodegeneration with ubiquitin-positive pathology (Rideout et al., 2004; Iwata et al., 2005a; Hara et al., 2006; Komatsu et al., 2006). It is not known whether autophagy is strictly a parallel degradation system, or whether it is a compensatory degradation system when the UPS is impaired; furthermore, if there is a compensatory interaction between these systems, the molecular link is not known. Pandey et al. show that autophagy acts as a compensatory degradation system when the UPS is impaired in *Drosophila melanogaster*, and that histone deacetylase 6 (HDAC6), a microtubule-associated deacetylase that interacts with polyubiquitinated proteins (Kawaguchi et al., 2003), is an essential mechanistic link in this compensatory interaction. The data presented in Pandey et al. show that compensatory autophagy is induced in response to mutations affecting the

proteasome and in response to UPS impairment in a fly model of the neurodegenerative disease spinobulbar muscular atrophy caused by polyglutamine tract expansion in the androgen receptor (AR). Furthermore, expression of HDAC6 is sufficient to rescue degeneration associated with UPS dysfunction *in vivo* in an autophagy-dependent manner. The work presented in this appendix specifically demonstrates that HDAC6 rescues degeneration in flies expressing polyglutamine-expanded AR by facilitating AR turnover.

Introduction

Neurodegenerative diseases such as Parkinson's disease, Alzheimer's disease, familial amyotrophic lateral sclerosis, and the polyglutamine diseases are characterized by the accumulation of toxic misfolded protein species (Ross and Poirier, 2004). These misfolded proteins result in cytotoxicity and neuronal death through mechanisms that are poorly understood. Polyglutamine diseases constitute a family of nine dominantly-inherited neurodegenerative diseases caused by expansion of a polymorphic polyglutamine (CAG) tract within the disease protein (Zoghbi and Orr, 2000).

Spinobulbar muscular atrophy (SBMA) belongs to the polyglutamine disease family and results from polyglutamine expansion within the androgen receptor (AR) gene (La Spada et al., 1991). Polyglutamine disease manifests when the glutamine repeat reaches a critical threshold, and polyglutamine repeat length is strongly correlated with disease severity (Doyu et al., 1992). The expanded polyglutamine repeat confers a toxic gain of function to the normal gene product (Warrick et al., 1998; Moulder et al., 1999; Marsh et al., 2000). Expanded polyglutamine proteins form intracellular aggregates that can coalesce into ubiquitin-positive protein inclusions (Taylor et al., 2003). Although it is unclear which species in the aggregation/inclusion process is toxic, it is likely that interventions directed at augmenting turnover of polyglutamine proteins will have therapeutic value (Taylor et al., 2003; Arrasate et al., 2004).

HDAC6 is a cytoplasmic deacetylase that contains two deacetylase domains, a ubiquitin-binding zinc finger domain, and a dynein-binding domain (Seigneurin-Berny et al., 2001;

Kawaguchi et al., 2003). Deacetylase targets of HDAC6 include HSP90, α -tubulin, and the actin binding protein cortactin (Hubbert et al., 2002; Kovacs et al., 2005; Zhang et al., 2007). HDAC6 binds misfolded, ubiquitinated proteins and facilitates their retrograde microtubule trafficking into specialized cellular structures termed “aggresomes” (Johnston et al., 1998; Kawaguchi et al., 2003). Aggresomes form in response to misfolded protein stress and represent an adaptive response that serves to sequester toxic proteins and facilitate their degradation (Taylor et al., 2003; Arrasate et al., 2004; Tanaka et al., 2004; Burnett and Pittman, 2005). HDAC6 has been shown to be required for aggresome formation, and its activity can protect against misfolded protein stress *in vitro* (Kawaguchi et al., 2003). However, aggresomes are primarily a cell culture phenomenon and their relevance to misfolded protein disease pathogenesis remains unclear. Furthermore, the role of HDAC6 in mediating misfolded protein turnover has not been explored *in vivo*. In the present study, we investigated the role of HDAC6 in the autophagic pathway and examined how HDAC6 levels influence the phenotypes associated with expression of misfolded, toxic proteins.

Materials and Methods

Fly stocks

All *Drosophila* stocks were maintained on standard media in 25°C incubators unless otherwise noted. DHT (Steraloids) was mixed with freshly made food once it had cooled to <50°C to a final concentration of 1 mM. To generate AR transgenic flies, cDNA encoding full length human AR with 12, 77, or 121 CAG repeats was subcloned into pUAST (Brand and Perrimon, 1993). The cDNA for dHDAC6 was generated from EST LD43531 which encodes 1128 amino acids corresponding to HDAC6-RA on Flybase. Kpn1 and Xba1 restriction sites were included in the 5' and 3' primers, respectively for subcloning into the vector pAc5.1/V5 (Invitrogen). The dHDAC6 cDNA plus in-frame V5 tag was subsequently subcloned into pUAST. UAS-atg6-IR flies were described previously (Scott et al., 2004). Inverted repeats for UAS-atg12-IR flies were generated with primers 5'-ggcgcgccTATCC TTCTGAACGCCACTG-3' and 5'-gcggaattcCTTAGCAAAGTCATGTGCG TATCG-3' as described previously (Scott et al., 2004).

Transgenic *Drosophila* lines were generated using standard techniques (Rubin and Spradling, 1982). The GMR-GAL4 line was obtained from the Bloomington Stock Center (Bloomington). AR20Q and AR52Q flies were provided by Kenichi Takeyama. *Elav*-GeneSwitch flies were described previously (Osterwalder et al., 2001). Eye phenotypes of 1-day-old anesthetized flies were evaluated with a Leica MZ APO stereomicroscope and photographed with a Leica DFC320 digital camera.

SEM

SEM samples were collected and fixed in 2.5% glutaraldehyde (EMSin PBS, and post-fixed for 15-30 minutes in 1.5% osmium tetroxide (Stevens Metallurgical) in PBS.

Samples were then dehydrated in ethanol, immersed in hexamethyldisilazane (Polysciences Inc.) and dried in a desiccator for three days. Specimens were then coated with gold:palladium using a Denton DV-503 vacuum evaporator, and analyzed using an AMRAY 1820D scanning electron microscope.

Protein turnover assay

UAS-AR or UAS-AR; UAS-dHDAC6-V5 transgenic flies were combined with flies expressing GeneSwitch GAL4 under the *elav* pan-neuronal enhancer. All flies were maintained at 25°C for the duration of the experiment. To monitor protein turnover *in vivo*, 1-day-old adult flies of the appropriate genotype were collected and starved for 12 hours in a vial that contained only a kimwipe soaked with 3 ml of water. After starvation, flies were placed in a vial that contained a kimwipe soaked with 3 ml of 500 μ M RU486 dissolved in a 2% sucrose solution (minus DHT condition) or 500 μ M RU486 and 1 mM DHT in a 2% sucrose solution (plus DHT condition) for 1 hour, and then transferred to a vial containing normal food (minus DHT condition) or food containing 1 mM DHT (plus DHT condition) until collected for extract preparation. Five flies were collected every 2.5 hours up to 20 hours, heads were removed, crushed in RIPA buffer, sonicated, and analyzed by Western blot. AR, actin, and V5-tagged HDAC6 protein levels were assessed by immunoblot using antibodies against AR (N20, Santa Cruz

Biotech), 119 α -actin (119, Santa Cruz Biotech), and V5 epitope (Sigma). Quantification of luminescence was performed with a Kodak IS2000RT instrument and Kodak Molecular Imaging software. Minus DHT experiments were performed in quadruplicate and plus DHT experiments in triplicate. Mean AR/actin ratios and standard error of the mean were plotted on a logarithmic scale.

Results and Discussion

HDAC6 suppresses degeneration associated with misfolded protein stress

To determine whether overexpression of histone deacetylase 6 (HDAC6) could suppress degeneration associated with misfolded protein stress, flies expressing polyglutamine-expanded androgen receptor (AR) in eye tissue were crossed to flies expressing *Drosophila* HDAC6 (dHDAC6). As the ligand for AR is required for toxicity, AR52-expressing flies reared on food without ligand showed no degenerative phenotype (Fig. A2.1.A). However, flies reared on food containing dihydrotestosterone (DHT), the ligand for AR, demonstrate a degenerative rough-eye phenotype characterized by supernumerary bristles and ommatidial disorganization, collapse, and pitting (Fig. A2.1.B). Ectopic expression of dHDAC6 strongly suppressed the ligand-dependent degenerative phenotype in flies expressing polyglutamine-expanded AR (Fig. A2.1.C). Thus, overexpression of dHDAC6 protects cells from polyglutamine toxicity *in vivo*.

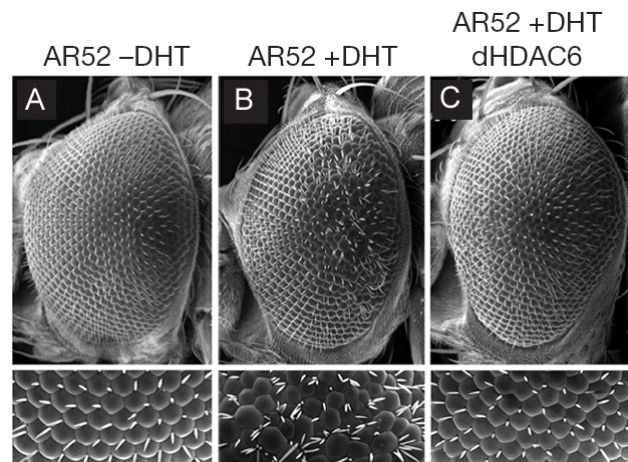


Figure A2.1. HDAC6 rescues degeneration in SBMA flies. SEM images of fly eyes expressing the indicated transgenes. Flies were reared either with or without DHT as indicated. **(A)** Normal eyes in AR52 flies reared without DHT. **(B)** Rough eyes in AR52 flies reared with DHT. **(C)** Degeneration was suppressed by expression of dHDAC6. DHT = dihydrotestosterone.

HDAC6 accelerates the turnover of misfolded proteins

We hypothesized that ectopic dHDAC6 suppressed degeneration in AR-expressing flies by promoting autophagic degradation of aberrant protein. Thus, we examined AR-expressing flies and determined that overexpression of dHDAC6 led to lower steady-state levels of polyglutamine-expanded AR (Fig. A2.2.A). In contrast, inhibition of autophagy by knockdown of the autophagy genes *atg6* or *atg12* resulted in higher steady state levels of AR (Fig. A2.2.A). Altered steady-state levels occurred despite no significant change in RNA levels (data not shown), suggesting that dHDAC6 accelerates the rate of AR degradation. To investigate this further, we adapted the inducible GeneSwitch (GS) expression system to monitor protein turnover *in vivo*. This system utilizes a GAL4-progesterone receptor fusion protein that is only active and able to induce expression of UAS-driven transgenes when a progesterone receptor ligand such as RU486 is administered (Osterwalder et al., 2001). Using this system, we tested whether dHDAC6 overexpression increases the rate of turnover of AR52 in *Drosophila* neuronal tissue *in vivo*. In *elav*-GS;UAS-AR52 flies, no RU486-mediated expression was detected prior to induction of protein expression (data not shown). To induce expression, starved flies were fed sucrose media containing RU486 for one hour, which resulted in a pulse of expression that became detectable within 2 hours, peaked after approximately 10 hours, and then gradually decayed (Fig. A2.2.B-C). In *elav*-GS;UAS-AR52;UAS-dHAD6 flies, there was a parallel induction of AR52 expression, but an accelerated rate of decay (Fig. A2.2.C-D). We estimated the half-life of AR52 *in vivo* by regression analysis using AR52 levels between 10-20 hours post-induction and determined that co-expression of

dHDAC6 reduced the half-life by approximately 2-fold (Fig. A2.2.C). Importantly, co-expression of dHDAC6 not only accelerated the turnover of AR52 monomers, but also high molecular weight aggregates that were trapped in the stacking gel (Fig. A2.2.B, D). This suggests augmented turnover of AR when dHDAC6 levels are increased.

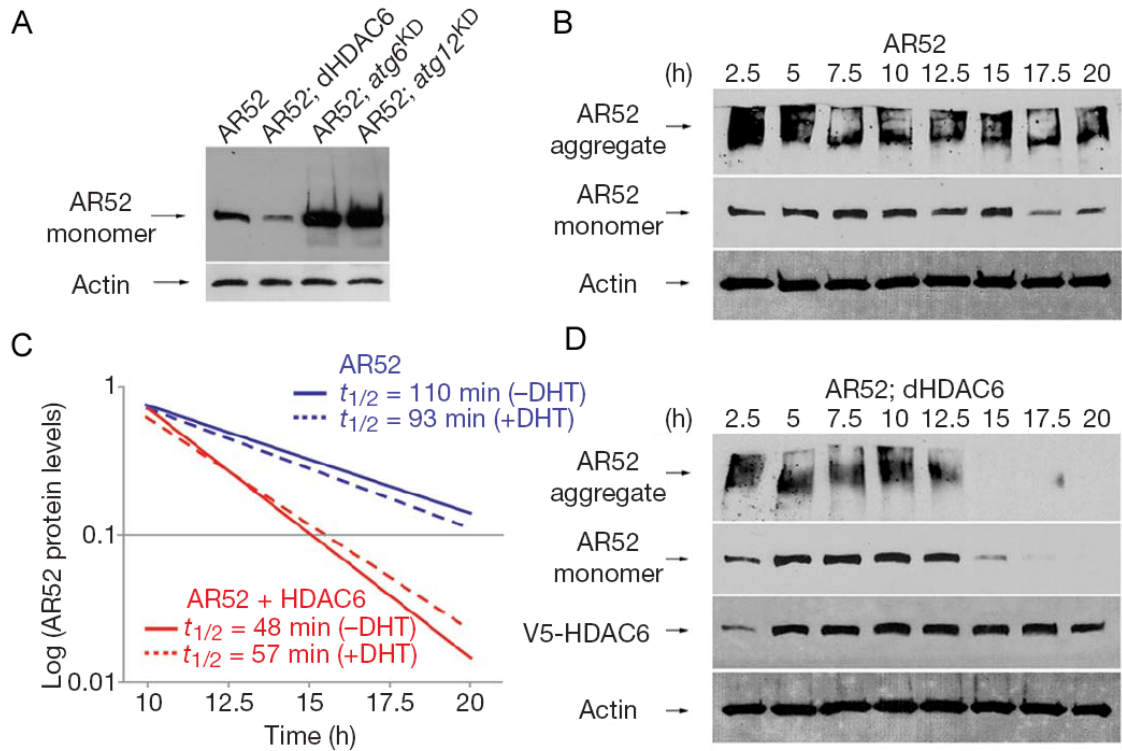


Figure A2.2. HDAC6 accelerates the turnover of polyglutamine-expanded AR. (A, B, D) Western blots from flies expressing the indicated transgenes. (A) Steady-state levels of AR52 protein are reduced in flies overexpressing dHDAC6, but are elevated in flies in which *atg6* or *atg12* has been knocked down. (B) Western blots showing the temporal profile of AR52 protein monomer and high molecular weight aggregate levels after a brief pulse of expression. (C) A logarithmic plot of AR52/actin ratios was used to determine the line of best fit by regression analysis ($y=Ae^{-Kx}$). $R^2=0.9117$ (AR52 -DHT), $R^2=0.7808$ (AR52 +DHT), $R^2=0.9719$ (HDAC6 + (AR52 -DHT)), $R^2=0.9644$ (HDAC6 + (AR52 +DHT)). Half-life was determined by the slope of the best fit line with the equation $t_{1/2} = 0.693/K$. Half-life of AR52 in vivo was reduced ~2-fold in flies co-expressing dHDAC6 and did not differ significantly in the presence (broken lines) or absence (solid lines) of DHT. (D) Flies co-expressing dHDAC6 showed a nearly identical profile of induced expression as in (B), but AR protein decayed at an accelerated rate. Exogenous dHDAC6 was detected by immunoblot against the V5 epitope.

Together, these results suggest that HDAC6 can dramatically suppress degeneration associated with overexpression of toxic, misfolded proteins *in vivo*. Furthermore, our results suggest that the suppressing effect of HDAC6 is mediated by acceleration of protein turnover through the autophagic pathway since HDAC6-mediated suppression of degeneration requires autophagy (data not shown). As HDAC6 both binds ubiquitinated proteins and is able to traffic along microtubules, HDAC6 may play a role in directing misfolded proteins to autophagic machinery or may more directly regulate autophagic vacuole maturation, trafficking, or fusion. Future experiments will address the specific role of HDAC6 in facilitating the autophagic degradation of misfolded proteins.

References

- Ahlberg J, Marzella L, Glaumann H (1982) Uptake and degradation of proteins by isolated rat liver lysosomes. Suggestion of a microautophagic pathway of proteolysis. *Lab Invest* 47:523-532.
- Aita VM, Liang XH, Murty VV, Pincus DL, Yu W, Cayanis E, Kalachikov S, Gilliam TC, Levine B (1999) Cloning and genomic organization of beclin 1, a candidate tumor suppressor gene on chromosome 17q21. *Genomics* 59:59-65.
- Ali BR, Wasmeier C, Lamoreux L, Strom M, Seabra MC (2004) Multiple regions contribute to membrane targeting of Rab GTPases. *J Cell Sci* 117:6401-6412.
- Andres DA, Seabra MC, Brown MS, Armstrong SA, Smeland TE, Cremers FP, Goldstein JL (1993) cDNA cloning of component A of Rab geranylgeranyl transferase and demonstration of its role as a Rab escort protein. *Cell* 73:1091-1099.
- Anglade P, Vyas S, Javoy-Agid F, Herrero MT, Michel PP, Marquez J, Mouatt-Prigent A, Ruberg M, Hirsch EC, Agid Y (1997) Apoptosis and autophagy in nigral neurons of patients with Parkinson's disease. *Histol Histopathol* 12:25-31.
- Arico S, Petiot A, Bauvy C, Dubbelhuis PF, Meijer AJ, Codogno P, Ogier-Denis E (2001) The tumor suppressor PTEN positively regulates macroautophagy by inhibiting the phosphatidylinositol 3-kinase/protein kinase B pathway. *J Biol Chem* 276:35243-35246.
- Arrasate M, Mitra S, Schweitzer ES, Segal MR, Finkbeiner S (2004) Inclusion body formation reduces levels of mutant huntingtin and the risk of neuronal death. *Nature* 431:805-810.
- Arstila AU, Trump BF (1968) Studies on cellular autophagocytosis. The formation of autophagic vacuoles in the liver after glucagon administration. *Am J Pathol* 53:687-733.
- Auer-Grumbach M, Wagner K, Timmerman V, De Jonghe P, Hartung HP (2000a) Ulceromutilating neuropathy in an Austrian kinship without linkage to hereditary motor and sensory neuropathy IIB and hereditary sensory neuropathy I loci. *Neurology* 54:45-52.
- Auer-Grumbach M, De Jonghe P, Wagner K, Verhoeven K, Hartung HP, Timmerman V (2000b) Phenotype-genotype correlations in a CMT2B family with refined 3q13-q22 locus. *Neurology* 55:1552-1557.
- Barisic N, Claeys KG, Sirotkovic-Skerlev M, Lofgren A, Nelis E, De Jonghe P, Timmerman V (2008) Charcot-Marie-Tooth disease: a clinico-genetic confrontation. *Ann Hum Genet* 72:416-441.
- Berg TO, Fengsrud M, Stromhaug PE, Berg T, Seglen PO (1998) Isolation and characterization of rat liver amphisomes. Evidence for fusion of autophagosomes with both early and late endosomes. *J Biol Chem* 273:21883-21892.
- Bergoffen J, Scherer SS, Wang S, Scott MO, Bone LJ, Paul DL, Chen K, Lensch MW, Chance PF, Fischbeck KH (1993) Connexin mutations in X-linked Charcot-Marie-Tooth disease. *Science* 262:2039-2042.
- Brand AH, Perrimon N (1993) Targeted gene expression as a means of altering cell fates and generating dominant phenotypes. *Development* 118:401-415.
- Brett CL, Plemel RL, Lobinger BT, Vignali M, Fields S, Merz AJ (2008) Efficient termination of vacuolar Rab GTPase signaling requires coordinated action by a GAP and a protein kinase. *J Cell Biol* 182:1141-1151.
- Brickner JH, Fuller RS (1997) SOI1 encodes a novel, conserved protein that promotes TGN-endosomal cycling of Kex2p and other membrane proteins by modulating the function of two TGN localization signals. *J Cell Biol* 139:23-36.
- Bright NA, Gratian MJ, Luzio JP (2005) Endocytic delivery to lysosomes mediated by concurrent fusion and kissing events in living cells. *Curr Biol* 15:360-365.

- Brunger AT, Adams PD, Clore GM, DeLano WL, Gros P, Grosse-Kunstleve RW, Jiang JS, Kuszewski J, Nilges M, Pannu NS, Read RJ, Rice LM, Simonson T, Warren GL (1998) Crystallography & NMR system: A new software suite for macromolecular structure determination. *Acta Crystallogr D Biol Crystallogr* 54:905-921.
- Bucci C, Thomsen P, Nicoziani P, McCarthy J, van Deurs B (2000) Rab7: a key to lysosome biogenesis. *Mol Biol Cell* 11:467-480.
- Burnett BG, Pittman RN (2005) The polyglutamine neurodegenerative protein ataxin 3 regulates aggresome formation. *Proc Natl Acad Sci U S A* 102:4330-4335.
- Bursch W (2001) The autophagosomal-lysosomal compartment in programmed cell death. *Cell Death Differ* 8:569-581.
- Cabrera M, Ostrowicz CW, Mari M, LaGrassa TJ, Reggiori F, Ungermann C (2009) Vps41 phosphorylation and the Rab Ypt7 control the targeting of the HOPS complex to endosome-vacuole fusion sites. *Mol Biol Cell* 20:1937-1948.
- Cai Y, Chin HF, Lazarova D, Menon S, Fu C, Cai H, Sclafani A, Rodgers DW, De La Cruz EM, Ferro-Novick S, Reinisch KM (2008) The structural basis for activation of the Rab Ypt1p by the TRAPP membrane-tethering complexes. *Cell* 133:1202-1213.
- Campenot RB (1977) Local control of neurite development by nerve growth factor. *Proc Natl Acad Sci U S A* 74:4516-4519.
- Cantalupo G, Alifano P, Roberti V, Bruni CB, Bucci C (2001) Rab-interacting lysosomal protein (RILP): the Rab7 effector required for transport to lysosomes. *Embo J* 20:683-693.
- Caplan S, Hartnell LM, Aguilar RC, Naslavsky N, Bonifacino JS (2001) Human Vam6p promotes lysosome clustering and fusion in vivo. *J Cell Biol* 154:109-122.
- Cardoso C, Leventer RJ, Ward HL, Toyo-Oka K, Chung J, Gross A, Martin CL, Allanson J, Pilz DT, Olney AH, Mutchinick OM, Hirotsune S, Wynshaw-Boris A, Dobyns WB, Ledbetter DH (2003) Refinement of a 400-kb critical region allows genotypic differentiation between isolated lissencephaly, Miller-Dieker syndrome, and other phenotypes secondary to deletions of 17p13.3. *Am J Hum Genet* 72:918-930.
- Caviston JP, Holzbaur EL (2006) Microtubule motors at the intersection of trafficking and transport. *Trends Cell Biol* 16:530-537.
- Ceresa BP, Bahr SJ (2006) rab7 activity affects epidermal growth factor:epidermal growth factor receptor degradation by regulating endocytic trafficking from the late endosome. *J Biol Chem* 281:1099-1106.
- Chai A, Withers J, Koh YH, Parry K, Bao H, Zhang B, Budnik V, Pennetta G (2008) hVAPB, the causative gene of a heterogeneous group of motor neuron diseases in humans, is functionally interchangeable with its Drosophila homologue DVAP-33A at the neuromuscular junction. *Hum Mol Genet* 17:266-280.
- Chavrier P, Gorvel JP, Stelzer E, Simons K, Gruenberg J, Zerial M (1991) Hypervariable C-terminal domain of rab proteins acts as a targeting signal. *Nature* 353:769-772.
- Chen XJ, Levedakou EN, Millen KJ, Wollmann RL, Soliven B, Popko B (2007) Proprioceptive sensory neuropathy in mice with a mutation in the cytoplasmic Dynein heavy chain 1 gene. *J Neurosci* 27:14515-14524.
- Chevalier-Larsen ES, Wallace KE, Pennise CR, Holzbaur EL (2008) Lysosomal proliferation and distal degeneration in motor neurons expressing the G59S mutation in the p150Glued subunit of dynein. *Hum Mol Genet* 17:1946-1955.
- Chow CY, Zhang Y, Dowling JJ, Jin N, Adamska M, Shiga K, Szigeti K, Shy ME, Li J, Zhang X, Lupski JR, Weisman LS, Meisler MH (2007) Mutation of FIG4 causes neurodegeneration in the pale tremor mouse and patients with CMT4J. *Nature* 448:68-72.

- Ciechanover A (2005) Intracellular protein degradation: from a vague idea thru the lysosome and the ubiquitin-proteasome system and onto human diseases and drug targeting. *Cell Death Differ* 12:1178-1190.
- Ciechanover A, Brundin P (2003) The ubiquitin proteasome system in neurodegenerative diseases: sometimes the chicken, sometimes the egg. *Neuron* 40:427-446.
- Ciechanover A, Finley D, Varshavsky A (1984) Ubiquitin dependence of selective protein degradation demonstrated in the mammalian cell cycle mutant ts85. *Cell* 37:57-66.
- Claude P, Hawrot E, Dunis DA, Campenot RB (1982) Binding, internalization, and retrograde transport of 125I-nerve growth factor in cultured rat sympathetic neurons. *J Neurosci* 2:431-442.
- Cohen E, Bieschke J, Perciavalle RM, Kelly JW, Dillin A (2006) Opposing activities protect against age-onset proteotoxicity. *Science* 313:1604-1610.
- Conner SD, Schmid SL (2003) Regulated portals of entry into the cell. *Nature* 422:37-44.
- Cowtan K (1994) A CCP4 density modification package. *Joint CCP4 and ESF-EACBM Newsletter on Protein Crystallography* 31:34-38.
- Cuervo AM (2004) Autophagy: many paths to the same end. *Mol Cell Biochem* 263:55-72.
- Cuervo AM, Dice JF (1996) A receptor for the selective uptake and degradation of proteins by lysosomes. *Science* 273:501-503.
- Cuervo AM, Dice JF (2000) Age-related decline in chaperone-mediated autophagy. *J Biol Chem* 275:31505-31513.
- Cuervo AM, Stefanis L, Fredenburg R, Lansbury PT, Sulzer D (2004) Impaired degradation of mutant alpha-synuclein by chaperone-mediated autophagy. *Science* 305:1292-1295.
- Cui B, Wu C, Chen L, Ramirez A, Bearer EL, Li WP, Mobley WC, Chu S (2007) One at a time, live tracking of NGF axonal transport using quantum dots. *Proc Natl Acad Sci U S A* 104:13666-13671.
- D'Adamo P, Menegon A, Lo Nigro C, Grasso M, Gulisano M, Tamanini F, Bienvenu T, Gedeon AK, Oostra B, Wu SK, Tandon A, Valtorta F, Balch WE, Chelly J, Toniolo D (1998) Mutations in GDI1 are responsible for X-linked non-specific mental retardation. *Nat Genet* 19:134-139.
- De Jonghe P, Timmerman V, Ceuterick C, Nelis E, De Vriendt E, Lofgren A, Vercruyssen A, Verellen C, Van Maldergem L, Martin JJ, Van Broeckhoven C (1999) The Thr124Met mutation in the peripheral myelin protein zero (MPZ) gene is associated with a clinically distinct Charcot-Marie-Tooth phenotype. *Brain* 122 (Pt 2):281-290.
- Deinhardt K, Salinas S, Verastegui C, Watson R, Worth D, Hanrahan S, Bucci C, Schiavo G (2006) Rab5 and Rab7 control endocytic sorting along the axonal retrograde transport pathway. *Neuron* 52:293-305.
- Delcroix JD, Valletta JS, Wu C, Hunt SJ, Kowal AS, Mobley WC (2003) NGF signaling in sensory neurons: evidence that early endosomes carry NGF retrograde signals. *Neuron* 39:69-84.
- Delprato A, Lambright DG (2007) Structural basis for Rab GTPase activation by VPS9 domain exchange factors. *Nat Struct Mol Biol* 14:406-412.
- Deppmann CD, Mihalas S, Sharma N, Lonze BE, Niebur E, Ginty DD (2008) A model for neuronal competition during development. *Science* 320:369-373.
- Di Paolo G, De Camilli P (2006) Phosphoinositides in cell regulation and membrane dynamics. *Nature* 443:651-657.
- Dice JF (1990) Peptide sequences that target cytosolic proteins for lysosomal proteolysis. *Trends Biochem Sci* 15:305-309.
- Dice JF (2007) Chaperone-mediated autophagy. *Autophagy* 3:295-299.

- Dirac-Svejstrup AB, Sumizawa T, Pfeffer SR (1997) Identification of a GDI displacement factor that releases endosomal Rab GTPases from Rab-GDI. *EMBO J* 16:465-472.
- Donati A, Cavallini G, Paradiso C, Vittorini S, Pollera M, Gori Z, Bergamini E (2001) Age-related changes in the regulation of autophagic proteolysis in rat isolated hepatocytes. *J Gerontol A Biol Sci Med Sci* 56:B288-293.
- Dong G, Medkova M, Novick P, Reinisch KM (2007) A catalytic coiled coil: structural insights into the activation of the Rab GTPase Sec4p by Sec2p. *Mol Cell* 25:455-462.
- Dong J, Chen W, Welford A, Wandinger-Ness A (2004) The proteasome alpha-subunit XAPC7 interacts specifically with Rab7 and late endosomes. *J Biol Chem* 279:21334-21342.
- Doyu M, Sobue G, Mukai E, Kachi T, Yasuda T, Mitsuma T, Takahashi A (1992) Severity of X-linked recessive bulbospinal neuronopathy correlates with size of the tandem CAG repeat in androgen receptor gene. *Ann Neurol* 32:707-710.
- Dunn WA, Jr., Cregg JM, Kiel JA, van der Klei IJ, Oku M, Sakai Y, Sibirny AA, Stasyk OV, Veenhuis M (2005) Pexophagy: the selective autophagy of peroxisomes. *Autophagy* 1:75-83.
- Dupuis L, Fergani A, Braunstein KE, Eschbach J, Holl N, Rene F, Gonzalez De Aguilar JL, Zoerner B, Schwalenstocker B, Ludolph AC, Loeffler JP (2009) Mice with a mutation in the dynein heavy chain 1 gene display sensory neuropathy but lack motor neuron disease. *Exp Neurol* 215:146-152.
- Eathiraj S, Pan X, Ritacco C, Lambright DG (2005) Structural basis of family-wide Rab GTPase recognition by rabenosyn-5. *Nature* 436:415-419.
- Einarsdottir E, Carlsson A, Minde J, Toolanen G, Svensson O, Solders G, Holmgren G, Holmberg D, Holmberg M (2004) A mutation in the nerve growth factor beta gene (NGFB) causes loss of pain perception. *Hum Mol Genet* 13:799-805.
- Eitzen G, Will E, Gallwitz D, Haas A, Wickner W (2000) Sequential action of two GTPases to promote vacuole docking and fusion. *EMBO J* 19:6713-6720.
- Emsley P, Cowtan K (2004) Coot: model-building tools for molecular graphics. *Acta Crystallogr D Biol Crystallogr* 60:2126-2132.
- Entchev EV, Schwabedissen A, Gonzalez-Gaitan M (2000) Gradient formation of the TGF-beta homolog Dpp. *Cell* 103:981-991.
- Esters H, Alexandrov K, Iakovenko A, Ivanova T, Thoma N, Rybin V, Zerial M, Scheidig AJ, Goody RS (2001) Vps9, Rabex-5 and DSS4: proteins with weak but distinct nucleotide-exchange activities for Rab proteins. *J Mol Biol* 310:141-156.
- Evgrafov OV et al. (2004) Mutant small heat-shock protein 27 causes axonal Charcot-Marie-Tooth disease and distal hereditary motor neuropathy. *Nat Genet* 36:602-606.
- Feng Y, Press B, Wandinger-Ness A (1995) Rab 7: an important regulator of late endocytic membrane traffic. *J Cell Biol* 131:1435-1452.
- Ferguson CJ, Lenk GM, Meisler MH (2009) Defective autophagy in neurons and astrocytes from mice deficient in PI(3,5)P2. *Hum Mol Genet* 18:4868-4878.
- Florez-McClure ML, Hohsfield LA, Fonte G, Bealor MT, Link CD (2007) Decreased Insulin-Receptor Signaling Promotes the Autophagic Degradation of beta-Amyloid Peptide in *C. elegans*. *Autophagy* 3.
- Florez-McClure ML, Linseman DA, Chu CT, Barker PA, Bouchard RJ, Le SS, Laessig TA, Heidenreich KA (2004) The p75 neurotrophin receptor can induce autophagy and death of cerebellar Purkinje neurons. *J Neurosci* 24:4498-4509.
- Fukui K, Sasaki T, Imazumi K, Matsuura Y, Nakanishi H, Takai Y (1997) Isolation and characterization of a GTPase activating protein specific for the Rab3 subfamily of small G proteins. *J Biol Chem* 272:4655-4658.

- Gozuacik D, Kimchi A (2004) Autophagy as a cell death and tumor suppressor mechanism. *Oncogene* 23:2891-2906.
- Gu F, Gruenberg J (1999) Biogenesis of transport intermediates in the endocytic pathway. *FEBS Lett* 452:61-66.
- Gutierrez MG, Munafo DB, Beron W, Colombo MI (2004) Rab7 is required for the normal progression of the autophagic pathway in mammalian cells. *J Cell Sci* 117:2687-2697.
- Haas AK, Fuchs E, Kopajtich R, Barr FA (2005) A GTPase-activating protein controls Rab5 function in endocytic trafficking. *Nat Cell Biol* 7:887-893.
- Hadano S et al. (2001) A gene encoding a putative GTPase regulator is mutated in familial amyotrophic lateral sclerosis 2. *Nat Genet* 29:166-173.
- Hafezparast M et al. (2003) Mutations in dynein link motor neuron degeneration to defects in retrograde transport. *Science* 300:808-812.
- Hanna MC, Blackstone C (2009) Interaction of the SPG21 protein ACP33/masparidin with the aldehyde dehydrogenase ALDH16A1. *Neurogenetics* 10:217-228.
- Hara T, Nakamura K, Matsui M, Yamamoto A, Nakahara Y, Suzuki-Migishima R, Yokoyama M, Mishima K, Saito I, Okano H, Mizushima N (2006) Suppression of basal autophagy in neural cells causes neurodegenerative disease in mice. *Nature* 441:885-889.
- Harrison RE, Bucci C, Vieira OV, Schroer TA, Grinstein S (2003) Phagosomes fuse with late endosomes and/or lysosomes by extension of membrane protrusions along microtubules: role of Rab7 and RILP. *Mol Cell Biol* 23:6494-6506.
- Hayasaka K, Himoro M, Sato W, Takada G, Uyemura K, Shimizu N, Bird TD, Conneally PM, Chance PF (1993) Charcot-Marie-Tooth neuropathy type 1B is associated with mutations of the myelin P0 gene. *Nat Genet* 5:31-34.
- Heerssen HM, Pazyra MF, Segal RA (2004) Dynein motors transport activated Trks to promote survival of target-dependent neurons. *Nat Neurosci* 7:596-604.
- Hollenbeck PJ (1993) Products of endocytosis and autophagy are retrieved from axons by regulated retrograde organelle transport. *J Cell Biol* 121:305-315.
- Houlden H, King RH, Muddle JR, Warner TT, Reilly MM, Orrell RW, Ginsberg L (2004) A novel RAB7 mutation associated with ulcero-mutilating neuropathy. *Ann Neurol* 56:586-590.
- Huang EJ, Reichardt LF (2001) Neurotrophins: roles in neuronal development and function. *Annu Rev Neurosci* 24:677-736.
- Hubbert C, Guardiola A, Shao R, Kawaguchi Y, Ito A, Nixon A, Yoshida M, Wang XF, Yao TP (2002) HDAC6 is a microtubule-associated deacetylase. *Nature* 417:455-458.
- Ikeda Y, Dick KA, Weatherspoon MR, Gincel D, Armbrust KR, Dalton JC, Stevanin G, Durr A, Zuhlke C, Burk K, Clark HB, Brice A, Rothstein JD, Schut LJ, Day JW, Ranum LP (2006) Spectrin mutations cause spinocerebellar ataxia type 5. *Nat Genet* 38:184-190.
- Ilieva HS, Yamanaka K, Malkmus S, Kakinohana O, Yaksh T, Marsala M, Cleveland DW (2008) Mutant dynein (Loa) triggers proprioceptive axon loss that extends survival only in the SOD1 ALS model with highest motor neuron death. *Proc Natl Acad Sci U S A* 105:12599-12604.
- Indo Y, Tsuruta M, Hayashida Y, Karim MA, Ohta K, Kawano T, Mitsubuchi H, Tonoki H, Awaya Y, Matsuda I (1996) Mutations in the TRKA/NGF receptor gene in patients with congenital insensitivity to pain with anhidrosis. *Nat Genet* 13:485-488.
- Itzen A, Pylypenko O, Goody RS, Alexandrov K, Rak A (2006) Nucleotide exchange via local protein unfolding--structure of Rab8 in complex with MSS4. *EMBO J* 25:1445-1455.
- Iwata A, Riley BE, Johnston JA, Kopito RR (2005a) HDAC6 and microtubules are required for autophagic degradation of aggregated huntingtin. *J Biol Chem* 280:40282-40292.

- Iwata A, Christianson JC, Bucci M, Ellerby LM, Nukina N, Forno LS, Kopito RR (2005b) Increased susceptibility of cytoplasmic over nuclear polyglutamine aggregates to autophagic degradation. *Proc Natl Acad Sci U S A* 102:13135-13140.
- Jager S, Bucci C, Tanida I, Ueno T, Kominami E, Saftig P, Eskelinen EL (2004) Role for Rab7 in maturation of late autophagic vacuoles. *J Cell Sci* 117:4837-4848.
- Jia K, Hart AC, Levine B (2007) Autophagy genes protect against disease caused by polyglutamine expansion proteins in *Caenorhabditis elegans*. *Autophagy* 3:21-25.
- Johansson M, Lehto M, Tanhuanpaa K, Cover TL, Olkkonen VM (2005) The oxysterol-binding protein homologue ORP1L interacts with Rab7 and alters functional properties of late endocytic compartments. *Mol Biol Cell* 16:5480-5492.
- Johansson M, Rocha N, Zwart W, Jordens I, Janssen L, Kuijl C, Olkkonen VM, Neefjes J (2007) Activation of endosomal dynein motors by stepwise assembly of Rab7-RILP-p150Glued, ORP1L, and the receptor betalll spectrin. *J Cell Biol* 176:459-471.
- Johnston JA, Ward CL, Kopito RR (1998) Aggresomes: a cellular response to misfolded proteins. *J Cell Biol* 143:1883-1898.
- Jordanova A, De Jonghe P, Boerkoel CF, Takashima H, De Vriendt E, Ceuterick C, Martin JJ, Butler IJ, Mancias P, Pappasozomenos S, Terespolsky D, Potocki L, Brown CW, Shy M, Rita DA, Tournev I, Kremensky I, Lupski JR, Timmerman V (2003) Mutations in the neurofilament light chain gene (NEFL) cause early onset severe Charcot-Marie-Tooth disease. *Brain* 126:590-597.
- Jordens I, Fernandez-Borja M, Marsman M, Dusseljee S, Janssen L, Calafat J, Janssen H, Wubbolts R, Neefjes J (2001) The Rab7 effector protein RILP controls lysosomal transport by inducing the recruitment of dynein-dynactin motors. *Curr Biol* 11:1680-1685.
- Kabeya Y, Mizushima N, Ueno T, Yamamoto A, Kirisako T, Noda T, Kominami E, Ohsumi Y, Yoshimori T (2000) LC3, a mammalian homologue of yeast Apg8p, is localized in autophagosome membranes after processing. *Embo J* 19:5720-5728.
- Kabuta T, Suzuki Y, Wada K (2006) Degradation of amyotrophic lateral sclerosis-linked mutant Cu,Zn-superoxide dismutase proteins by macroautophagy and the proteasome. *J Biol Chem* 281:30524-30533.
- Kajiho H, Saito K, Tsujita K, Kontani K, Araki Y, Kurosu H, Katada T (2003) RIN3: a novel Rab5 GEF interacting with amphiphysin II involved in the early endocytic pathway. *J Cell Sci* 116:4159-4168.
- Kamal A, Goldstein LS (2002) Principles of cargo attachment to cytoplasmic motor proteins. *Curr Opin Cell Biol* 14:63-68.
- Kawaguchi Y, Kovacs JJ, McLaurin A, Vance JM, Ito A, Yao TP (2003) The deacetylase HDAC6 regulates aggresome formation and cell viability in response to misfolded protein stress. *Cell* 115:727-738.
- Kegel KB, Kim M, Sapp E, McIntyre C, Castano JG, Aronin N, DiFiglia M (2000) Huntingtin expression stimulates endosomal-lysosomal activity, endosome tubulation, and autophagy. *J Neurosci* 20:7268-7278.
- Keller A, Nesvizhskii AI, Kolker E, Aebersold R (2002) Empirical statistical model to estimate the accuracy of peptide identifications made by MS/MS and database search. *Anal Chem* 74:5383-5392.
- Kenyon C (2005) The plasticity of aging: insights from long-lived mutants. *Cell* 120:449-460.
- Kim I, Rodriguez-Enriquez S, Lemasters JJ (2007) Selective degradation of mitochondria by mitophagy. *Arch Biochem Biophys* 462:245-253.
- Kimura S, Noda T, Yoshimori T (2007) Dissection of the autophagosome maturation process by a novel reporter protein, tandem fluorescent-tagged LC3. *Autophagy* 3:452-460.

- Kirkegaard K, Taylor MP, Jackson WT (2004) Cellular autophagy: surrender, avoidance and subversion by microorganisms. *Nat Rev Microbiol* 2:301-314.
- Klionsky DJ, Cuervo AM, Seglen PO (2007) Methods for monitoring autophagy from yeast to human. *Autophagy* 3:181-206.
- Klionsky DJ, Elazar Z, Seglen PO, Rubinsztein DC (2008) Does bafilomycin A1 block the fusion of autophagosomes with lysosomes? *Autophagy* 4:849-950.
- Koike M, Shibata M, Waguri S, Yoshimura K, Tanida I, Kominami E, Gotow T, Peters C, von Figura K, Mizushima N, Saftig P, Uchiyama Y (2005) Participation of autophagy in storage of lysosomes in neurons from mouse models of neuronal ceroid-lipofuscinoses (Batten disease). *Am J Pathol* 167:1713-1728.
- Koike M, Nakanishi H, Saftig P, Ezaki J, Isahara K, Ohsawa Y, Schulz-Schaeffer W, Watanabe T, Waguri S, Kametaka S, Shibata M, Yamamoto K, Kominami E, Peters C, von Figura K, Uchiyama Y (2000) Cathepsin D deficiency induces lysosomal storage with ceroid lipofuscin in mouse CNS neurons. *J Neurosci* 20:6898-6906.
- Komatsu M, Waguri S, Chiba T, Murata S, Iwata J, Tanida I, Ueno T, Koike M, Uchiyama Y, Kominami E, Tanaka K (2006) Loss of autophagy in the central nervous system causes neurodegeneration in mice. *Nature* 441:880-884.
- Kondo Y, Kanzawa T, Sawaya R, Kondo S (2005) The role of autophagy in cancer development and response to therapy. *Nat Rev Cancer* 5:726-734.
- Kovacs JJ, Murphy PJ, Gaillard S, Zhao X, Wu JT, Nicchitta CV, Yoshida M, Toft DO, Pratt WB, Yao TP (2005) HDAC6 regulates Hsp90 acetylation and chaperone-dependent activation of glucocorticoid receptor. *Mol Cell* 18:601-607.
- Kuhlenbaumer G, Young P, Hunermund G, Ringelstein B, Stogbauer F (2002) Clinical features and molecular genetics of hereditary peripheral neuropathies. *J Neurol* 249:1629-1650.
- Kuma A, Matsui M, Mizushima N (2007) LC3, an autophagosome marker, can be incorporated into protein aggregates independent of autophagy: caution in the interpretation of LC3 localization. *Autophagy* 3:323-328.
- Kuriyama H, Asakawa S, Minoshima S, Maruyama H, Ishii N, Ito K, Gejyo F, Arakawa M, Shimizu N, Kuwano R (2000) Characterization and chromosomal mapping of a novel human gene, ANKHZN. *Gene* 253:151-160.
- Kwon JM, Elliott JL, Yee WC, Ivanovich J, Scavarda NJ, Moolsintong PJ, Goodfellow PJ (1995) Assignment of a second Charcot-Marie-Tooth type II locus to chromosome 3q. *Am J Hum Genet* 57:853-858.
- La Spada AR, Wilson EM, Lubahn DB, Harding AE, Fischbeck KH (1991) Androgen receptor gene mutations in X-linked spinal and bulbar muscular atrophy. *Nature* 352:77-79.
- Laird FM, Farah MH, Ackerley S, Hoke A, Maragakis N, Rothstein JD, Griffin J, Price DL, Martin LJ, Wong PC (2008) Motor neuron disease occurring in a mutant dynactin mouse model is characterized by defects in vesicular trafficking. *J Neurosci* 28:1997-2005.
- LaMonte BH, Wallace KE, Holloway BA, Shelly SS, Ascano J, Tokito M, Van Winkle T, Howland DS, Holzbaur EL (2002) Disruption of dynein/dynactin inhibits axonal transport in motor neurons causing late-onset progressive degeneration. *Neuron* 34:715-727.
- Landers JE, Leclerc AL, Shi L, Virkud A, Cho T, Maxwell MM, Henry AF, Polak M, Glass JD, Kwiatkowski TJ, Al-Chalabi A, Shaw CE, Leigh PN, Rodriguez-Leyza I, McKenna-Yasek D, Sapp PC, Brown RH, Jr. (2008) New VAPB deletion variant and exclusion of VAPB mutations in familial ALS. *Neurology* 70:1179-1185.
- Lanzetti L, Rybin V, Malabarba MG, Christoforidis S, Scita G, Zerial M, Di Fiore PP (2000) The Eps8 protein coordinates EGF receptor signalling through Rac and trafficking through Rab5. *Nature* 408:374-377.

- Lapierre LA, Tuma PL, Navarre J, Goldenring JR, Anderson JM (1999) VAP-33 localizes to both an intracellular vesicle population and with occludin at the tight junction. *J Cell Sci* 112 (Pt 21):3723-3732.
- Lev S, Ben Halevy D, Peretti D, Dahan N (2008) The VAP protein family: from cellular functions to motor neuron disease. *Trends Cell Biol* 18:282-290.
- Levine B, Klionsky DJ (2004) Development by self-digestion: molecular mechanisms and biological functions of autophagy. *Dev Cell* 6:463-477.
- Levy JR, Sumner CJ, Caviston JP, Tokito MK, Ranganathan S, Ligon LA, Wallace KE, LaMonte BH, Harmison GG, Puls I, Fischbeck KH, Holzbaur EL (2006) A motor neuron disease-associated mutation in p150Glued perturbs dynactin function and induces protein aggregation. *J Cell Biol* 172:733-745.
- Liang XH, Kleeman LK, Jiang HH, Gordon G, Goldman JE, Berry G, Herman B, Levine B (1998) Protection against fatal Sindbis virus encephalitis by beclin, a novel Bcl-2-interacting protein. *J Virol* 72:8586-8596.
- Loewen CJ, Roy A, Levine TP (2003) A conserved ER targeting motif in three families of lipid binding proteins and in Opi1p binds VAP. *EMBO J* 22:2025-2035.
- Luzio JP, Pryor PR, Bright NA (2007) Lysosomes: fusion and function. *Nat Rev Mol Cell Biol* 8:622-632.
- Marrosu MG, Vaccargiu S, Marrosu G, Vannelli A, Cianchetti C, Muntoni F (1998) Charcot-Marie-Tooth disease type 2 associated with mutation of the myelin protein zero gene. *Neurology* 50:1397-1401.
- Marsh JL, Walker H, Theisen H, Zhu YZ, Fielder T, Purcell J, Thompson LM (2000) Expanded polyglutamine peptides alone are intrinsically cytotoxic and cause neurodegeneration in *Drosophila*. *Hum Mol Genet* 9:13-25.
- McCray BA, Skordalakes E, Taylor JP (2009) Disease mutations in Rab7 result in unregulated nucleotide exchange and inappropriate activation. *Hum Mol Genet*.
- Meggough F, Bienfait HM, Weterman MA, de Visser M, Baas F (2006) Charcot-Marie-Tooth disease due to a de novo mutation of the RAB7 gene. *Neurology* 67:1476-1478.
- Melendez A, Tallozy Z, Seaman M, Eskelinen EL, Hall DH, Levine B (2003) Autophagy genes are essential for dauer development and life-span extension in *C. elegans*. *Science* 301:1387-1391.
- Mersiyanova IV, Perepelov AV, Polyakov AV, Sitnikov VF, Dadali EL, Oparin RB, Petrin AN, Evgrafov OV (2000) A new variant of Charcot-Marie-Tooth disease type 2 is probably the result of a mutation in the neurofilament-light gene. *Am J Hum Genet* 67:37-46.
- Mizuno K, Kitamura A, Sasaki T (2003) Rabring7, a novel Rab7 target protein with a RING finger motif. *Mol Biol Cell* 14:3741-3752.
- Moulder KL, Onodera O, Burke JR, Strittmatter WJ, Johnson EM, Jr. (1999) Generation of neuronal intranuclear inclusions by polyglutamine-GFP: analysis of inclusion clearance and toxicity as a function of polyglutamine length. *J Neurosci* 19:705-715.
- Muchowski PJ, Wacker JL (2005) Modulation of neurodegeneration by molecular chaperones. *Nat Rev Neurosci* 6:11-22.
- Murshudov GN, Vagin AA, Dodson EJ (1997) Refinement of macromolecular structures by the maximum-likelihood method. *Acta Crystallogr D Biol Crystallogr* 53:240-255.
- Myllykangas L, Tyynela J, Page-McCaw A, Rubin GM, Haltia MJ, Feany MB (2005) Cathepsin D-deficient *Drosophila* recapitulate the key features of neuronal ceroid lipofuscinoses. *Neurobiol Dis* 19:194-199.
- Nelis E, Erdem S, Van Den Bergh PY, Belpaire-Dethiou MC, Ceuterick C, Van Gerwen V, Cuesta A, Pedrola L, Palau F, Gabreels-Festen AA, Verellen C, Tan E, Demirci M, Van

- Broeckhoven C, De Jonghe P, Topaloglu H, Timmerman V (2002) Mutations in GDAP1: autosomal recessive CMT with demyelination and axonopathy. *Neurology* 59:1865-1872.
- Nesvizhskii AI, Keller A, Kolker E, Aebersold R (2003) A statistical model for identifying proteins by tandem mass spectrometry. *Anal Chem* 75:4646-4658.
- Nishimura AL, Mitne-Neto M, Silva HC, Richieri-Costa A, Middleton S, Cascio D, Kok F, Oliveira JR, Gillingwater T, Webb J, Skehel P, Zatz M (2004) A mutation in the vesicle-trafficking protein VAPB causes late-onset spinal muscular atrophy and amyotrophic lateral sclerosis. *Am J Hum Genet* 75:822-831.
- Nishimura Y, Hayashi M, Inada H, Tanaka T (1999) Molecular cloning and characterization of mammalian homologues of vesicle-associated membrane protein-associated (VAMP-associated) proteins. *Biochem Biophys Res Commun* 254:21-26.
- Nixon RA, Yang DS, Lee JH (2008) Neurodegenerative lysosomal disorders: a continuum from development to late age. *Autophagy* 4:590-599.
- Nixon RA, Wegiel J, Kumar A, Yu WH, Peterhoff C, Cataldo A, Cuervo AM (2005) Extensive involvement of autophagy in Alzheimer disease: an immuno-electron microscopy study. *J Neuropathol Exp Neurol* 64:113-122.
- Noda T, Ohsumi Y (1998) Tor, a phosphatidylinositol kinase homologue, controls autophagy in yeast. *J Biol Chem* 273:3963-3966.
- Ohsumi Y (2001) Molecular dissection of autophagy: two ubiquitin-like systems. *Nat Rev Mol Cell Biol* 2:211-216.
- Orr HT (2002) Lurcher, nPIST, and autophagy. *Neuron* 35:813-814.
- Osterwalder T, Yoon KS, White BH, Keshishian H (2001) A conditional tissue-specific transgene expression system using inducible GAL4. *Proc Natl Acad Sci U S A* 98:12596-12601.
- Otomo A, Hadano S, Okada T, Mizumura H, Kunita R, Nishijima H, Showguchi-Miyata J, Yanagisawa Y, Kohiki E, Suga E, Yasuda M, Osuga H, Nishimoto T, Narumiya S, Ikeda JE (2003) ALS2, a novel guanine nucleotide exchange factor for the small GTPase Rab5, is implicated in endosomal dynamics. *Hum Mol Genet* 12:1671-1687.
- Overly CC, Hollenbeck PJ (1996) Dynamic organization of endocytic pathways in axons of cultured sympathetic neurons. *J Neurosci* 16:6056-6064.
- Paduch M, Jelen F, Otlewski J (2001) Structure of small G proteins and their regulators. *Acta Biochim Pol* 48:829-850.
- Pan X, Eathiraj S, Munson M, Lambright DG (2006) TBC-domain GAPs for Rab GTPases accelerate GTP hydrolysis by a dual-finger mechanism. *Nature* 442:303-306.
- Pandey UB, Nie Z, Batlevi Y, McCray BA, Ritson GP, Nedelsky NB, Schwartz SL, DiProspero NA, Knight MA, Schuldiner O, Padmanabhan R, Hild M, Berry DL, Garza D, Hubbert CC, Yao TP, Baehrecke EH, Taylor JP (2007) HDAC6 rescues neurodegeneration and provides an essential link between autophagy and the UPS. *Nature* 447:859-863.
- Patterson GH, Lippincott-Schwartz J (2002) A photoactivatable GFP for selective photolabeling of proteins and cells. *Science* 297:1873-1877.
- Pei L, Peng Y, Yang Y, Ling XB, Van Eyndhoven WG, Nguyen KC, Rubin M, Hoey T, Powers S, Li J (2002) PRC17, a novel oncogene encoding a Rab GTPase-activating protein, is amplified in prostate cancer. *Cancer Res* 62:5420-5424.
- Pennetta G, Hiesinger PR, Fabian-Fine R, Meinertzhagen IA, Bellen HJ (2002) Drosophila VAP-33A directs bouton formation at neuromuscular junctions in a dosage-dependent manner. *Neuron* 35:291-306.
- Perkins DN, Pappin DJ, Creasy DM, Cottrell JS (1999) Probability-based protein identification by searching sequence databases using mass spectrometry data. *Electrophoresis* 20:3551-3567.

- Perlson E, Jeong GB, Ross JL, Dixit R, Wallace KE, Kalb RG, Holzbaur EL (2009) A switch in retrograde signaling from survival to stress in rapid-onset neurodegeneration. *J Neurosci* 29:9903-9917.
- Petersen A, Larsen KE, Behr GG, Romero N, Przedborski S, Brundin P, Sulzer D (2001) Expanded CAG repeats in exon 1 of the Huntington's disease gene stimulate dopamine-mediated striatal neuron autophagy and degeneration. *Hum Mol Genet* 10:1243-1254.
- Petiot A, Ogier-Denis E, Blommaert EF, Meijer AJ, Codogno P (2000) Distinct classes of phosphatidylinositol 3'-kinases are involved in signaling pathways that control macroautophagy in HT-29 cells. *J Biol Chem* 275:992-998.
- Pickart CM (2004) Back to the future with ubiquitin. *Cell* 116:181-190.
- Potterton E, Briggs P, Turkenburg M, Dodson E (2003) A graphical user interface to the CCP4 program suite. *Acta Crystallogr D Biol Crystallogr* 59:1131-1137.
- Puls I, Jonnakuty C, LaMonte BH, Holzbaur EL, Tokito M, Mann E, Floeter MK, Bidus K, Drayna D, Oh SJ, Brown RH, Jr., Ludlow CL, Fischbeck KH (2003) Mutant dynactin in motor neuron disease. *Nat Genet* 33:455-456.
- Qu X, Yu J, Bhagat G, Furuya N, Hibshoosh H, Troxel A, Rosen J, Eskelinen EL, Mizushima N, Ohsumi Y, Cattoretti G, Levine B (2003) Promotion of tumorigenesis by heterozygous disruption of the beclin 1 autophagy gene. *J Clin Invest* 112:1809-1820.
- Raiborg C, Rusten TE, Stenmark H (2003) Protein sorting into multivesicular endosomes. *Curr Opin Cell Biol* 15:446-455.
- Rak A, Pylypenko O, Niculae A, Pyatkov K, Goody RS, Alexandrov K (2004) Structure of the Rab7:REP-1 complex: insights into the mechanism of Rab prenylation and choroideremia disease. *Cell* 117:749-760.
- Rak A, Pylypenko O, Durek T, Watzke A, Kushnir S, Brunsveld L, Waldmann H, Goody RS, Alexandrov K (2003) Structure of Rab GDP-dissociation inhibitor in complex with prenylated YPT1 GTPase. *Science* 302:646-650.
- Ratnaparkhi A, Lawless GM, Schweizer FE, Golshani P, Jackson GR (2008) A Drosophila model of ALS: human ALS-associated mutation in VAP33A suggests a dominant negative mechanism. *PLoS One* 3:e2334.
- Ravikumar B, Duden R, Rubinsztein DC (2002) Aggregate-prone proteins with polyglutamine and polyalanine expansions are degraded by autophagy. *Hum Mol Genet* 11:1107-1117.
- Ravikumar B, Berger Z, Vacher C, O'Kane CJ, Rubinsztein DC (2006) Rapamycin pre-treatment protects against apoptosis. *Hum Mol Genet* 15:1209-1216.
- Ravikumar B, Acevedo-Arozena A, Imarisio S, Berger Z, Vacher C, O'Kane CJ, Brown SD, Rubinsztein DC (2005) Dynein mutations impair autophagic clearance of aggregate-prone proteins. *Nat Genet* 37:771-776.
- Ravikumar B, Vacher C, Berger Z, Davies JE, Luo S, Oroz LG, Scaravilli F, Easton DF, Duden R, O'Kane CJ, Rubinsztein DC (2004) Inhibition of mTOR induces autophagy and reduces toxicity of polyglutamine expansions in fly and mouse models of Huntington disease. *Nat Genet* 36:585-595.
- Raymond CK, Howald-Stevenson I, Vater CA, Stevens TH (1992) Morphological classification of the yeast vacuolar protein sorting mutants: evidence for a prevacuolar compartment in class E vps mutants. *Mol Biol Cell* 3:1389-1402.
- Regazzi R, Kikuchi A, Takai Y, Wollheim CB (1992) The small GTP-binding proteins in the cytosol of insulin-secreting cells are complexed to GDP dissociation inhibitor proteins. *J Biol Chem* 267:17512-17519.
- Rideout HJ, Lang-Rollin I, Stefanis L (2004) Involvement of macroautophagy in the dissolution of neuronal inclusions. *Int J Biochem Cell Biol* 36:2551-2562.

- Rink J, Ghigo E, Kalaidzidis Y, Zerial M (2005) Rab conversion as a mechanism of progression from early to late endosomes. *Cell* 122:735-749.
- Rocha N, Kuijl C, van der Kant R, Janssen L, Houben D, Janssen H, Zwart W, Neeffjes J (2009) Cholesterol sensor ORP1L contacts the ER protein VAP to control Rab7-RILP-p150 Glued and late endosome positioning. *J Cell Biol* 185:1209-1225.
- Rojas R, van Vlijmen T, Mardones GA, Prabhu Y, Rojas AL, Mohammed S, Heck AJ, Raposo G, van der Sluijs P, Bonifacino JS (2008) Regulation of retromer recruitment to endosomes by sequential action of Rab5 and Rab7. *J Cell Biol* 183:513-526.
- Romero Rosales K, Peralta ER, Guenther GG, Wong SY, Edinger AL (2009) Rab7 activation by growth factor withdrawal contributes to the induction of apoptosis. *Mol Biol Cell* 20:2831-2840.
- Ross CA, Poirier MA (2004) Protein aggregation and neurodegenerative disease. *Nat Med* 10 Suppl:S10-17.
- Rubin GM, Spradling AC (1982) Genetic transformation of *Drosophila* with transposable element vectors. *Science* 218:348-353.
- Rubinsztein DC (2006) The roles of intracellular protein-degradation pathways in neurodegeneration. *Nature* 443:780-786.
- Sandow SL, Heydon K, Weible MW, 2nd, Reynolds AJ, Bartlett SE, Hendry IA (2000) Signalling organelle for retrograde axonal transport of internalized neurotrophins from the nerve terminal. *Immunol Cell Biol* 78:430-435.
- Sapp E, Schwarz C, Chase K, Bhide PG, Young AB, Penney J, Vonsattel JP, Aronin N, DiFiglia M (1997) Huntingtin localization in brains of normal and Huntington's disease patients. *Ann Neurol* 42:604-612.
- Sarkar S, Perlstein EO, Imarisio S, Pineau S, Cordenier A, Maglathlin RL, Webster JA, Lewis TA, O'Kane CJ, Schreiber SL, Rubinsztein DC (2007) Small molecules enhance autophagy and reduce toxicity in Huntington's disease models. *Nat Chem Biol* 3:331-338.
- Sasaki T, Kikuchi A, Araki S, Hata Y, Isomura M, Kuroda S, Takai Y (1990) Purification and characterization from bovine brain cytosol of a protein that inhibits the dissociation of GDP from and the subsequent binding of GTP to smg p25A, a ras p21-like GTP-binding protein. *J Biol Chem* 265:2333-2337.
- Sato Y, Fukai S, Ishitani R, Nureki O (2007) Crystal structure of the Sec4p.Sec2p complex in the nucleotide exchanging intermediate state. *Proc Natl Acad Sci U S A* 104:8305-8310.
- Saxena S, Bucci C, Weis J, Kruttgen A (2005) The small GTPase Rab7 controls the endosomal trafficking and neuritogenic signaling of the nerve growth factor receptor TrkA. *J Neurosci* 25:10930-10940.
- Schroer TA (2004) Dynactin. *Annu Rev Cell Dev Biol* 20:759-779.
- Schubert U, Anton LC, Gibbs J, Norbury CC, Yewdell JW, Bennink JR (2000) Rapid degradation of a large fraction of newly synthesized proteins by proteasomes. *Nature* 404:770-774.
- Schulte-Herbruggen O, Braun A, Rochlitzer S, Jockers-Scherubl MC, Hellweg R (2007) Neurotrophic factors--a tool for therapeutic strategies in neurological, neuropsychiatric and neuroimmunological diseases? *Curr Med Chem* 14:2318-2329.
- Scott RC, Schuldiner O, Neufeld TP (2004) Role and regulation of starvation-induced autophagy in the *Drosophila* fat body. *Dev Cell* 7:167-178.
- Seabra MC, Brown MS, Goldstein JL (1993) Retinal degeneration in choroideremia: deficiency of rab geranylgeranyl transferase. *Science* 259:377-381.
- Seals DF, Eitzen G, Margolis N, Wickner WT, Price A (2000) A Ypt/Rab effector complex containing the Sec1 homolog Vps33p is required for homotypic vacuole fusion. *Proc Natl Acad Sci U S A* 97:9402-9407.

- Seaman MN, McCaffery JM, Emr SD (1998) A membrane coat complex essential for endosome-to-Golgi retrograde transport in yeast. *J Cell Biol* 142:665-681.
- Seaman MN, Harbour ME, Tattersall D, Read E, Bright N (2009) Membrane recruitment of the cargo-selective retromer subcomplex is catalysed by the small GTPase Rab7 and inhibited by the Rab-GAP TBC1D5. *J Cell Sci*.
- Seigneurin-Berny D, Verdel A, Curtet S, Lemerrier C, Garin J, Rousseaux S, Khochbin S (2001) Identification of components of the murine histone deacetylase 6 complex: link between acetylation and ubiquitination signaling pathways. *Mol Cell Biol* 21:8035-8044.
- Shacka JJ, Klocke BJ, Young C, Shibata M, Olney JW, Uchiyama Y, Saftig P, Roth KA (2007) Cathepsin D deficiency induces persistent neurodegeneration in the absence of Bax-dependent apoptosis. *J Neurosci* 27:2081-2090.
- Sikorska B, Liberski PP, Giraud P, Kopp N, Brown P (2004) Autophagy is a part of ultrastructural synaptic pathology in Creutzfeldt-Jakob disease: a brain biopsy study. *Int J Biochem Cell Biol* 36:2563-2573.
- Simpson MA, Cross H, Proukakis C, Pryde A, Hershberger R, Chatonnet A, Patton MA, Crosby AH (2003) Maspardin is mutated in mast syndrome, a complicated form of hereditary spastic paraplegia associated with dementia. *Am J Hum Genet* 73:1147-1156.
- Sivars U, Aivazian D, Pfeffer SR (2003) Yip3 catalyses the dissociation of endosomal Rab-GDI complexes. *Nature* 425:856-859.
- Skehel PA, Martin KC, Kandel ER, Bartsch D (1995) A VAMP-binding protein from *Aplysia* required for neurotransmitter release. *Science* 269:1580-1583.
- Skinner PJ, Vierra-Green CA, Clark HB, Zoghbi HY, Orr HT (2001) Altered trafficking of membrane proteins in purkinje cells of SCA1 transgenic mice. *Am J Pathol* 159:905-913.
- Soldati T, Shapiro AD, Svejstrup AB, Pfeffer SR (1994) Membrane targeting of the small GTPase Rab9 is accompanied by nucleotide exchange. *Nature* 369:76-78.
- Soussan L, Burakov D, Daniels MP, Toister-Achituv M, Porat A, Yarden Y, Elazar Z (1999) ERG30, a VAP-33-related protein, functions in protein transport mediated by COPI vesicles. *J Cell Biol* 146:301-311.
- Spinosa MR, Progida C, De Luca A, Colucci AM, Alifano P, Bucci C (2008) Functional characterization of Rab7 mutant proteins associated with Charcot-Marie-Tooth type 2B disease. *J Neurosci* 28:1640-1648.
- Stein MP, Feng Y, Cooper KL, Welford AM, Wandinger-Ness A (2003) Human VPS34 and p150 are Rab7 interacting partners. *Traffic* 4:754-771.
- Street VA, Bennett CL, Goldy JD, Shirk AJ, Kleopa KA, Tempel BL, Lipe HP, Scherer SS, Bird TD, Chance PF (2003) Mutation of a putative protein degradation gene LITAF/SIMPLE in Charcot-Marie-Tooth disease 1C. *Neurology* 60:22-26.
- Stroupe C, Collins KM, Fratti RA, Wickner W (2006) Purification of active HOPS complex reveals its affinities for phosphoinositides and the SNARE Vam7p. *EMBO J* 25:1579-1589.
- Sudhof TC, Rothman JE (2009) Membrane fusion: grappling with SNARE and SM proteins. *Science* 323:474-477.
- Suter U, Scherer SS (2003) Disease mechanisms in inherited neuropathies. *Nat Rev Neurosci* 4:714-726.
- Tall GG, Barbieri MA, Stahl PD, Horazdovsky BF (2001) Ras-activated endocytosis is mediated by the Rab5 guanine nucleotide exchange activity of RIN1. *Dev Cell* 1:73-82.
- Tanaka M, Kim YM, Lee G, Junn E, Iwatsubo T, Mouradian MM (2004) Aggresomes formed by alpha-synuclein and synphilin-1 are cytoprotective. *J Biol Chem* 279:4625-4631.

- Tang BS, Zhao GH, Luo W, Xia K, Cai F, Pan Q, Zhang RX, Zhang FF, Liu XM, Chen B, Zhang C, Shen L, Jiang H, Long ZG, Dai HP (2005) Small heat-shock protein 22 mutated in autosomal dominant Charcot-Marie-Tooth disease type 2L. *Hum Genet* 116:222-224.
- Taylor JP, Hardy J, Fischbeck KH (2002) Toxic proteins in neurodegenerative disease. *Science* 296:1991-1995.
- Taylor JP, Tanaka F, Robitschek J, Sandoval CM, Taye A, Markovic-Plese S, Fischbeck KH (2003) Aggresomes protect cells by enhancing the degradation of toxic polyglutamine-containing protein. *Hum Mol Genet* 12:749-757.
- Terman A (1995) The effect of age on formation and elimination of autophagic vacuoles in mouse hepatocytes. *Gerontology* 41 Suppl 2:319-326.
- Terman A, Brunk UT (2004) Lipofuscin. *Int J Biochem Cell Biol* 36:1400-1404.
- Terman A, Dalen H, Brunk UT (1999) Ceroid/lipofuscin-loaded human fibroblasts show decreased survival time and diminished autophagocytosis during amino acid starvation. *Exp Gerontol* 34:943-957.
- Toth ML, Simon P, Kovacs AL, Vellai T (2007) Influence of autophagy genes on ion-channel-dependent neuronal degeneration in *Caenorhabditis elegans*. *J Cell Sci* 120:1134-1141.
- Traut TW (1994) Physiological concentrations of purines and pyrimidines. *Mol Cell Biochem* 140:1-22.
- Trojanowski JQ, Lee VM (2000) "Fatal attractions" of proteins. A comprehensive hypothetical mechanism underlying Alzheimer's disease and other neurodegenerative disorders. *Ann N Y Acad Sci* 924:62-67.
- Tsuda H, Han SM, Yang Y, Tong C, Lin YQ, Mohan K, Haueter C, Zoghbi A, Harati Y, Kwan J, Miller MA, Bellen HJ (2008) The amyotrophic lateral sclerosis 8 protein VAPB is cleaved, secreted, and acts as a ligand for Eph receptors. *Cell* 133:963-977.
- Ullrich O, Stenmark H, Alexandrov K, Huber LA, Kaibuchi K, Sasaki T, Takai Y, Zerial M (1993) Rab GDP dissociation inhibitor as a general regulator for the membrane association of rab proteins. *J Biol Chem* 268:18143-18150.
- Ure DR, Campenot RB (1997) Retrograde transport and steady-state distribution of 125I-nerve growth factor in rat sympathetic neurons in compartmented cultures. *J Neurosci* 17:1282-1290.
- Valentijn LJ, Baas F, Wolterman RA, Hoogendijk JE, van den Bosch NH, Zorn I, Gabreels-Festen AW, de Visser M, Bolhuis PA (1992a) Identical point mutations of PMP-22 in Trembler-J mouse and Charcot-Marie-Tooth disease type 1A. *Nat Genet* 2:288-291.
- Valentijn LJ, Bolhuis PA, Zorn I, Hoogendijk JE, van den Bosch N, Hensels GW, Stanton VP, Jr., Housman DE, Fischbeck KH, Ross DA, et al. (1992b) The peripheral myelin gene PMP-22/GAS-3 is duplicated in Charcot-Marie-Tooth disease type 1A. *Nat Genet* 1:166-170.
- van den Hurk JA, van de Pol TJ, Molloy CM, Brunsmann F, Ruther K, Zrenner E, Pinckers AJ, Pawlowitzki IH, Bleeker-Wagemakers EM, Wieringa B, et al. (1992) Detection and characterization of point mutations in the choroideremia candidate gene by PCR-SSCP analysis and direct DNA sequencing. *Am J Hum Genet* 50:1195-1202.
- van der Sluijs P, Hull M, Webster P, Male P, Goud B, Mellman I (1992) The small GTP-binding protein rab4 controls an early sorting event on the endocytic pathway. *Cell* 70:729-740.
- Vanlandingham PA, Ceresa BP (2009) Rab7 regulates late endocytic trafficking downstream of multivesicular body biogenesis and cargo sequestration. *J Biol Chem* 284:12110-12124.
- Verhoeven K, De Jonghe P, Coen K, Verpoorten N, Auer-Grumbach M, Kwon JM, FitzPatrick D, Schmedding E, De Vriendt E, Jacobs A, Van Gerwen V, Wagner K, Hartung HP, Timmerman V (2003) Mutations in the small GTP-ase late endosomal protein RAB7 cause Charcot-Marie-Tooth type 2B neuropathy. *Am J Hum Genet* 72:722-727.

- Vitelli R, Santillo M, Lattero D, Chiariello M, Bifulco M, Bruni CB, Bucci C (1997) Role of the small GTPase Rab7 in the late endocytic pathway. *J Biol Chem* 272:4391-4397.
- Vollmer P, Will E, Scheglmann D, Strom M, Gallwitz D (1999) Primary structure and biochemical characterization of yeast GTPase-activating proteins with substrate preference for the transport GTPase Ypt7p. *Eur J Biochem* 260:284-290.
- Wang CW, Klionsky DJ (2003) The molecular mechanism of autophagy. *Mol Med* 9:65-76.
- Ward WF (2002) Protein degradation in the aging organism. *Prog Mol Subcell Biol* 29:35-42.
- Warner LE, Mancias P, Butler IJ, McDonald CM, Keppen L, Koob KG, Lupski JR (1998) Mutations in the early growth response 2 (EGR2) gene are associated with hereditary myelinopathies. *Nat Genet* 18:382-384.
- Warrick JM, Paulson HL, Gray-Board GL, Bui QT, Fischbeck KH, Pittman RN, Bonini NM (1998) Expanded polyglutamine protein forms nuclear inclusions and causes neural degeneration in *Drosophila*. *Cell* 93:939-949.
- Waterman-Storer CM, Karki S, Holzbaur EL (1995) The p150Glued component of the dynactin complex binds to both microtubules and the actin-related protein capping protein (Arp-1). *Proc Natl Acad Sci U S A* 92:1634-1638.
- Weber T, Zemelman BV, McNew JA, Westermann B, Gmachl M, Parlati F, Sollner TH, Rothman JE (1998) SNAREpins: minimal machinery for membrane fusion. *Cell* 92:759-772.
- Weir ML, Klip A, Trimble WS (1998) Identification of a human homologue of the vesicle-associated membrane protein (VAMP)-associated protein of 33 kDa (VAP-33): a broadly expressed protein that binds to VAMP. *Biochem J* 333 (Pt 2):247-251.
- Wennerberg K, Rossman KL, Der CJ (2005) The Ras superfamily at a glance. *J Cell Sci* 118:843-846.
- Wilkin M, Tongngok P, Gensch N, Clemence S, Motoki M, Yamada K, Hori K, Taniguchi-Kanai M, Franklin E, Matsuno K, Baron M (2008) *Drosophila* HOPS and AP-3 complex genes are required for a Deltex-regulated activation of notch in the endosomal trafficking pathway. *Dev Cell* 15:762-772.
- Worthylake DK, Rossman KL, Sondek J (2000) Crystal structure of Rac1 in complex with the guanine nucleotide exchange region of Tiam1. *Nature* 408:682-688.
- Wu M, Wang T, Loh E, Hong W, Song H (2005) Structural basis for recruitment of RILP by small GTPase Rab7. *EMBO J* 24:1491-1501.
- Wurmser AE, Sato TK, Emr SD (2000) New component of the vacuolar class C-Vps complex couples nucleotide exchange on the Ypt7 GTPase to SNARE-dependent docking and fusion. *J Cell Biol* 151:551-562.
- Xiao GH, Shoarinejad F, Jin F, Golemis EA, Yeung RS (1997) The tuberous sclerosis 2 gene product, tuberin, functions as a Rab5 GTPase activating protein (GAP) in modulating endocytosis. *J Biol Chem* 272:6097-6100.
- Yamamoto A, Cremona ML, Rothman JE (2006) Autophagy-mediated clearance of huntingtin aggregates triggered by the insulin-signaling pathway. *J Cell Biol* 172:719-731.
- Yang Y, Hentati A, Deng HX, Dabbagh O, Sasaki T, Hirano M, Hung WY, Ouahchi K, Yan J, Azim AC, Cole N, Gascon G, Yagmour A, Ben-Hamida M, Pericak-Vance M, Hentati F, Siddique T (2001) The gene encoding alsin, a protein with three guanine-nucleotide exchange factor domains, is mutated in a form of recessive amyotrophic lateral sclerosis. *Nat Genet* 29:160-165.
- Ye H, Kuruvilla R, Zweifel LS, Ginty DD (2003) Evidence in support of signaling endosome-based retrograde survival of sympathetic neurons. *Neuron* 39:57-68.
- Young P, Suter U (2001) Disease mechanisms and potential therapeutic strategies in Charcot-Marie-Tooth disease. *Brain Res Brain Res Rev* 36:213-221.

- Yu L, Alva A, Su H, Dutt P, Freundt E, Welsh S, Baehrecke EH, Lenardo MJ (2004) Regulation of an ATG7-beclin 1 program of autophagic cell death by caspase-8. *Science* 304:1500-1502.
- Yu WH, Cuervo AM, Kumar A, Peterhoff CM, Schmidt SD, Lee JH, Mohan PS, Mercken M, Farmery MR, Tjernberg LO, Jiang Y, Duff K, Uchiyama Y, Naslund J, Mathews PM, Cataldo AM, Nixon RA (2005) Macroautophagy--a novel Beta-amyloid peptide-generating pathway activated in Alzheimer's disease. *J Cell Biol* 171:87-98.
- Yue Z (2007) Regulation of neuronal autophagy in axon: implication of autophagy in axonal function and dysfunction/degeneration. *Autophagy* 3:139-141.
- Yue Z, Jin S, Yang C, Levine AJ, Heintz N (2003) Beclin 1, an autophagy gene essential for early embryonic development, is a haploinsufficient tumor suppressor. *Proc Natl Acad Sci U S A* 100:15077-15082.
- Yue Z, Horton A, Bravin M, DeJager PL, Selimi F, Heintz N (2002) A novel protein complex linking the delta 2 glutamate receptor and autophagy: implications for neurodegeneration in lurcher mice. *Neuron* 35:921-933.
- Zhang X, Yuan Z, Zhang Y, Yong S, Salas-Burgos A, Koomen J, Olashaw N, Parsons JT, Yang XJ, Dent SR, Yao TP, Lane WS, Seto E (2007) HDAC6 modulates cell motility by altering the acetylation level of cortactin. *Mol Cell* 27:197-213.
- Zhang XM, Walsh B, Mitchell CA, Rowe T (2005) TBC domain family, member 15 is a novel mammalian Rab GTPase-activating protein with substrate preference for Rab7. *Biochem Biophys Res Commun* 335:154-161.
- Zoghbi HY, Orr HT (2000) Glutamine repeats and neurodegeneration. *Annu Rev Neurosci* 23:217-247.
- Zoncu R, Perera RM, Balkin DM, Pirruccello M, Toomre D, De Camilli P (2009) A phosphoinositide switch controls the maturation and signaling properties of APPL endosomes. *Cell* 136:1110-1121.
- Zuchner S, Vance JM (2006) Mechanisms of disease: a molecular genetic update on hereditary axonal neuropathies. *Nat Clin Pract Neurol* 2:45-53.
- Zuchner S, Nouredine M, Kennerson M, Verhoeven K, Claeys K, De Jonghe P, Merory J, Oliveira SA, Speer MC, Stenger JE, Walizada G, Zhu D, Pericak-Vance MA, Nicholson G, Timmerman V, Vance JM (2005) Mutations in the pleckstrin homology domain of dynamin 2 cause dominant intermediate Charcot-Marie-Tooth disease. *Nat Genet* 37:289-294.
- Zuchner S et al. (2004) Mutations in the mitochondrial GTPase mitofusin 2 cause Charcot-Marie-Tooth neuropathy type 2A. *Nat Genet* 36:449-451.
- Zweifel LS, Kuruvilla R, Ginty DD (2005) Functions and mechanisms of retrograde neurotrophin signalling. *Nat Rev Neurosci* 6:615-625.